This book specializes in groundwater monitoring and environmental impact assessments. It has revealed the groundwater pollution evaluation, remediation and radiological risk assessments which represent one of the main activities. The effort in these fields was clearly noticed due to the presence of necessary scientific contributions in groundwater monitoring, mapping the contamination channels, remediation of high radiotoxicity risks level, decontaminating of highly radioactive zones and building materials. The excellence of these book has provided a baseline for civil engineers and water resources managements on safer areas to drill boreholes for quality and consumable groundwater-based drinking in basement terrain.

Dr. Omeje Maxwell is currently teaching Physics at Covenant University,Ota, Ogun State, Nigeria. I hold Ph.D Physics of Universiti Teknologi Malaysia, M.Sc Geophysics of Federal University of Technology,Yola and B.sc Industrial Physics of Enugu State University of Science & Technology,Enugu,Nigeria with specialization in Environmental Geopysics.

978-3-659-95532-7

Radioactivity on Groundwater of Abuja

Omeje Maxwell
Husin Wagiran

Radiotoxicity Risk of Rocks& Groundwater of Abuja,Northcentral Nigeria

LAP LAMBERT Academic Publishing

Maxwell, Wagiran

Omeje Maxwell
Husin Wagiran

Radiotoxicity Risk of Rocks& Groundwater of Abuja,Northcentral Nigeria

Omeje Maxwell
Husin Wagiran

Radiotoxicity Risk of Rocks& Groundwater of Abuja,Northcentral Nigeria

LAP LAMBERT Academic Publishing

Impressum / Imprint
Bibliografische Information der Deutschen Nationalbibliothek: Die Deutsche Nationalbibliothek verzeichnet diese Publikation in der Deutschen Nationalbibliografie; detaillierte bibliografische Daten sind im Internet über http://dnb.d-nb.de abrufbar.

Bibliographic information published by the Deutsche Nationalbibliothek: The Deutsche Nationalbibliothek lists this publication in the Deutsche Nationalbibliografie; detailed bibliographic data are available in the Internet at http://dnb.d-nb.de.

Coverbild / Cover image: www.ingimage.com

Verlag / Publisher:
LAP LAMBERT Academic Publishing
ist ein Imprint der / is a trademark of
OmniScriptum GmbH & Co. KG
Bahnhofstraße 28, 66111 Saarbrücken, Deutschland / Germany
Email: info@omniscriptum.com

Herstellung: siehe letzte Seite /
Printed at: see last page
ISBN: 978-3-659-95532-7

Zugl. / Approved by: Universiti Teknologi malaysia, Diss., 2014

RADIOMETRIC INTERPRETATION OF GEOLOGIC DATA AND ITS EFFECT ON GROUNDWATER IN ABUJA, NORTH-CENTRAL NIGERIA

OMEJE MAXWELL

Faculty of Science
Universiti Teknologi Malaysia

I dedicate this work

To my dear wife and family

Whose love, kindness, patience and prayers have brought me this far

ACKNOWLEDGEMENT

To God be all Glory, honour, majesty and praise for his mercies, protection and care throughout the course of this research work. I wish to express my profound gratitude to my able supervisors, Prof. Dr. Husin Wagiran; indeed a father to me, Prof .Dr. Noorddin Ibrahim and Dr. Soheil Sabri who despite their tight schedules still had time to scrutinize this work offering with constructive advice where necessary. A very big thanks to Mr. S. K. Lee who from the beginning of this research took it upon himself to assist to the end. Also to my uncles in the likes of Dr. Ugwuoke Paulinus, Mr. Gebriel Ezema, Mr. Ugwuoke Peter Ifeanychukwu, Prince Ugwuoke, Rev. Paul Okereke, Mr & Mrs. Chima Cyracus Agbo, Mr. Ottih Gerry, Mr. Ugwu Earnest Ozoemena and Oha Andrew Ifeanyi for their financial and academic supports.

Thanks and appreciations to all the staff and my friends in the Physics Department who contributed in this research work. Many thanks to all people who helped me in my study, in particular, Dr. Ibrahim Alnour, Dr. Yasser Alajerami, Dr. Muneer Saleh, Mohamad Gulbahar, Nuraddeen Nasiru Getso, Abubaka Sadiqu Aliyu, Aminu Saidu, Azadeh Rafaei and lab Staff Mr Saiful Bin Rashid, Mr Mohammad Abdullah Bin Lasimin, Abdusalami Gital, Mr Jaffar and Puan Anissa.

Special thanks to my late parents and all the members of my family that supported me with patience and encouragements.

ABSTRACT

The purpose of this study is to evaluate the quality of groundwater in different locations for water consumption at Dei-Dei, Kubwa, Gosa and Lugbe area of Abuja, North-Central Nigeria. Vertical electric sounding and shuttle radar topography mission was used to determine the depth of groundwater bearing formation and map lineaments structures underlying the area. Boreholes with the geophysical log data were drilled and rock samples in each layer lithologically were collected for γ-ray analysis. The activity concentrations of ^{238}U, ^{232}Th, and ^{40}K from the borehole rock samples were determined using high-purity germanium γ-detector. The activity concentration of radionuclides in Dei-Dei borehole has a mean value of 30.1 ± 2.9 Bq kg^{-1} for ^{238}U; 67.2 ± 5.2 Bq kg^{-1} for ^{232}Th, and 832.3 ± 105.0 Bq kg^{-1} for ^{40}K. Kubwa borehole has a mean value of 34.4 ± 3.2 Bq kg^{-1} for ^{238}U; 60.5 ± 5.4 Bq kg^{-1} for ^{232}Th and 573.1± 72.0 Bq kg^{-1} for ^{40}K. At Gosa borehole, ^{238}U has a mean value of 26.1 ± 2.5 Bq kg^{-1}, 62.8 ± 4.8 Bq kg^{-1} for ^{232}Th and 573.3 ± 73.0 Bq kg^{-1} for ^{40}K. At Lugbe borehole ^{238}U has a mean value of 20.0 ± 2.0 Bq kg^{-1}, 46.8 ± 4.9 Bq kg^{-1} for ^{232}Th and 915.2 ± 116.1 Bq $kg^{-1}$for ^{40}K . Significantly higher concentration of ^{238}U and ^{232}Th occurred in samples collected from Dei-Dei borehole was attributed to granitic intrusions produced by denudation and tectonism. Inductively coupled plasma mass spectrometry (ICP-MS) was used to determine the concentrations of ^{238}U and toxic elements (i.e. Pb, Cr, Cd, Zn, Ni, As and Mg) in water samples collected from the boreholes and public water supply in the study area. The activity concentration of ^{238}U in groundwater-based drinking was noted higher at Lugbe borehole with a value of 2736 μBq L^{-1} when compared with other boreholes. In the study area, the inhabitants permanently used water from the boreholes for daily drinking and household requirements. The annual effective dose was estimated to be in the range from 1.46 x 10^{-5} to 9.03 x 10^{-5} mSv yr^{-1} for boreholes with the highest value noted in Lugbe borehole with a value of 9.03 x 10^{-5} mSv yr^{-1}. The group receives about 5.55 x 10^{-5} mSv of the annual collective effective dose in the study area due to ^{238}U in drinking water. The highest radiological risks for cancer mortality and morbidity were found to be low, with highest values of 1.03 × 10^{-7} and 1.57 × 10^{-7} obtained from Lugbe borehole. The chemical toxicity risk of ^{238}U in drinking water over a life time consumption has a mean value of 4.0 x 10^{-3} μg kg^{-1} day^{-1} with highest value of 6.0 x 10^{-3} μg kg^{-1} day^{-1} obtained from Dei-Dei and Lugbe boreholes. The elemental concentration of Pb was noted to be higher than the recommended permissible limit at Lugbe borehole and Public Nigeria Water Board with values of 0.014 and 0.012 mg L^{-1}, respectively. Other results obtained were below the recommended acceptable level by World Health Organization and United State Environmental Protection Agency. Results of the measurements could be of importance in radio-epidemiological assessment, diagnosis and prognosis of uranium induced cancer in the population of the inhabitants of Abuja.

ABSTRAK

Tujuan kajian ini adalah untuk menilai kualiti air bawah tanah di kedudukan berbeza sebagai sumber air bagi kegunaan di kawasan Dei-Dei, Kubwa, Gosa dan Lugbe di Abuja, Utara-Tengah Nigeria. Pembunyian elektrik menegak dan misi topografi radar olak-alik digunakan bagi menentukaan kedalaman pembentukan takungan air bawah tanah dan struktur garisan peta di bawah permukaan kawasan tersebut. Lubang gerek dengan data log geofizik digerudi dan sampel batuan pada setiap lapisan litoligik diambil untuk analisis sinar-γ. Kepekatan keaktifan ^{238}U, ^{232}Th dan ^{40}K daripada sampel batuan lubang gerek ditentukan dengan mengunakan pengesan sinar-γ germanium berketulenan tinggi. Kepekatan keaktifan radionuklid di lubang gerek Dei-Dei mempunyai nilai min 30.1 ± 2.9 Bq kg^{-1} bagi ^{238}U; 67.2 ± 5.2 Bq kg^{-1} bagi ^{232}Th, dan 832.3 ± 105.0 Bq kg^{-1} bagi ^{40}K. Lubang gerek Kubwa mempunyai nilai min 34.4 ± 3.2 Bq kg^{-1} bagi ^{238}U; 60.5 ± 5.4 Bq kg^{-1} bagi ^{232}Th dan 573.1± 72.0 Bq kg^{-1} bagi ^{40}K. Lubang gerek Gosa mempunyai nilai min 26.1 ± 2.5 Bq kg^{-1} bagi ^{238}U , 62.8 ± 4.8 Bq kg^{-1} bagi ^{232}Th dan 573.3 ± 73.0 Bq kg^{-1} bagi ^{40}K. Lubang gerek Lugbe mempunyai nilai min 20.0 ± 2.0 Bq kg^{-1} bagi ^{238}U, 46.8 ± 4.9 Bq kg^{-1} bagi ^{232}Th dan 915.2 ± 116.1 Bq kg^{-1} bagi ^{40}K. Kepekatan tinggi yang ketara bagi ^{238}U dan ^{232}Th didapati pada sampel yang diambil dari lubang gerek Dei-Dei adalah disebabkan penerjahan granitik yang dihasilkan oleh penggondolan dan tektonisme. Spektrometer jisim plasma gandingan teraruh (ICP-MS) digunakan untuk menentukan kepekatan ^{238}U dan unsur toksik (Pb, Cr, Cd, Zn, Ni, As dan Mg) dalam sampel air yang diambil dari lubang gerek yang sama dan pembekal air awam di kawasan kajian. Kepekatan keaktifan ^{238}U dalam air bawah tanah yang diminum didapati tinggi di lubang gerek Lugbe dengan nilai 2736 μBq L^{-1} jika dibandingkan dengan lubang gerek yang lain. Di kawasan kajian, penghuni menggunakan air dari lubang gerek secara tetap sebagai minuman harian dan keperluan isi rumah. Dos berkesan tahunan telah dianggarkan dalam julat antara 1.46 x 10^{-5} hingga 9.03 x 10^{-5} mSv tahun^{-1} bagi lubang gerek dengan nilai tertinggi didapati pada lubang gerek Lugbe dengan nilai 9.03 x 10^{-5} mSv tahun^{-1}. Kumpulan tersebut menerima dos berkesan terkumpul kira-kira 5.55 x 10^{-5} mSv di kawasan kajian akibat kandungan ^{238}U dalam air minuman. Risiko radiologi tertinggi bagi mortaliti kanser dan morbiditi kanser didapati rendah dengan nilai tertinggi masing-masing ialah 1.03 × 10^{-7} and 1.57 × 10^{-7} yang didapati dari lubang gerek Lugbe. Risiko toksik kimia dari ^{238}U dalam air minuman bagi penggunaan seumur hidup mempunyai nilai min 4.0 x 10^{-3} μg kg^{-1} hari^{-1} dengan nilai tertinggi 6.0 x 10^{-3} μg kg^{-1} hari^{-1} yang diperoleh dari lubang gerek Dei-Dei and Lugbe. Kepekatan unsur Pb didapati lebih tinggi daripada had yang dibenarkan yang disyorkan, masing-masing didapati di lubang gerek Lugbe dan bekalan air awam dengan nilai masing-masing adalah 0.014 dan 0.01 mg L^{-1}. Hasil lain yang didapati adalah di bawah nilai aras yang diterima yang disyorkan oleh Organisasi Kesihatan Sedunia dan Agensi Perlindungan Alam Sekitar Amerika Syarikat. Hasil pengukuran adalah sangat penting dalam penilaian radio-epidemiologi, diagnosis dan prognosis kanser akibat uranium bagi penduduk Abuja.

TABLE OF CONTENTS

LIST OF TABLES

LIST OF FIGURES

LIST OF ABBREVIATION

AB	-	Distance from point A to B of the current electrode spacing
AT	-	Average time
BW	-	Body weight
CNSC	-	Canadian nuclear safety commission
Cpm	-	Count per minute
DC	-	Direct current
ED	-	Exposure duration
EF	-	Exposure frequency
EPA	-	Environmental protection agency
EPC	-	Exposure point concentration
GM	-	Geiger muller
GPS	-	Geographical positioning system
HPGe	-	High purity germanium
IAEA	-	International atomic energy agency
ICRP	-	International commission on radiological protection
ICP-MS	-	Inductively coupled plasma mass spectrometry
IR	-	Ingestion rate
LADD	-	Life average daily dose
LFI	-	Limited field investigation
NAA	-	Neutron activation analysis
NASA	-	National aeronautics and space administration
ND	-	Not detected
NE	-	North east
NNE	-	North north east
NOR	-	Natural occurring radionuclide
NORM	-	Natural occurring radioactive material

NRC	-	Nuclear regulatory commission
MCA	-	Multi-channel analyzer
MNA	-	Malaysian nuclear agency
MDA	-	Minimum detectable activity
MINT	-	Malaysian institute of nuclear technology research
PPM	-	Parts per million
PPB	-	Parts per billion
PSI	-	Pound per square inch
QF	-	Quality factor
RAD	-	Radiation absorbed dose
REM	-	Roentgen equivalent man
REV	-	Representative elementary volume
RFD	-	Reference dose
SL	-	Site layer
SRTM	-	Shuttle radar topography mission
SRTM-DEM	-	Shuttle radar topographic mission-digital elevation model
SSW	-	South south west
STUK	-	Säteilyturvakeskus strålsäkerhetscentralen (radiation and nuclear safety authority Finland)
SW	-	South West
TP	-	Technical procedure
UNFPA	-	United nations population fund
UNICEF	-	United nations internationl Children's emergency fund
UNSCEAR	-	United nations scientific committee on the effect of atomic radiation
U(IV)	-	Uranous
USSGS	-	US geological survey
VES	-	Vertical electrical sounding
X-SAR	-	X-band synthetic aperture radar
SI	-	International system of units
WHO	-	World health organisation
WSW-ENE	-	West South West- East North East
XRF	-	X-ray fluorescence

LIST OF SYMBOLES

Al_2O_3	-	Aluminium oxide
As	-	Arsenic
A_{samp}	-	The specific activity concentration of sample
A_{std}	-	The specific activity concentration of the standard sample
BqL^{-1}	-	Becquerel per litre
CaO	-	Calcium oxide
$CaCO_2$	-	Calcium carbonates (calcite)
Cd	-	Cadmium
Co	-	Cobalt
CO_3^{2-}	-	Carbonate
Cr	-	Chromium
C_{samp}	-	Concentration of sample
C^{std}	-	Concentration of the standard sample
E_{BE}	-	Binding energy
E_e	-	Kinetic energy
Eh	-	Oxidation potential
Eγ	-	Gamma energy
F	-	Fluoride
Fe_2O_3	-	Iron oxide
K	-	Potassium
KCl	-	Potassium chloride
K_2O	-	Potasium oxide
m	-	Sample mean
M	-	Molecular weight
Mg	-	Magnesium

Mg	-	Magnesium
MgO	-	Magnesium oxide
MnO	-	Manganese oxide
n^-	-	n-doped material
N	-	Number of atoms
Na_2O	-	Sodium oxide
Ni	-	Nickel
N_{samp}	-	Net count of photopeak area of sample collected
N_{std}	-	Net counts of photopeak area of the standard sample
P^+	-	P-doped material
P_2O_5	-	Phosphorus oxide
pH	-	Potential hydrogen
Pb	-	Lead
$Pb(OH)^+$	-	Lead hydroxide
$Pb(OH)_2$	-	Lead (II) hydroxide
P0	-	Polonium
R	-	Lifetime cancer risk
R	-	Roentgen
SiO_2	-	Silicon oxide
SO_4	-	Tetraoxosulphate (VI)
T_d	-	Decay time
Th	-	Thorium
TiO_2	-	Titanium oxide
u	-	Atomic mass unit
U	-	Uranium
U_2^{2+}	-	Uranyl
U_3O_8	-	Uranium trioxide
U^{4+}	-	Uranous
UO_2	-	Uraninite
W_{samp}	-	The weight of the sample collected
W_{std}	-	The weight of the standard sample
Zn	-	zinc
$ZnSO_4$	-	Zinc sulphate

U	-	Potential,in volt.
m	-	Mass of the element
r	-	Risk coefficient
α	-	Alpha particle
β	-	Beta particle
γ	-	Gamma radiation
ε	-	Efficiency
θ	-	Volumetric water content
λ	-	Disintegration constant
μ	-	Micron
$\mu g\ L^{-1}$	-	Micron gram per litre
ρ	-	Resistivity of the medium
δ_{est}	-	Standard deviation
δ_{SE}	-	Standard error
1D	-	One dimensional
2D	-	Two dimensional
^{204}Pb	-	Lead-204
^{206}Pb	-	Lead-206
^{207}Pb	-	Lead-207
^{208}Pb	-	Lead-208
^{208}Tl	-	Thallium-208
^{210}Pb	-	Lead-210
^{210}Po	-	Polonium- 210
^{211}Pb	-	Lead-211
^{212}Po	-	Polonium- 212
^{214}Bi	-	Bismuth- 214
^{220}Rn	-	Radon- 220
^{222}Rn	-	Radon- 222
^{223}Ra	-	Radium-223
^{224}Ra	-	Radium-224
^{226}Ra	-	Radium -226
^{228}Ac	-	Actinium-228
^{228}Ra	-	Radium-228

^{233}Pa	-	Protactinium- 233
^{234}U	-	Uranium- 234
^{235}U	-	Uranium- 235
^{236}U	-	Uranium-236
^{238}U	-	Uranium -238
pH	-	Neptunium- 239
^{40}K	-	Potassium- 40

LIST OF APPENDICES

CHAPTER 1

INTRODUCTION

1.1 Introduction

Ionizing radiation in natural environment was discovered in 1899 and it is said to originate from radioactivity in environmental materials like rivers, ground waters, soils and rocks (Lowder, 1990). The natural radionuclides, ^{238}U, ^{232}Th and ^{40}K are present in the earth crust (Evans, 1969). Humans are usually exposed to some natural background radiations which are the naturally occurring radioactive material (NORM) (U.S. EPA, 1993). The presence of these (NORM) in soil, rocks, water, and air, alongside the cosmic radiation result in continuous and unavoidable internal and external radiation exposures of humans (UNSCEAR, 2000). The NORM in the earth and water of an environment mainly occur as progeny of ^{238}U, ^{235}U and ^{232}Th isotopes which are distributed by natural geological and geochemical processes in addition to potassium ^{40}K and small quantities of fission-product residues such as ^{137}Cs from atmospheric weapon tests (Trimble, 1968). In many countries, extensive work has been carried out to evaluate the risks associated with NORM (NRC,1999; UNSCEAR, 2000). Thus, it has been established that the specific levels of terrestrial environmental radiation are related to the geological composition of each lithologically separated area, and to the content of ^{238}U, ^{232}Th and ^{40}K in the rock from which soils originate in each area (Abd El-mageed *et al.,* 2011; Maxwell *et al*., 2013a; Tzortzis and Tsertos, 2004; UNSCEAR, 2000; Xinwei and Xiaolon, 2008).

Uranium occurs as a trace element in the earth's crust and is typically present in the concentration of 1-10 ppm in granite and in clastic sediments of granitic origin and thorium is typically present in concentrations ranging between 3 and 30 ppm in crustal minerals. The average concentration of potassium in crustal rocks is approximately 2.5% with a range from 0.1% to 5% or more On the other hand, thorium occurs mostly in sediment (IAEA, 1989).

In 2006, limited field investigation (LFI) involving uranium in the subsurface at the Hanford Site's 300 Area in Washington, yielded unexpectedly high concentrations of uranium in groundwater samples collected at two of the four characterization boreholes (Williams *et al.*, 2007). The samples were obtained during drilling and came from stratigraphic intervals in the unconfined aquifer that is not monitored by the existing well network. The occurrences appeared to be restricted to an interval of relatively finer-grained sediment within the Ring old Formation. A subsequent investigation was carried out which involved drilling and characterization activities at four new locations near the initial discovery. This report presents the fresh information obtained since the LFI characterization report (Williams *et al.*, 2007) regarding uranium contamination beneath the 300 Area (Peterson *et al.,* 2008). It was estimated that approximately 650,000 m^3 of groundwater beneath the 300 area investigated are affected by uranium at concentrations that exceed the drinking water standard of 30 μg L^{-1}.

Naturally occurring radionuclides are manly from three different decay chains (^{235}U, ^{238}U and ^{232}Th). One of the longest-lived nuclides is ^{232}Th with a half-life of 1.405 x 10^{10} years. ^{236}U was the immediate parent of ^{232}Th with a life of 2.342 x 10^7 years thus is not found in the environment anymore and ^{238}U refers to the second longest series. 99.2745% by weight of ^{238}U, 0.7200% of ^{235}U, and 0.0055% of ^{234}U are the estimated naturally occurring uranium (Pfennig *et al.,* 1998).

The activity concentrations of ^{238}U, ^{232}Th and ^{40}K in groundwater are connected to the activity concentrations of ^{238}U and ^{232}Th of aquifer bearing formation, and their decay products in subsurface rock formation. This occurs as a result of reactions between groundwater, soil and bedrock which release quantities of

dissolved mineral components depending on the mineralogical and geochemical composition of the rock formation (IAEA, 1990; Langmuir, 1978). It also depends on the chemical composition of the water, degree of weathering of the subsurface rock formation, redox conditions and the residence time of groundwater in subsurface water bearing formation, (Durrance, 1986). ^{238}U and ^{232}Th decay series in soils, bedrocks and groundwater system is controlled by the chemical substances, radioactive decay and surrounding physical factors. As a result of these controlled processes, the radioactive elements either leach into the groundwater or to the surrounding, resulting into decay series of disequilibrium of nuclides (Durrance, 1986).

In Nigeria, NORM levels have been studied in surface soils in Ijero-Ekiti (Ajayi *et al*., 1995), in soil and water around Cement Company in Ewekoro (Jibiri et al., 1999) and in rocks found in Ekiti (Ajayi and Ajayi, 1999). Only insignificant levels of NORM were identified by (Ajayi *et al*., 1995). The health risks to human are real which is not defined in this geological condition. The activity concentration of these radionuclides is yet to be defined in the environment and no epidemiological studies to quantify the risk from all natural radionuclides in drinking water.

In this study, the main emphasis is to determine the risk areas in subsurface structures (lithology) and to examine activity levels of naturally occurring radionuclides in different raw water sources at Dei-Dei, Kubwa, Gosa, and Lugbe boreholes in order to evaluate the exposure to the inhabitants in the area. The study areas are bounded by latitudes 8^o 53`N - $9^o$ 13`N and longitudes 7^o 00`E - $7^o$ 30` E. The borehole points are in the coordinates lat: 9^o 6'52"N and long: 7^o 15'39"E (Dei-Dei), lat: 9^o 6' 16.7" N and long: 7^o 16' 26.0"E (Kubwa), lat: 8^o 56' 45.6" N and long: 7^o 13' 26.2" E (Gosa) and lat: 8^o 59' 2.3" N and long: 7^o 23' 7.8"E (Lugbe).

1.2 Problem Statement

In Nigeria, the case for conjunctive use of surface and groundwater supply, where available, to meet the ever increasing demand cannot be over-emphasized. However, relating the available resources to demand, the population finds it difficult to access quality water for consumption. Nigeria has been ranked the third in world's poorest countries in gaining access to water and sanitation according to World Health Organization report 2012. A report from (Godknows, 2012) noted that the World Health organization and UNICEF ranked Nigeria third behind China and India, in countries with largest population without adequate water and sanitation. The study area (Abuja) had a master plan in 1979 which projected population in the region to be 5.8 million people by 2026. The recent population of Abuja is 2, 759,829 at 2013 and the most recent is 3,028,807 at 2014 report (UNIFPA, 2014).

The Water Board has a designed capacity with the pre-plan which is not in phase with the city growth in the recent time. The increase in demand for water has led to compulsory alternative sources to defray the deficit. Majority of the public water supplies come from the borehole of reasonable depths. The water has been consumed without treatment and during drilling processes it cuts across so many rock formations. The radioelement exists in this rock formation like granite to some extent could contaminate the groundwater system through leaching and weathering processes. The natural radioactivity of ground water is derived primarily from radioactive rocks, soil and mineral with which the water has been in contact. There are three naturally radioactive elements: the uranium series, the thorium series and potassium-40.

The ground water is not considered acceptable to the public, organism and plantation if activity concentration value exceeds 1 Bq L^{-1} as recommended by IAEA and Annual effective dose exceeds 1 mSv y^{-1} as suggested by World Health Organisation (WHO, 2008). As a result, most of the public in the satellite towns and suburbs are not aware of the potential problems associated with aquifer bearing rocks constituting radioactive elements. In the same way, it leaches into the groundwater through chemical weathering and physical processes which is being consumed daily

by the public. The study of these radionuclides in groundwater of the suburbs of Abuja has become important because many residents of the area embark on the development of private boreholes without the knowledge of the health risk associated with the naturally occurring radionuclides.

1.3 Research Objectives

The primary aim of this work is to gather new information on the occurrence of natural radioactivity in groundwater based drinking water and to reduce the radiation exposure to Abuja inhabitants. In order to achieve this aim, the objectives of this work are

1. To investigate the depth to aquifer bearing formation and the subsurface structures that controls the groundwater system using Vertical Electrical Sounding (VES) and Shuttle Radar Topography Mission (SRTM).

2. To determine the activity concentration of ^{238}U, ^{232}Th and ^{40}K in different layers of the subsurface lithology so as to infer the source rock that poses higher activity level.

3. To determine the corresponding geologic rock type that attributes such high level of natural radionuclides so as to set a baseline that will help geologists and hydrologists in groundwater resources on basement terrain areas how to drill hydrogeologically motivated boreholes in safer aquifer bearing formations for public consumption.

4. To investigate the occurrence of ^{238}U and toxic elements in groundwater and to obtain representative estimates of the effective dose to borehole users (private wells) in the study area.

1.4 Research Scope

The first part of the study was to determine the suitable sites for groundwater bearing formation (aquifer) at Dei-Dei, 70 m, Kubwa, 60 m, Gosa, 50 m and Lugbe, 40 m in Abuja, Northcentral Nigeria using Vertical Electrical Sounding (VES) integrated with 88 lineaments (fractures) extracted from Hill-shaded Shuttle Radar Topography Mission (SRTM) data.

Secondly, the comparison of activity concentrations of ^{238}U, ^{232}Th and ^{40}K in different layers of subsurface structures in the study area were determined such as to trace the source rock that constitute higher activity concentrations of ^{238}U, ^{232}Th and ^{40}K.

Thirdly, the rock layers with the highest activity level and geological type that contributed such high level of radionuclides in subsurface formation.

Finally, determination of activity concentrations of ^{238}U, ^{232}Th and ^{40}K in groundwater to estimate the exposure to the inhabitants of Abuja people who rely on groundwater based drinking water for consumption. Its purpose was to evaluate the suitability of different sites as locations for obtaining groundwater for consumption.

The scope of this work described in Figure 1.1 shows how radionuclides from the environment, soil, bedrock are being transferred to human through groundwater source from reasonable depths of varying rock formation to the aquiferous zone (groundwater host rock) below ground level. The exposure is by ingesting the water that comes from such formation with high dissolved uranium, thorium and potassium rich minerals due to water-rock interactions. The movements across the fractured zones through the recharging channels that supply the water to the aquifer are to be evaluated for the contamination level of the radionuclides to the inhabitants.

The scope of this study presented in a flowchart with structure of the study discussed in Figure 1.1 has two segments:

1. The first segment describes the occurance of radionuclides and the exposure to Abuja people.

2. The second part discussed the structure of the study to attain the purpose of this work.

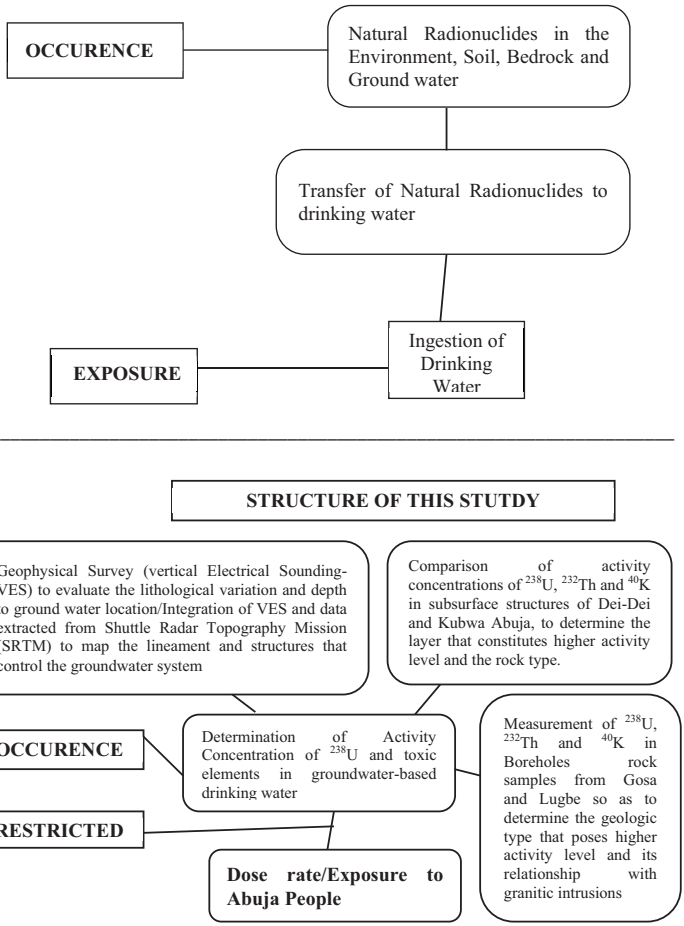

Figure 1.1 The flowchart of the Scope of work and the Structure of the study

1.5 Significance of the Study

1. The identification of radioactive source rock that constitute higher activity concentrations of ^{238}U, ^{232}Th and ^{40}K in subsurface layers will assist professionals in hydrogeology and water resources management: civil engineers, environmental engineers, geologists and hydrologists who are engaged in the investigation, management, and protection of groundwater resources on areas to drill boreholes for the safety of the inhabitants who rely on groundwater based drinking water for consumption.

2. It will identify the occurrence of radionuclides in groundwater and obtain representative estimate for the effective dose to the users of private wells in Abuja caused by ^{238}U, ^{232}Th and ^{40}K.

3. It will equally reveal the geologic conditions that will help to monitor the activity levels in groundwater by Geophysicists/Geochemists such as geologic rock units, weathering, chemical complexation and oxidations.

4. Importantly, to serve as guidance for the water resources management and effective utilization in Abuja.

5. Furthermore, this study contributes significant and general information on baseline to the people of Abuja on their groundwater consumption status.

1. 6 Research Hypotheses:

H_1 = alternative hypothesis

- The layers with high metamorphosed granitic intrusion will report higher activity concentration of ^{238}U, ^{232}Th, and ^{40}K.
- The layers that are highly fractured and techtonized will be noted higher, which will be attributed to oxidation of uranium in aqueous phase.

H_o = null hypothesis

- Granitic intrusion has no effect on activity concentration of ^{238}U, ^{232}Th and ^{40}K.
- There will be no difference in Th/U ratio in different layers
- The ^{238}U and ^{232}Th activity does not increase with acidity of soil/rock
- Weathering and metamorphism do not modify the ^{238}U, ^{232}Th and ^{40}K to readily leach from pegimatite and granites and redeposit in sediment at large distance from the source rocks.
- Weathering does not have impact in decreasing the Th/U ratio.

1.7 Thesis Organization

This thesis consists of five chapters. Chapter 1 presents the introduction of the natural occurring radionuclides; problem statement; objectives of the study; scope of the study; significance of the study; Research hypothesis and development of conceptual model.

Chapter 2 involves a literature review of geophysical methods for groundwater investigation, radioactive study and radioactivity, natural occurring radionuclides in groundwater, natural occurring radionuclides in Nigeria, Groundwater flow concept, groundwater formation in Nigeria. Chapter 3 discusses the instrumentation for geophysical data acquisition and methods, groundwater flow model, methodology and calculations of elemental concentrations using comparison method for gamma spectrometry including HPGe detector and experimental procedures, methods and calculations for neutron activation analysis, geochemical characterization method using XRF, method of water analysis using inductively coupled plasma spectrometry (ICP-MS). Chapter 4 covers the results for geophysical interpretation, comparison of NAA and direct method (gamma ray spectrometry using HPGe detector), determination of elemental concentrations of ^{238}U, ^{232}Th and ^{40}K in (ppm) and Bq kg^{-1} in studied samples and interpretations, geochemical characterization and interpretation of the mineral contents in the rock sample obtained in the four boreholes in the study area, interpretation of ICP-MS results for both groundwater samples from the same four boreholes and Water Board from the study area . Chapter 5 summarized the conclusion of the research work and suggestions.

CHAPTER 2

LITERATURE REVIEW

2.1 Introduction

The aim of this chapter is to review the methods and theoretical principles upon which the present work depends on and according to the objectives of the work.

2.2 Radioactive Studies

Some naturally occurring substances consist of nuclei which makes them unstable. Thus, these substances spontaneously transform into more stable product atoms. They are said to be radioactive and the transformation process is known as radioactive decay. The first investigation of uranium salt in 1896 observed the blackening of photographic emulsion in the vicinity of uranium compound. This was subsequently attributed to radiation being emitted by uranium. Radioactive decay is usually accompanied by the nuclear radiation emission of charged particles, alpha, beta and gamma rays which are denoted by the Greek letters alpha (α), beta (β) and gamma (γ).

2.2.1 Radioactivity

The activity of radioisotope source is defined as its rate of decay. Radioactive isotope emits radiation and therefore its activity will decrease as the time passes. The radiation emitted can be either alpha-, beta- or gamma- radiation, and a given source may emit radiation of more than one type in its decay process to a stable isotope. It is important to note that this decay is a completely random process. During radioactive decay, the mass of the sample will decrease, due to the emission of alpha- or beta-particle, but the total number of atoms will remain constant. Gamma-emission takes place from an excited nucleus with no change of nucleon or proton number. Alpha-emission reduces the nucleon number by four and the proton number by two. Beta-emission leaves the nucleon number unchanged but increases or decreases the proton number by one.

2.3 Natural Radioelements

This section reviews basic radiation geophysics, discussing briefly the primary natural radioelements of potassium, uranium and thorium.

2.3.1 Potassium (K)

Potassium is a radioelement by virtue of the radioactive ^{40}K isotope which has an abundance of 0.012 % in natural potassium. The gamma rays from the ^{40}K are monoenergetic with energy of 1461 keV and are emitted at a rate of 3.3 quanta s^{-1} kg^{-1}. In crustal materials, potassium is carried by the feldspar orthoclase (K feldspar), the muscovite and biotite micas, and the clay mineral illites. The average concentration of potassium in crustal rocks is approximately 2.5 % potassium with a

range from 0.1 to 5 % or more. Pure quartz sand, limestone, or serpentinized ultramafic rock is material of particularly low potassium content, (IAEA, 1989).

2.3.2 Uranium (U)

Uranium is an element comprised of three radioactive isotopes of mass number 238, 235 and 234. ^{238}U (99.3% abundance) and ^{235}U (0.7% abundance) are primaeval nuclides which are transformed into stable lead isotopes through successive alpha and beta decays. ^{234}U (< 0.01% abundance) is intermediate radionuclide in the decay series formed by ^{238}U. The disintegration series of ^{238}U is shown in Figure 2.1.

One gram of uranium is an indirect source of almost 50 000 photon emissions per second of which over 90 % originate from the ^{238}U decay series. Nearly two thirds of the ^{238}U photons are gamma rays with energies of between 242 and 2448 keV. They are principally emitted by two decaying uranium daughter nuclei, ^{214}Pb and ^{214}Bi (Table 2.1). About one third of the ^{238}U photons are X and gamma rays with energies of less than 100 keV. A small contribution to the uranium decay series includes gamma rays with energy of 185.7 keV, emitted by ^{235}U. Uranium occurs as a trace element in the earth's crust and is typically present in concentrations of 1 to 10 ppm in granite and in clastic sediments of granitic origin. In oxidizing environments, uranium forms the hexavalent uranyl ion which may be transported by groundwater and redeposited in sediments with a content of organic material, (IAEA, 1989).

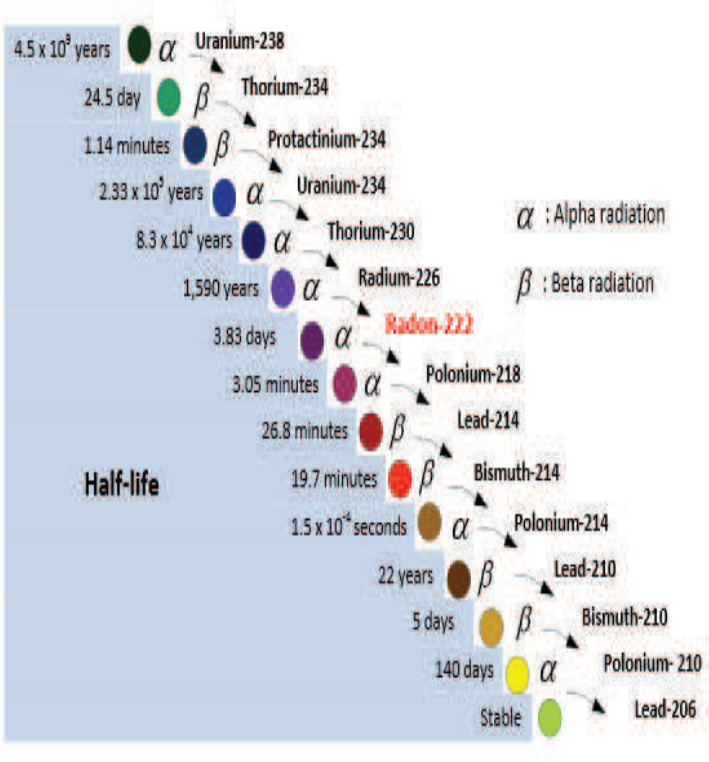

Figure 2.1 Disintegration series of ^{238}U. (Principal members only: isotopes constitution less than 0.2% of the decay products are omitted.) Source: Canadian Nuclear Safety Commission, (CNSC).

Table 2.1: Principal Gamma Ray Emissions in the ^{238}U Decay Series

Source Nuclide	Gamma Ray Energy (keV)	Relative Intensity[a] (%)
Pb-214	242	7.6
Pb-214	295	18.9
Pb-214	350	37.1
Bi-214	609	42.8
Bi-214	666	14.0
Bi-214	768	4.8
Bi-214	1120	15.0
Bi-214	1238	6.1
Bi-214	1378	4.3
Bi-214	1765	15.9
Bi-214	2204	5.3

[a] Photons per hundred decays of the source nuclide.

2.3.3 Thorium (Th)

Thorium is formed by the primaeval nuclide ^{232}Th which decays into stable lead through nuclear transformation similar to those in the two uranium decay series as shown in Figure 2.2. One gram of thorium results in emission of approximately 15 000 photons per second and about one third of these are X-rays of energies up to 105 keV. The others are gamma rays with energies from 129 to 2615 keV. Most of the gamma rays originate from decaying ^{228}Ac, ^{208}Tl and ^{212}Pb (Table 2.2).

In the crustal materials, the concentration between 3 and 30 ppm of thorium level was reported. Much of the thorium contained in sediments may be carried by

kaolinite or other minerals of the clay fraction or in heavy resistant minerals such as zircron and monazite, (IAEA, 1989).

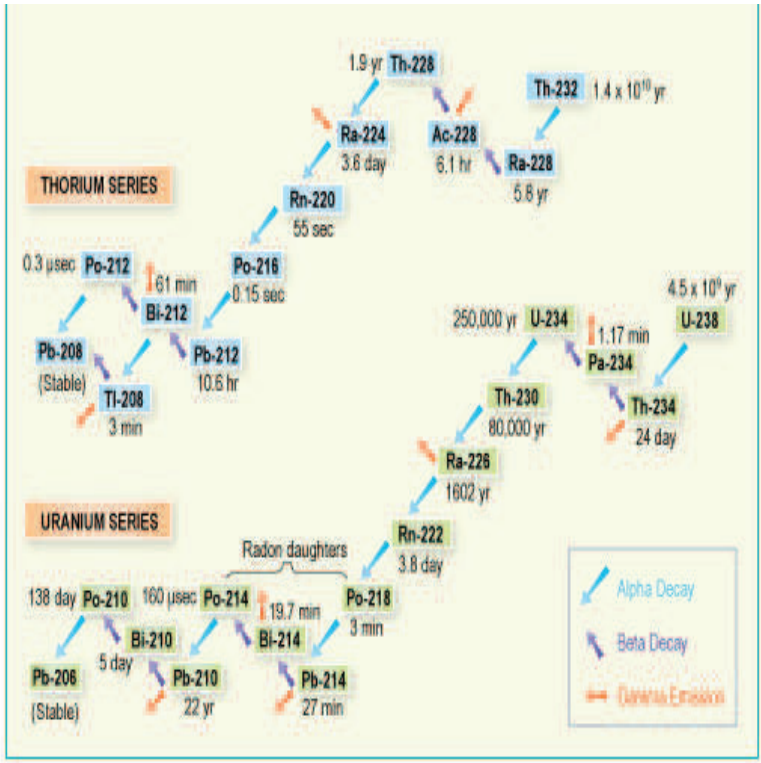

Figure 2.2 Disintegration series of thorium.(Source: World Nuclear Association Registered in England, UK)

Table 2.2: Principal Gamma Ray Emissions in the ^{232}Th Decay Series

Source Nuclide	Gamma Ray Energy (keV)	Relative Intensity[a] (%)
Pb-212	239	44.6
Ac-228	338	12.4
Tl-208	511	8.1
Tl-208	583	31.0
Bi-212	727	6.7
Ac-228	795	5.0
Ac-228	840	10.2
Ac-228	911	30.0
Ac-228	965	5.6
Ac-228	969	18.1
Tl-208	2615	36.0

[a] Photons per hundred decays of the source nuclide.

2.4 Geochemistry and Chemistry of Natural Radionuclides in Groundwater

^{222}Rn is a naturally occurring radioactive gas in the ^{238}U decay series with a half-life of 3.82 days. It is the most significant isotope of radon due to longer half-life. The other isotopes, ^{220}Rn and ^{219}Rn have half-lives of 55 seconds and 4 seconds respectively. The occurrence in groundwater is principally linked to the type of rock which the water has been extracted, (Cottem, 1990). In groundwater, ^{222}Rn occurs in ferrous condition and its level of activity may differ from few Bq L^{-1} to Bq L^{-1} in thousands. ^{222}Rn of higher activity level was found in reasonable deep subsurface aquifer formation. In an exposed terrain of surface water, ^{222}Rn activity level is found to be very low (Aieta *et al.* 1987, Salonen, 1994).

In the subsurface groundwater formation, the activity concentration of ^{222}Rn is highly dependent on the activity level of ^{226}Ra in aquifer bearing rock and soil,

rock permeability and the degree of ^{222}Rn emanation (Veeger and Ruderman, 1998). ^{222}Rn activity concentration is not affected by the chemical composition associated with the groundwater; rather, its mobility is affected by the movement of gaseous phase as well as the liquid phase, (Juntunen, 1991, Salih *et al.* 2004). The distance of transport of ^{222}Rn in groundwater is in the range of some metres because of its short half-life. The disequilibrium between ^{222}Rn and other ^{238}U decay series is caused by the ^{222}Rn escape in diffusive state (Salih, 2004).

Due to the inert nature of ^{222}Rn, it lacks the formation of chemical compounds in an environment at the range of neutral conditions or adsorbs surrounding materials in an environment. However, the correlations between elements in stable conditions and ^{222}Rn in subsurface groundwater system which was observed to be weak correlations were investigated by (Salih *et al.,* 2004). It was observed that ionic formation of fluoride in groundwater, in low pH media, affect the mobility of ^{222}Rn. ^{222}Rn transport in groundwater is higher at lower fluoride concentrations.

Natural occurring unstable radioactive elements are found in all rocks, soil and water. The common long-lived radioactive elements, ^{238}U and ^{232}Th, decay slowly to yield other radioelements, such as radium, which undergo radioactive decay. Radium has four natural isotopes: ^{223}Ra, ^{224}Ra, ^{226}Ra and ^{228}Ra. ^{226}Ra and ^{228}Ra are moderately soluble in water. Radium penetrate the subsurface groundwater system by the dissolution of aquifer bearing rocks, desorption from the sediment surfaces and ejection of minerals from decay series of radioactive materials in the bedrock (Lucas, 1985). In groundwater, the activity level has a strong relationship with bedrock structural mechanism such as complexation and precipitation-dissolution which influence the mobility of radium in groundwater system. The water-rock interaction depends on the chemical composition of the bedrock that hosts the groundwater which is related to the relationship of the structural mechanism of aquifer bearing formation, (IAEA, 1990). In groundwater investigation, the higher level of ^{226}Ra and ^{228}Ra activity concentrations was reported from saline water (IAEA, 1990).

Saline waters with low movement, radium occurs as uncomplexed Ra^{2+} cations. Weak complexes which may be caused by sulphate and carbonate anions are likely to be found in water that the salinity is very low and has no influence on the mobility of radium. The most abundant isotopes of radium are ^{226}Ra and ^{228}Ra with half-lives of 1600 years and 5.8 years, respectively. In low saline groundwater, the ratio of ^{226}Ra to ^{228}Ra is widely varied. In the previous report, values from 0.07 to 41 were noted. In saline water, the ratio of ^{226}Ra to ^{228}Ra ranges from 0.44 to 4 were reported in previous work elsewhere which was observed to be lower than the ratio ^{226}Ra to ^{228}Ra in low saline water, (IAEA, 1990). Natural occurring radium has been observed at high activity level in groundwater from two reasonable deep aquifers underlying northern Illinoise used for public water supply and was attributed to the dissolution of aquifer bearing rocks, desorption from the sediment surfaces and ejection of minerals from decay series of radioactive materials in the bedrock (Lucas, 1985).

^{238}U and ^{234}U are the most predominant form of uranium in groundwater system. Aieta *et al.*, (1987) reported that due to little abundance of ^{235}U in earth's crust, it occurs in low concentration in groundwater. The oxidation states of uranium are +III, +IV, +V and +VI of which +IV or +VI state occur in groundwater in as a result of water rock interaction. Langmuir (1978) noted that the level of activity concentration in aquifer bearing rock determines the activity concentration in groundwater and other proximity of uranium-riche aquifer materials, the oxidation and potential hydrogen ions (pH) state of uranium. Other factors such as the presence of fluoride and carbonate coupled with other species like phosphate concentrations can form insoluble minerals or complexes uranium. The activity level of ^{238}U in groundwater is influenced by the hydroxides of manganese and iron and high sorption properties of organic constituents found in water.

Groundwater with pH less than neutral and oxygen deficient, the ^{238}U is much better stable in the form of +IV uranous (U^{4+}) than +VI in oxidized condition of uranyl, (UO_2^{2+}). Durrance (1986) reported that uranous species oxidizes to be in soluble form of uranyl species under the condition of oxidation to +VI.

Langmuir (1978) noted that ^{238}U chemically immobile in the +IV state. It was as a result of the precipitation in a wide range of natural condition. ^{238}U transport is increased in orders of magnitude in oxidized form of hexavalent state which could be the less soluble nature of uranous species than the uranyl species. However, the complexes of uranyl in the state of natural oxidized form are stable than the uranous conditions of complexes natural condition especially in groundwater system with more of organic matter.

The mineral content of ^{238}U in the host rock located in subsurface formation determines its solubility. Langmuir (1978) reported that ^{238}U found in rock mineral like uraninite (UO_2) or calcite ($CaCO_2$), in a normal condition, there are possibilities of leaching from the host rock into the groundwater system. It was found that the oxidation and leaching of ^{238}U increases in the present of carbonate which forms complexes of stable uranyl (Hostetler and Garrels, 1962).

Langmuir (1978) noted that uranium always form complex in groundwater with the dominant species in the oxidation (redox) potential and the activity of potential hydrogen ion (pH). Uranium complexing with organic matter are being studied. Crancon and Lee (2003) observed that fulvic and humic acids are the most essential ligands in natural condition, noted that uranium transports and precipitates in groundwater in these acids solute. Ivanovich and Harmon (1982) reported that humic and fulvic acids varies according to pH with the degree of ionization as well as the formation of uranium complexes which depends on pH of the groundwater system. Under acid condition, organic materials in groundwater plays essential role in the adsorption of uranium in subsurface water-rock interaction, (Lee, 2003; Silva and Nitshe, 1995).

2.4.1 Disequilibrium of Radioactivity in Groundwater

Durrance (1986) noted that ^{238}U and ^{232}Th decay series in soils, bedrocks and groundwater system is controlled by the chemical substances, radioactive decay and surrounding physical factors. As a result of these controlled processes, the radioactive element either leach into the groundwater or to the surrounding, resulting into decay series of disequilibrium of nuclides as shown in Figure 2.3. Ivanovich and Harmon (1982) reported that some daughter nuclides of ^{238}U and ^{232}Th have short half-life to be fractioned from the parent nuclides. ^{222}Rn for instance, has short-lived daughters. ^{210}Pb may be at equilibrium with the progenitor, ^{226}Ra if ^{222}Rn is found to be negligible in diffusion. A radioactive process of secular equilibrium occurs when the process of the system is not interfered with. In such condition of equilibrium, the parent nuclides activity concentration and its daughter nuclides activity are equal, which reduces with the half-life of the source nuclides (parent).

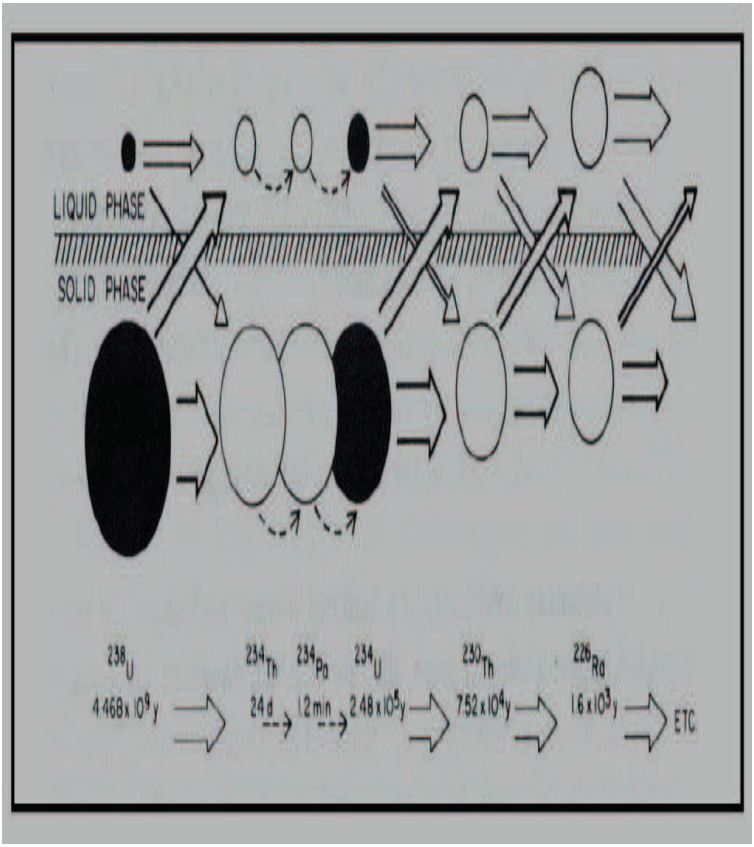

Figure 2.3 Disequilibrium of ^{238}U decay series nuclides. It indicates that the concentration is higher in solid phase (rock minerals) than liquid phase (groundwater), the migration of solid phase of the daughter nuclides to the liquid phase is the direction of the movements (Durrance 1986, Ivanovich and Harmon, 1982).

In subsurface aquifer bearing formation, there is interaction between the soil, aquifer rock materials and groundwater. Von Gunten and Benes (1995) reported that since there is interaction between the water and the bedrock interface, the possibilities of radionuclides leaching into the groundwater system by desorption and

dissolution or even erosion means or by radioactive decay atomic recoil is likely to take place. In groundwater system, elemental particles and radioactive isotopic disequilibrium occur within uranium- and thorium- series nuclides which were found to be greatest in deep groundwaters, such as boreholes with reasonable depths. The chemical and physical characteristics of the nuclides in boreholes were the reasons for the disequilibrium in groundwater which complexes the nuclides and cause them to be mobile when dissolved in water, (Salonen and Huikuri, 2002).

In the subsurface formation, Durrance (1986) reported that the measured activity concentrations of isotopes of ^{238}U and ^{234}U are equal. Ivanovich and Harmon (1982) noted that the activity level of ^{234}U almost greater than the ^{238}U activity concentration in groundwater. Salonem and Huikuri (2002) discovered that the ratio of ^{234}U to ^{238}U in subsurface drilled well in Finnish was 2 with a range of 1-3 at confidence level of 95 %. The lower activity concentration of ^{234}U and ^{238}U results in higher activity ratio in groundwater. Ivanovich and Harmon, 1982, reported the higher activity ratio of ^{234}U to 238U in groundwater to be about 30.

Durrance (1986) reported that in igneous rock formation, the occurrence of uranium is in undissolved state of +IV, which could be oxidized to form +VI, with a multiple magnitude order in soluble form than uranium in the form of +IV state. In this process, ^{234}Th may interact with atoms of oxygen due to alpha recoil and generate oxygen radicals in ^{234}U contents in oxygen-rich rock formation and get the uranium content in the formation oxidized. The considering of ^{232}Th fractions in chemical composition is not an important mechanism, (Suksi 2001).

2.4.2 Groundwater Colloids and Particles

In groundwater, the mobility of radioactive elements is influenced by the movements of the colloids and other particles in the water. Particle sizes of about 1-450 nm called colloids and other ions, complexes and constituents of groundwater

settles with very low velocity in the aquifer water formation (Degueldre *et al.* 2000). The fine clay particles, silica, some transition metals, humic and fulvic acids are the colloids found in natural subsurface groundwater system. Lieser *et al*., (1990), noted that certain level of colloidal humic substance increase was observed at the near surface. Tiny particles form aggregates and particles of larger sizes are settled onto the sediments below the bottom.

In groundwater system, transition metals and other metal hydroxides, acids of fulvic and humic are termed as the carriers of colloidal particles which adsorb or co-precipitate with radionuclides in colloidal form with other elements in water bearing formation. This is termed as the first group. The particles of intrinsic colloid are termed as the second group which are formed by radionuclides materials. The possibility of intrinsic colloidal formation is unlikely since the mass concentration in groundwater is low and the constant of the solubility does not exceed the limit (Lieser *et al.* 1990, Silva and Nitsche 1995).

2.4.3 Activity Concentrations of Natural Occurring Radioelements Reported in Different Countries

The various activity concentrations of ^{238}U and ^{226}Ra in groundwater have been carried out in many countries and the results are summarized in Tables 2.3 and 2.4 respectively. The results obtained in different countries cannot be compared to each other, since few areas that are restricted were examined for the activity levels.

Table 2.3: Concentrations of ^{238}U in groundwater from different Countries.

Nuclide	Country	Water Source	Number of Samples	Mean	Maximum	Reference
^{238}U (Bq L^{-1})	Sweden	D	328	14.3	427	Isam Salih et al. 2002
	Finland	D	7000	32	20 000	Salonen & Huikuri 2002
		G	5000	1.6	89	Juntunen 1991, Makelainen *et al*. 2002
	Norway	D	476	34	750	Midtgard *et al*., 1998
		D	150	6	3000	Banks *et al.,* 1998
	Ukraine	D	520	30.4	570	Zelensky *et al.,* 1993
	Switzerland	DW	360	<2	80.6	Deflorin *et al.,* 2004, UNSCEAR 2000
		M	42	<2	<10	Deflorin *et al.,* 2004
	Spain	D	345	145	1500	Fernandez *et al.,* 1992
		G	345	32	43	Fernandez *et al.,* 1992
	Germany	G + D	14	1.15	5.1	Gans *et al.,* 1987
	China	G +D	110	1.4	13.4	Zhou *et al.,* 2001
	Brazil	G + D	88	0.08	667	Almeida *et al.,* 2004
	France	G + D	54	8.7	24.4	Saumande *et al.,* 1973
	Slovenia	G	500	0.51	4.2	Kobal et al.1990
	Italy	DW	-	-	10.5	UNSCEAR 2000
	Colorado, North (USA)	D	566	18.6	<200	Zielinski *et al.,* 1995
	Colorado, South (USA)	D	170	31.6	>200	Zielinski *et al.,* 1995

* D= Drilled Well, G= Groundwater (dug wells and springs), T= Tap water, DW= Drinking water, M= Mineral water.

Table 2.4: Concentrations of ^{226}Ra in groundwater from different Countries.

Nuclide	Country	Water Source	Number of Samples	Mean	Maximum	Reference
^{226}Ra (Bq L^{-1})	Finland	D	2700	0.06	49	Salonen & Huikuri 2002
		G	2200	0.01	2.0	Makelainen *et al.,* 2002
	Sweden	D	328	0.26	4.9	Isam Salih *et al.,* 2002
	Denmark	D	79	-	0.55	Ulbak & Klinder, 1984
	Ukraine	D	520	0.38	5.2	Zelensky *et al.,* 1993
	Switzerland	DW	360	<0.02	1.5	Deflorin *et al.,* 2004, UNSCEAR 2000.
	Switzerland	M	42	0.035	0.13	Deflorin *et al.,* 2004
	Spain	D	345	0.84	9.26	Fernandez *et al.,* 1992
		G	345	0.025	0.07	Fernandez *et al.,* 1992
		D	32	1.0	4.0	Soto *et al.,* 1988
	Germany	G + D	192	0.15	6.29	Gans *et al.,* 1988
	China	G + D	428	0.03	0.94	Zhou *et al.,* 2001
	Brazil	G + D	88	0.02	0.49	Almeida *et al.,* 2004
	France	G + D	54	0.08	0.53	Saumande *et al.,* 1973
	Slovenia	G	500	0.02	0.51	Kobal *et al.,* 1990
	United Kingdom	DW	-	-	0.18	UNSCEAR 2000
	Poland	D	6	0.104	0.33	Grzybowska *et al.,*1983
	Italy	DW	-	-	1.2	UNSCEAR 2000
	Maine (USA)	D	33	2.4	27	Smith *et al.,*1961

*D= Drilled Well, G= Groundwater (dug wells and springs), T= Tap water, DW= Drinking water, M= Mineral water.

1) = number of drilled well and dug well samples all together

2) = ^{238}U concentration is calculated from total activity concentration of (^{238}U and ^{234}U) using isotope ratio of 2 and factor 80.6 to convert Bq L^{-1} to µg L^{-1}

3) = geometric mean

4) = median

5) = median and maximum values are estimated from cumulative frequency diagrams

2.4.4 Activity concentration of natural radionuclides in Nigeria

The natural radioactivity levels in rocks depend on the type and location of rock formation. Rocks fall into three main divisions namely, the sedimentary formation, metamorphic and igneous rocks. Sedimentary rocks are derived from igneous rocks. Igneous rocks are composed mainly of silicates and free silica. The principal rock types are granite, granodiorite, diorite, syemite, basalt, eclogite, peridotite and dunite. In Nigeria, previous studies on radionuclides have been carried out in soil, bedrocks and water. Few of the reported works are discussed below.

The Gamma-emitting radionuclides in rocks and soils of Saunder Quarry site in Abeokuta, South-Western Nigeria were measured by Okeyedi, (2012). He concluded that the granite rock used for building and construction purposes from the study area would be rich in natural occurring radionuclides (NOR).

In the same studies above, the radioactivity levels of rock and soil and the corresponding external exposures in Navy Quarry site of the same area were determined. He concluded that the food crops grown on the soil of the study area will be rich in NOR.

In 2011, Gbadebo, determined the radionuclide distribution in the granitic rocks and soils of abandoned quarry sites, Abeokuta, South-western Nigeria and concluded that the observed radionuclides are based on local geology of the area and these radionuclides will serve as a possible source of radiation to the local quarry workers and nearby residents alike.

The radioactivity of Jos Tin mine tailing in Northern Nigeria was measured by Usikalu *et al*., (2011). It was however observed that the radionuclides can act as a source for external radon exhalation for those dwelling 500 m away from the site.

2.5 Groundwater Concept

Groundwater flows through porous media, fractured media, and large passage through weathered zones in subsurface terrain. Porous media consists of solid material and voids or pore spaces. Porous media contains relatively small openings in the solid materials as permeable which allows the flow of water through the media. The porous media that are of interest in groundwater flow includes natural soil, unconsolidated sediments, and sedimentary rocks. The size range of particles in soil is referred to as the soil texture. Grain size determines the particle size classification. The fraction of clay, silt, sand in soil texture has been described by soil texture triangle (US Soil Conservation Service, 1951). Each point on the triangle corresponds to different percentage by mass (weight of clay, sand and silt.

The subsurface occurrence of groundwater can be divided into vadose zone (zone of operation) and zone of saturation. The vadose zone, also called the unsaturated or partially saturated zone is the subsurface media above the water table. The term vadose is derived from the latin vadosus, meaning shallow. Groundwater originates through infiltration, influent streams, seepages from reservoirs, artificial recharge, condensation, seepage from ocean, water trapped in the sedimentary rock (connate water), and juvenile water (volcanic, magmatic and cosmic). Any significant quantity of subsurface water stored in subsurface formation defines an aquifer. An aquifer may be defined as a formation that contains sufficient saturated permeable material to yield significant quantities of water to well, (Lohman *et al.,* 1972). Aquifers are usually of large area extent and are essentially underground storage reservoirs. They may be overlain or underlain by confining bed, which is relatively impermeable material adjacent to the aquifer. Typical example of aquifers can be found in Figure 2.4.

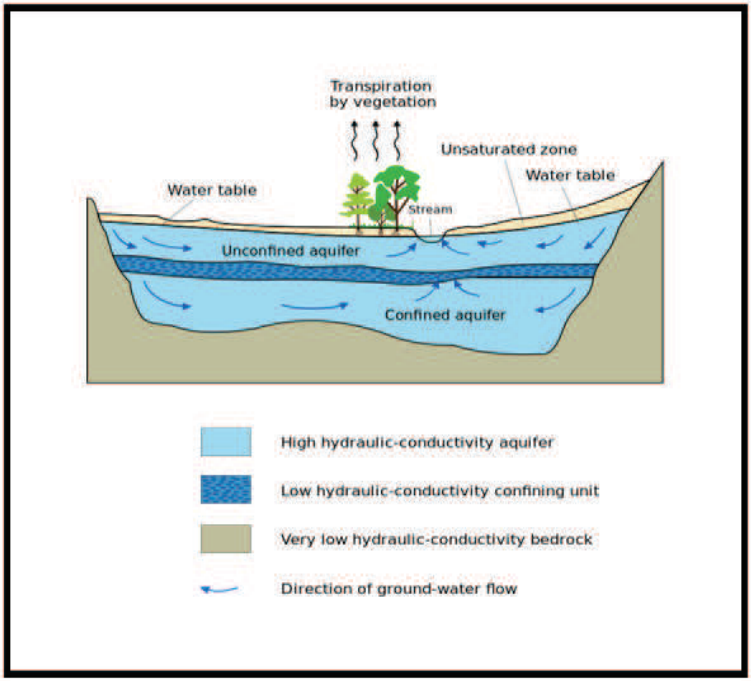

Figure 2.4 Typical flow directions in a cross-sectional view of confined and unconfined aquifers system (source:Wikipedia.org/wiki/aquifer)

2.5.1 Different Types of Confining Beds

Figure 2.4 indicates typical flow directions in a cross sectional view of a simple confined or unconfined aquifer system. The system shows two aquifers with one aquitard (a confining or impermeable layer) between them, surrounded by the bedrock aquiclude, which is in contact with a gaining stream (typical in humid regions). The water table and unsaturated zone are also illustrated. An aquitard is a zone within the earth that restricts the flow of groundwater from one aquifer to another. An aquitard can sometimes, if completely impermeable, be called an

aquiclude or aquifuge. Aquitards are composed of layers of either clay or non-porous rock with low hydraulic conductivity. Further explanation of different types of confining beds is shown below.

(1) Aquiclude: A saturated but relatively impermeable materials that do not yield appreciable quantities of water to well; clay is an example.

(2) Aquifuge: A relatively impermeable formation neither containing nor transmitting water; solid granite belongs in this category.

(3) Aquitard – A saturated but poorly permeable stratum that impedes groundwater movements and does not yield water freely to wells, but they may transmit appreciably water to or from adjacent aquifers and, where sufficiently thick, may constitute an important groundwater storage zone; sandy clay is an example. (Todd, 1980).

2.5.2 Aquifer Properties

Aquifer performs two important functions- a storage function and a conduit function. In order words, aquifer stores water and also functions as a pipeline. When water is drained from a saturated material under the influence of gravity, only a portion of the total saturated volume in the pores is released. Part of the water is retained in the interstices due to the losses of the molecular attraction, adhesion and cohesion. The specific yield S_y, which is the storage term for unconfined aquifers, is the volume of water drained from a saturated sample of the unit volume ($1ft^3$ or $1m^3$) with a point decrease in the water table. Specific retention Sr is the quantity of water that is retained in the unit volume after gravity drainage.

The sum of specific yield and the specific retention for saturated aquifers is the porosity, $\alpha = S_y + S_r$. Porosity is the pore volume divided by total volume expressed in percent. Porosity represents the potential storage of an aquifer, but does not indicate the amount of water a porous material will yield. The storagetivity (or storage coefficient) of an aquifer is the volume of water the aquifer releases from or

takes into storage per unit surface area of an aquifer per unit decline or rise of head, (Tiddo, 1980).

2.5.3 Hydraulic Conductivity

It is also referred to as (coefficient of permeability) is the property related to the function of an aquifer. It is the nature of ease of moving groundwater through aquifers, with dimension of $\left(L/T\right)$. The hydraulic conductivity, K is the rate of flow of water through a cross-section of a unit area of aquifer under a unit hydraulic gradient. The hydraulic gradient is the head loss divided by the distance between two points. The hydraulic conductivity is commonly expressed in gallon per day ft^{-3} or ft d^{-1} or m d^{-1} in SI unit.

2.5.4 Heterogeneity and Anisotropy of Hydraulic Conductivity

In geologic formations, the hydraulic conductivity usually varies through space, referred to as heterogeneity. A geologic formation is homogenous if the hydraulic conductivity is independent of position in the formation, ie $K\ (x, y, z) =$ constant. A geologic formation is heterogeneous if the hydraulic conductivity is dependent on position in the formation, $K\ (x, y, z) \neq$ constant. Hydraulic conductivity may also show variations with the direction of measurement at a given point in the formation. A geologic formation is isotropic at a point if the hydraulic conductivity is independent of direction of measurement at the point, Kx $= Ky = Kz$. A geologic formation is anisotropic at a point if the hydraulic conductivity varies with direction, $Kx \neq Ky \neq Kz$.

2.5.5 Groundwater Movement

Groundwater in its natural state is invariably moving and this movement is governed by hydraulic principle. The flow through an aquifer is expressed by darcy's law, which is the foundation of groundwater hydraulics.

2.5.6 Darcy's Law

Ground water flow can be described quantitatively by Darcy's Law which was derived empirically by Henry Darcy from his experiments in 1856 of water flowing through filter sands. Darcy observed that in a given sand, the flow increased directly proportional to the difference in hydraulic head and inversely proportional to the length of flow or the flow rate through porous media is proportional to the head loss and inversely proportional to the length of the flow part, expressed mathematically as

Darcy's Law in Figure 2.5 can be expressed one dimensionally as:

$$q = \frac{Q}{A} = -K\frac{dh}{dl} \tag{2.1}$$

where

Q = flow rate

A = cross-sectional area through which water flow occur (m^2)

q = specific discharge, or flow rate Q, through cross-section area A , meter per day ($m\ d^{-1}$)

K = proportionally constant ($m\ d^{-1}$)

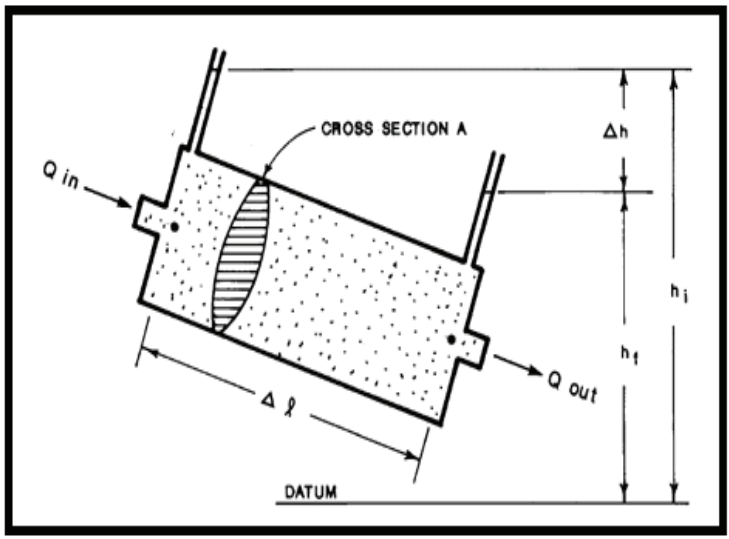

Figure 2.5 Darcy's experiment (after Freeze and Cherry, 1979)

However, it is important to realize that specific discharge is not the "speed" of ground water flow, but the flow per unit area. The average ground water velocity can be estimated by dividing the specific discharge, q, by the porosity, n:

$$- , \qquad (2.2)$$

where is the ground water or "Darcy" velocity.

2.6 Basement Terrain Groundwater in Nigeria

2.6.1 Groundwater occurrence in Basement Complex Rocks of Nigeria

Despite the favourable, large groundwater occurrence reported in the world over, the Nigerian situation appears to be restricted by the fact that more than half of the country is underlain by hard crystalline impervious rocks which are either igneous or metamorphic in origin. This rather extensive mass, of almost impermeable rocks underlies many of the semi-arid, and even the humid areas of the country, in which there is high scarcity of portable water. In these areas, therefore, a serious hydrogeological situation presents itself and water has to be found to meet the domestic, agricultural and industrial needs of the population (Offodile, 2002; Offodile, 1992; Offodile, 1975).

The hydrogeological characteristics of crystalline basement complex rocks in assessing the groundwater potential in Nigeria has the following hydrogeological sub provinces which is to be recognized:

(1) The younger granite complex area
(2) The metasediments, quartzites and schists complex area
(3) The older granite, migmatite and gneiss complex area.

2.6.2 The Older Granite and Gneisses Complex Area

The older granite, migmatite and gneissose rocks comprise the extensive mass of metamorphic rocks underlying most areas of the north and west of the country. The rocks include different textures of granites; coarse to fine, consisting

essentially of biotite, feldspars and quartz, which are indications of hydrogeological characteristics. While the coarse granites weathered into water bearing sandy residue, the syenitic rock types, with the predominance of unstable minerals eg. feldspars decompose into plastic or soft clays and other argillites which behave only as aquitards or aquicludes (Offodile, 2002; Offodile, 1992; Offodile, 1975).

Generally, only small amount of water can be obtained in the freshly unweathered bedrock below the weathered layers. Even when fractured, the clayey materials tend to seal the openings of the fractures and prevent water from being transmitted into the borehole (Offodile, 2002; Offodile, 1992; Offodile, 1975).

2.6.3 The metasediments, Quartzites and Schists Complex Area

It is difficult to distinguish the metasedimentary areas, as they often grade into the surrounding country rock which invariably are the older granite series. However, the hydrogeological properties depend on the texture of the metasediments, hence the schists and phyllites would be poor aquifers while the quartzites and pegmatites, where fractures would prevent opposite situations. It is not possible to describe case studies of these areas as no attempt has been made to distinguish the areas in borehole drilling programmes. However, the distinction is necessary for future programmes, to enable the determination of the hydrogeological area as a potential groundwater producing area (Offodile, 2002; Offodile, 1992; Offodile, 1975).

2.6.4 The Younger Granite/ Fluvio Volcanic Complex Area

The Younger Granite Complex comprises series of high level intrusive granite of different chemical compositions, within the basement complex. The

granitic series include alkali feldspar granite associated with rhyolites and minor gabbros and syenites. The emplacement of the rocks is preceded by a series of volcanic activities which is responsible for its peculiar geomorphologic and textural set up in Nigeria (Offodile, 2002; Offodile, 1992; Offodile, 1975)

2.6.5 The granite areas

The areas of extensive fracturing in Younger Granite often coincide with the broad depressions or valleys separating the areas of high relief. The Younger granite is characterized by a pronounced set of open joints which show a persistent northerly trend in the study area and contain a lot of water. As a result, shallow groundwater occurs almost everywhere in the decomposed zone overlying the fresh rock. This is extensively developed for domestic purposes by means of numerous boreholes and hand-dug wells (Offodile, 2002; Offodile, 1992).

2.6.6 Fluvio Volcanic Series

The fluvio volcanic series consists essentially of a series of hard, consolidated basalt bed, basalt boulders and decomposed basalt, often weathered to clay, invariably underlain by gravels or freshly weathered granite. The basaltic top is often lateritised. A typical setting is as recorded from Lugbe, using borehole sections and geophysical methods.

2.7 The Hydrogeologic System of Groundwater in Nigeria

The Nigerian hydrogeologic system is dominated by two main drainage systems, the Rivers Niger and Benue and their tributaries. Others are the braided north-south flowing rivers marking the coastline and emptying into the Atlantic Ocean, and the inland northeast network, rising from the middle northeast half of the country and feeding the Lake Chad. The Lake Chad, which is shared between Nigeria, Chad, Cameroon and Niger, is the only major inland water body in Nigeria in the northeastern corner of the country.

One of the main characteristic features of the rivers, in the Sahel region of the country, is the fact that they originate from the areas of, relatively, higher rainfall, invariably around the Jos Plateau and the Cameroon highlands. From the wet highland regions, the rivers flow over large expense of highly permeable and dry "thirsty" sandy land area before emptying into the Lake Chad or the upper part of the River Niger. The rivers are, therefore, very effective agents of recharge of the surface and underground waters, downstream; conveying water from areas of water surplus to areas of water deficit, (Schultz, 1976).

2.7.1 Groundwater Chemistry

The chemistry of water is determined by some constituents which occur in solution. These make up the major and minor constituents of water. The major constituents include elements of calcium, magnesium, sodium, potassium as cations and carbonates, bicarbonates, sulphates, chlorides and nitrates as anions. Other chemical constituents, occurring in low concentrations are boron, fluoride, silica, phosphate, sulphide, lithium and aluminum. The minor elements are generally not critical in the determination of the quality of groundwater (Offodile, 1975)

2.7.2 Groundwater classification in Nigeria

The chemical composition of groundwater in Nigeria varies considerably. The special characteristic in some hydrogeological environments are discussed below. However, on the basis of the chemical parameters, viz anionic and cationic concentrations, the groundwater in Nigeria can be classified into four groups as follows, (Offodile, 1976):

i. Predominantly calcium bicarbonate water
ii. Magnesium sulphate, sodium chloride calcium bicarbonate water
iii. Predominantly sodium chloride waters
iv. Magnesium sulphate water.

Most of the Nigerian groundwaters fall into this category of predominantly calcium bicarbonate water. The aquifers include carbonate rocks and sandstones in various stages of consolidation. But of interest, is the fact that most of Nigerian sandstone aquifers give high carbonate/bicarbonate chemical characteristics. Du Preeze (1975) made a similar observation about groundwater from Northern Nigeria. The observation could be attributed to the environment of deposition of the sands, and the matrix binding the sands being calcareous, or due to the infiltration of carbon dioxide rich rain-water derived from the atmosphere.

Some mine waters with a pH below 4 are known to have several hundreds to several thousands mg L^{-1} of Aluminum. Magnesium ions are mostly precipitated above pH of 10.5. The mobility of manganese, copper, vanadium and uranium is affected by the pH of the groundwater, though other processes, such as absorption, may be more effective in controlling their distribution (Du Preeze, 1975).

CHAPTER 3

METHODOLOGY

3.1 Introduction

Materials and methods used in this work were discussed according to the objectives proposed for this research. Firstly, for easy identifications of the study locations and the rocks that constitute the geology of the area were briefly discussed in this chapter.

3.1.1 The Study Area

The area of study forms part of the basement complex of North-Central Nigeria; with lithologic units falling under three main categories, which include: (1) Undifferentiated migmatite complex of Proterozoic to Archean origin, (2) Metavolcano-Sedimentary rocks of Late Proterozoic age and (3) Older Granite Complex of Late Precambrian - Lower Paleozoic age, also known as Pan-African Granites. All these rocks have been affected and deformed by the Pan-African thermotectonic event. Detailed reports of the lithological description, age, history, structure and geochemistry of the Basement Complex of Nigeria are given in Oyawoye, (1972), Black *et al*., (1979), Ajibade *et al.*, (1987), Rahaman, (1988), Caby, (1989), and Dada, (2008). Figure 3.1 is the geologic map of Nigeria with red arrow pointing the study area as part of the basement complex of Nigeria. The

accessibility map of the study locations is well represented in Appendix A indicating the points of VES. The geologic map of the study area and schematic 2D cross section is well represented in Appendix B.

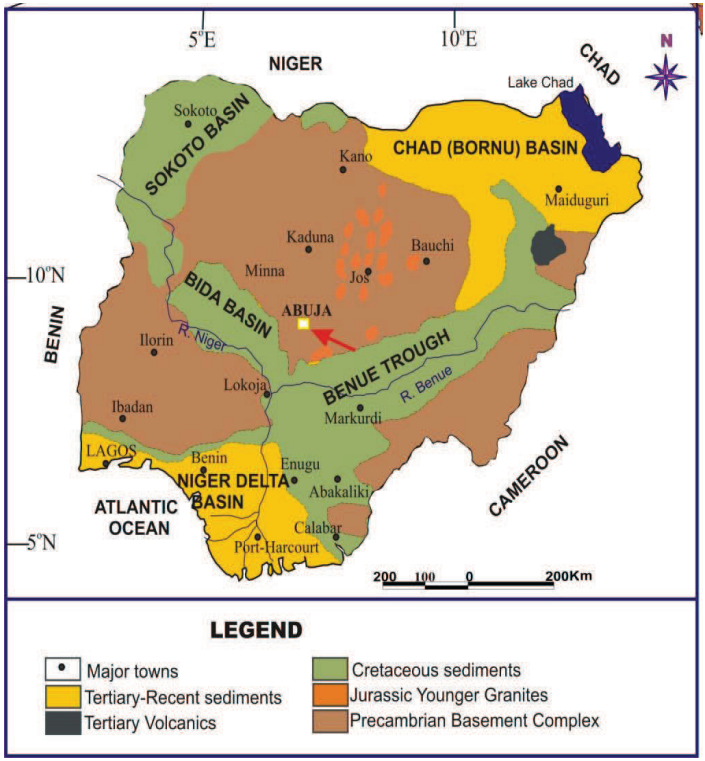

Figure 3.1 Geological map of Nigeria showing the position of Abuja (red arrow) in the basement complex of North Central Nigeria. (Modified from Obaje, 2009).

3.2 Materials and Methods for the Present Work

The methods used to materialize the aim of this research work are presented according to the objectives. They are as follows:

1) Geophysical survey using Vertical Electrical Sounding (VES) to determine the depth to the groundwater and lithological variation in resistivity.
2) Structural studied using Shuttle Radar Topography Mission (SRTM) data to map out the subsurface structures, joints and faults that control groundwater system and yields in the area
3) Modeling of groundwater movement and flow using MatLab.
4) Drilling of hydrogeologically motivated boreholes using 30 ton capacity Rig Machine attached to 25 ton capacity high pressure compressor made of INGERSOL.
5) Well log data (rock samples) collected sequentially with varying depth of about 70 m in Dei-Dei, 60 m in Kubwa, 50 m in Gosa and 40 m in Lugbe using hand-shovel with GPS for coordinate of the borehole point locations (GPS Model: Extrex 2000-2007).
6) Rock samples collected from the four boreholes accordingly were subjected to radionuclei analysis using High Purity Germanium Gamma spectrometer (HPGe)
7) The rock samples were also selected for geochemical characteristics using X-ray fluorescence (XRF) analysis.
8) The water samples collected from the same four boreholes drilled, hand-dug well and public water supply from the study area were analysed for activity of radionuclides and toxic elements using Inductively Coupled Plasma Mass Spectrometry (ICP-MS).

3.2.1 Geophysical Investigation

The search for groundwater in the study area was done by conventional method using Vertical Electrical Sounding (VES) for aquifer characterisation, depth to

basement terrain groundwater and integrated with Shuttle Radar Topography Mission (SRTM) for mapping out structures that control the groundwater system. The combination of both methods revealed detailed groundwater information in the study area especially at Gosa borehole.

3.2.2 Vertical Electrical Sounding (VES)

The search for groundwater was carried out through the use of electrical methods of near surface geophysical survey. The Schlumberger configuration in vertical electrical sounding (VES) was used to obtain field data. VES probes the vertical variation in resistivity of the subsurface, thereby indicating the presence of fluid and ionic concentration in the subsurface materials (Reynolds, 2011). VES also determine the depth to bedrock, delineate the various units that constitute the overburden (regolith), determine the degree of fracturing of the bedrock; all of which would help in making the choice for a feasible site for constructing a successful borehole. Figure 3.2 shows the simple configuration used for field data in this work (Schlumberger configuration). VES data for this work were obtained using the Allied OmegaC2 Terrameter as shown in Figure 3.3. The field data obtained was presented as curve of apparent resistivity values against half of the current electrode separation (AB/2) in metres on a log-log scale. The VES data obtained were analyzed using the WINRESIST 2004 Version computer software to improve the quality of the interpretation by iteration and modeling to goodness of fit. The practical field data acquisition using Schlumberger array of VES method is shown in Figure 3.4. The details of the results were discussed in Section 4.2.1 and 4.2.2 respectively.

From Figure 3.2, the mathematical application for the determination of apparent resistivity is derived.

$$V = U_M - U_N = \frac{\rho I}{2\pi}\left[\frac{1}{AM} - \frac{1}{BN} + \frac{1}{BN} - \frac{1}{AN}\right] \tag{3.1}$$

where,

U_M and U_N = potentials at M and N

AM= distance between electrodes A and M, etc

$$- \quad - \quad , \tag{3.2}$$

where is apparent resistivity

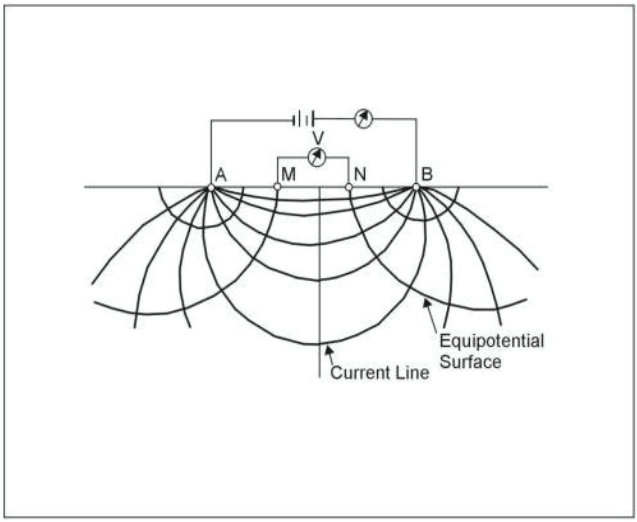

Figure 3.2 The Schlumberger array for resistivity measurements using pair of electrodes A and B lines for a pair of equipotentials on a half-space.

$$-\left[- \quad - \quad - \quad -\right] \tag{3.3}$$

$$- \tag{3.4}$$

= Current across A to

where K is the geometric factor which depends on the arrangement of the four electrodes and the lithology of the formation. Resistivity meters normally give a resistance value, $R = {}^{V}/_{I}$, so in practice the apparent resistivity value is calculated as stated in Equation 3.4. To determine the true subsurface resistivity, an inversion of the measured apparent resistivity values using a computer program must be carried

out. Instrument readings (current and voltage) are generally reduced to "apparent resistivity" values. The apparent resistivity is the resistivity of the half-space which would produce the observed instrument response for a given electrode spacing. Apparent resistivity is a weighted average of soil resistivities over the depth of investigation. For VES, a log-log plot of apparent resistivity versus electrode separation is obtained. This is sometimes referred to as the "sounding curve. The theoretical response is then compared with the observed field response and differences between the observed and the calculated were noted. The hypothetical earth model is then adjusted to create a response which more nearly fits the observed data. When this iterative process is automated it is referred to as "iterative inversion" or "optimization.

Figure 3.3 Campus OmegaC2 Terrameter

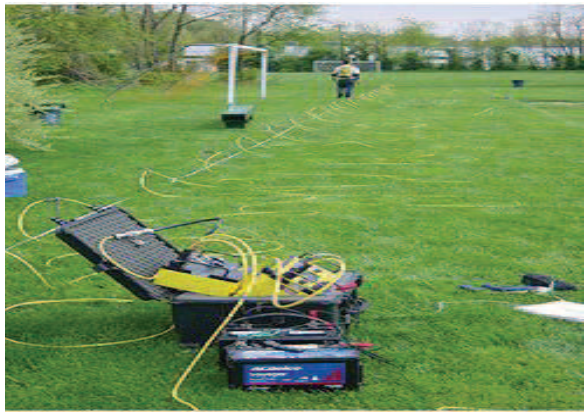

Figure 3.4 Practical field work using Campus Omega C2 resistivity for VES data acquisition

3.2.3 Shuttle Radar Topography Mission (SRTM)

The conventional method of geophysical survey using Vertical Electrical Sounding (VES) could not solve the problem of detailed subsurface information of water-rock interaction and low yield of borehole production in some parts of the study area, (e.g. Gosa) and groundwater sample is needed for radionuclides and toxic elemental studies for this present study. Moreso, the inhabitant's demand for water supply is on the increase for lack of explorable groundwater with good yield in the area (Gosa). A combination of conventional method (VES) with SRTM was used to actualize the objective of subsurface structural mapping and structural trends of fractures that control the groundwater system.

The Shuttle Radar Topography Mission (SRTM), a single pass interferometry mission flown in February 2000, generated elevation data at 90 m resolution for 80% of the Earth's surface in C-band. The SRTM-DEM data was downloaded from the

website: http://srtm.csi.cigar.org/ and subjected to hill-shading procedure using Idrisi 32 software to enhance linear features that could be major regional fractures. The analytical hill-shading algorithm in Idrisi32 is used to create the hill-shading image with the Sun azimuth angle set to 315^{o} (NW) and the Sun elevation angle set to 30^{o}. The lineaments were extracted and digitized on screen to create a lineament map and the lineament directions plotted on a rose diagram using GEOrientVer 9.5.0 software. The data used in this study was extracted in the SRTM-DEM as shown in in Appendix A. The details of the SRTM results were discussed in Section 4.2.3.

3.2.4 Application of SRTM

Application of remotely sensed data for groundwater investigation is becoming increasingly popular, especially in areas where conventional methods are inadequate in accurately demarcating hydrologic zones. Examples include the works of Galnett and Gardner, 1979; Edet, *et al.,* 1994; Bala *et al.*, 2000; Bala 2001. In a few case studies, it has successfully complemented conventional geophysical investigations (Goki *et al*., 2010; Anudu *et al.,* 2011). The use of Shuttle Radar Topographic Mission – Digital Elevation Model (SRTM-DEM) data for hydrogeologic studies has been reported in other parts of the world (Wright *et al.,* 2006; Valeriano *et al*., 2006; Grohmann *et al.*, 2007; Abdullah *et al.,* 2012; Maxwell et al., 2013a; Maxwell *et al.,* 2014). These reports show the reliability of SRTM for geophysical survey in structural studies and hydrogeologic studies.

3.2.5 Drilling of Borehole

The purpose of the borehole drilling in this research work was to collect different rock layer samples accordingly to the depth of the aquifer and equally groundwater samples. The boreholes were drilled with the help of 30 ton capacity Rig machine attached with high pressure compressor made of INGERSOL of 25 ton

capacity. The rocks were from clay and sand, and the medium was heterogeneous as the thickness of the different layers differed in the borehole. The cutting method of technical procedure (TP-8.0, Rev. 15, 2003) was used in this work. Figures 3.5a, 3.5b, 3.5c and 3.5d (Dei-Dei, Kubwa, Gosa and Lugbe) show typical drilling method of cuttings for rock sample collections in the study area for this present work.

(a)

(b)

(c)

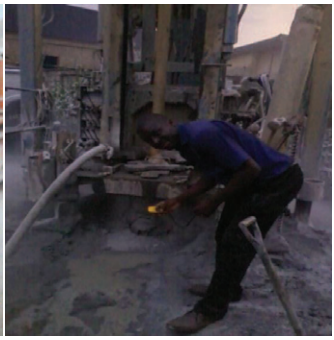

(d)

Figures 3.5 Drilling Point at the sites in Abuja, Nigeria (a) Dei-Dei, (b) Kubwa, (c) Gosa and (d) Lugbe boreholes

3.2.6 Sample Inventory

The identification of boundaries between layers with noticeably different particle sizes using visual manual logging method and record the thickness when the layer changes. Layer thickness change may range from less than one metre to tens of metres. Each layer was measured into the plastic bag accordingly. After boundary of distinct layers has been clearly marked on plastic bag with an indelible felt-tipped pen (Marker), the following records were documented for easy identification of each sample and the collection point.

(a) The date of the sample collections and the initials of the logger were recorded.
(b) The sample type for the rock samples, "SL" to designate a geologically logged core segment, Site and Layer type for SL were also recorded
(c) The depth interval for each layer (thickness) was recorded
(d) The layers were photographed digital camera.

The selected drilling sites for this research work are Dei-Dei, 70 m; Kubwa, 60 m; Gossa, 50 m and Lugbe 40 m borehole sites.

- **Dei-Dei borehole/site one (S1):** Eleven samples were collected from the drilling of site one (S1L1 to S1L11).
- **Kubwa borehole/site two (S2):** Nine samples were collected from the drilling of site two (S2L1 to S2L9).
- **Gosa borehole/site three (S3):** Six samples were collected from the drilling of site three (S3L1 to S3L6).
- **Lugbe borehole/site four (S4):** Five samples were collected from the drilling of site four (S4L1 to S4L5). In addition, labelled properly using borehole number and depth on each sample plastic bag.

At Dei-Dei borehole area, eleven rock samples were collected below ground level (blg) to a depth of about 70 m. The samples were labeled S1L1 to S1L11 indicating site one layer one to site one layer eleven below ground level. The samples collected according to layer variations in lithologies are presented in Table 3.1. The

drilling point coordinate, lat. 9^{o} 6'52"N and long.7^{o} 15'39"E, using GPS, Model: Extrex High Sensitivity 2000-2007 Garmin Ltd.

Table 3.1: Depth and lithologic unit of Dei-Dei borehole site

Sample ID	Depth (m)	Thickness (m)	Lithology Description
S1L1	0-4	4	Sandstone, brownish and ferruginous, interbedded with quartz feldspar
S1L2	4-10	6	Coarse sand with clay, bright red.
S1L3	10-11.3	1.3	Slightly micaceous Sandy clay, brownish pebbly, fine to coarse feldspar.
S1L4	11.3-18.5	7.2	Fin to coarse sandy clayey and gravel
S1L5	18.5-24	5.5	Sand. Brown, clayey at the top, fine to coarse
S1L6	24-33	9	Light grey coarse sand, granite gravel
S1L7	33-45	12	Silty sand feldspar, blackish to grey
S1L8	45-49	4	Grey silty sand, low grade
S1L9	49-57	8	Greyish to Purple silty sand
S1L10	57-64.5	7.5	Sand, fine to coarse, pebbly blackish to grey
S1L11	64.5-71.7	7.2	Sand, fine to medium-grained, blackish to grey becoming whitish from 69m

In the same way, at Kubwa borehole area, nine rock samples were collected below ground level (blg) to a depth of about 60 m. The samples were labeled S2L1 to S2L9 indicating site two layer one to site two layer nine below ground level. The

samples collected according to layer variations in lithology are presented in Table 3.2. The drilling point coordinate, lat. 9^{o} 6'16.7" N and long. 7^{o} 16'26.0"E, using GPS, Model: Extrex High Sensitivity 2000-2007 Garmin Ltd.

Table 3.2: Depth and lithologic unit of Kubwa borehole site.

Sample ID	Depth (m)	Thickness(m)	Lithology Description
S2L1	0-7	7	Brownish ash sandy clay gravely interbedded.
S2L2	7-13.4	6.4	Clay with bright red.
S2L3	13.4-21	7.6	Sandy clay micaceous, brownish with feldspar.
S2L4	21-29	8	Fine to coarse sandy clayey and gravel smoky
S2L5	29-36.4	7.4	Clay sandy, fine grain size, darkish ash feldspar
S2L6	36.4-43	6.6	Silty clay, interbedded, bright ash to glacy feldspar.
S2L7	43-44	1	Fine to coarse ashy sandy clay.
S2L8	44-51	7	Fine to coarse sand, greyish.
S2L9	51-61.1	10.1	Micaceous - gravely sandy, fine-medium coarse darkish to grey.

At Gosa borehole area, six sequential rock samples were collected below ground level (blg) to a depth of about 50 m. The samples were labeled S3L1 to S3L6 indicating site three layer one to site three layer six below ground level. The samples collected according to layer variation in lithology are presented in Table 3.3. The drilling point coordinate, Lat: 8^{o} 56' 45.6" N and Long: 7^{o} 13' 26.2" E, GPS- Model: Extrex High Sensitivity 2000-2007 Garmin Ltd) was used for determining the coordinates.

Table 3.3: Depth and lithologic units of Gosa borehole site.

Sample ID	Depth (m)	Thickness (m)	Lithology Description
S3L1	0-4	4	Sandy clay, reddish brown laterite top soil.
S3L2	4-10	6	Sandy clay, fine to medium, reddish to yellow.
S3L3	10-11.3	1.3	Clay sandy feldspar Yellowish brown pebbly
S3L4	11.3-18.5	7.2	Micaceous clayey, grey to black
S3L5	18.5-24	5.5	Sandy shinny greyish to black feldspar.
S3L6	24-33	9	Fine medium shinny, qartz interbeded, greyish ash feldspar

The last borehole drilled for this study at Lugbe area which was about 40 m deep. Five rock samples were collected below ground level (blg) and were labeled accordingly ranging from S4L1 to S4L5. The label identifies the samples as site four layer one to site four layer 5 (S4L1 to S4L5), respectively. The samples collected according to layer variation in lithology are presented in Table 3.4. The drilling point coordinate (lat: 8^{o} 59' 2.3" N and long: 7^{o} 23' 7.8"E), GPS- Model: Extrex High Sensitivity 2000-2007 Garmin Ltd) was used for determining the coordinate. All these drilled rock samples and information will be subjected for further analysis in this research work.

Table 3.4: Depth and lithologic unit of Lugbe borehole site.

Sample ID	Depth (m)	Thickness (m)	Lithology Description
S4L1	0-7	7	Laterite topsoil, yellowish brown
S4L2	7-16.8	9.8	Sandy clay, fine to coarse, brownish yellow.
S4L3	16.8-27	10.2	Clayey sandy, brownish ash, fine grain feldspar
S4L4	27-39	12	Sandy maicaceous, grey, interbedded with quatz feldspar
S4L5	39 -40	1	Fine to coarse, ashy to grey

3.3 Sampling and Sample Preparation for Gamma Ray Spectrometry Analysis

3.3.1 Rock Samples

A total of thirty one (31) samples collected from boreholes lithologies in Dei-Dei, Kubwa; Gosa and Lugbe were dried under the ambient temperature of 25-29^{o}C for some weeks and sealed back into the plastic sock in Nigeria. They were transported from Nigeria to Universiti Teknologi Malaysia, Nuclear Laboratory. The samples were first dried at 105^{o}C each overnight with two different ovens made of Jouan of Japan and Memmert, model Schutzart Din 40050-IP20 made in Western Germany, crushed with the help of Bico Pulverizer MFD by Bico Inc. UA Burbank, California. After crushing of each sample, high pressure compressor air with nozzle pipe was used to flush the remnant on the crushing machine and cleaned with tissue

to avoid cross-contamination before adding another sample. It was crushed to powder and passed through 250µm sieve mesh with the help of sieve shaker made by EFL 2000R and IMK11 Ende Cott Ltd, England. All the crushing and sieving were carried out in Applied Geophysics laboratory, Faculty of Petroleum, UTM, Johor Bahru. The oven used in this work to dry the rock samples at 105^{o}C is shown in Figure 3.6.

Figure 3.6 Ovum for drying the rock samples at Nuclear Lab. UTM (made of Jouan by Japan)

After drying the samples overnights, they were taken to the crushing machine which was set to the required sample size of 250 µm. The crushing machine used is shown in Figure 3.7

Figure 3.7 The rock sample crushing machine was set at 250 µm sizes in Applied Geophysics Lab., UTM (made by Bico Pulverizer MFD, Bico Inc. UA Burbank California)

Each rock sample was crushed to the size of 250 µ for this study was further passed through sieve shaker machine to achieve the required sample size of powdered form by using the sieve mesh. The sieve shaker machine is shown in Figure 3.8.

Figure 3.8 Sieve shaker machine sieving crushed rock samples through sieve mesh of 250 µm.

During crushing and sieving, to avoid cross contamination of the samples either on the sieve mesh or crushing machine, a high pressure air compressor was used to flush the residue of the samples on the body parts. The air compressor is shown in Figure 3.9

Figure 3.9 The high pressure air flushing machine that keeps the sieve mesh and crushing machine clean at each use to avoid cross-contamination of rock samples.

After sample sieving, it was temporarily put into the plastic bottle and labeled according to sample layers and the borehole site as shown in Figure 3.10 for easy identification before transferring to marinelli beaker to achieve secular equilibrium and for gamma counting.

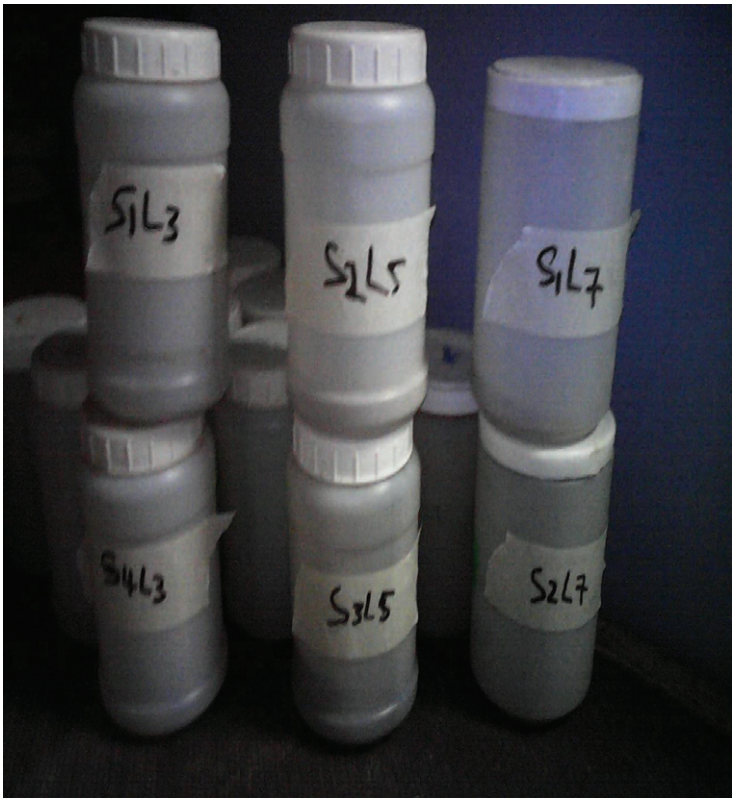

Figure 3.10 Temporary plastic bottle containing each sieved rock sample labeled according to sample site and layers.

3.3.2 Gamma-ray Detector –High Purity Germanium (HPGe)

Most semiconductor radiation-detectors are built around a p^{+}– I – n^{-} diode. The diode consists of a heavily p-doped material (p^{+}), an intrinsic material (i) and heavily n-doped material (n^{-}). Trivalent impurities are built into the p-doped

material, so this material has an excess of hole. The n-doped material has pentavalent impurities built in, which results in an excess of electrons. The intrinsic material, germanium, is a material with a very high degree of purity. These germanium diode detectors are referred to as High Purity Germanium-detector (HPGe).

When the n–type crystal an\d p^+–type material are brought into contact, the charge carrier will migrate over the junction; the electron migrate to p^+–material, the hole migrate to n- material. The combined effect of these migrations is a negative space charge on the p^+ –side and a positive space charge on the n^- –side of the junction. The space charge causes an electric field over the junction which opposes further migration of charge carriers. The zone over which the electric field extends has a very low density of charge carriers (± 100 charge carriers per cm^3) and is called the depletion zone. Because of the presence of the electric field in this zone, electron-hole pairs created within the depleted zone will be swept out, driving the electrons to the n^-–type material and the holes to the p^+–type material. However, only a small part of the detector will be depleted. Therefore, a reverse bias-voltage is applied which has a two-fold effect on the performance of the detector; it will increase the active volume of the detector and it will also speed up the charge collection.

As semiconductor detector, the primary electron (created by any of the gamma interactions) is slowed down creating electron-hole pairs. The number n of electron-hole pairs created in a semiconductor material is proportional to the deposited γ-ray energy E_{dep} according to:

$$n = \frac{E_{dep}}{E_{eh}} \tag{3.5}$$

with E_{eh}, the average energy required to create an electron-hole pair, which is in the order of a few eV only. Since only a few eV is needed to create information carriers in a semiconductor (in contrast to the approximately 30 eV in a scintillation detector) the number of information carriers is much larger in a semiconductor detector.

3.3.3 Gamma Ray Detection System for this Study

Experiments were carried out using the gamma ray spectrometry facilities at the Nuclear Lab. Faculty of Science, Universiti Teknologi Malaysia as shown in Figure 3.11. A high resolution spectrometer was used for the measurement of the gamma energy spectrum of emitted gamma-rays in the energy range between 50 keV and 2000 keV. The gamma ray spectrometry consists of a high purity germanium (HPGe) detector with a counting efficiency of 20%, a resolution of 1.8 keV for 1332 keV gamma ray emission of ^{60}Co. The detector used in gamma ray measurements was Canberra GC2018 with Genie-2000 software. The gamma detector was cooled by liquid nitrogen at 77 K for the purpose of reducing leakage current and thermal noise, and its warm-up sensor is coupled to the high voltage detector bias supply. The pre-amplifier was placed inside a lead shield to reduce background radiation (Tsoulfanidis, 1995). The decay isotopes, gamma energy and gamma disintegrations are shown in Table 3.5. The decay isotopes of gamma-ray energy and the block diagram of HPGe operation is shown in Figure 3.12 and 3.13, respectively

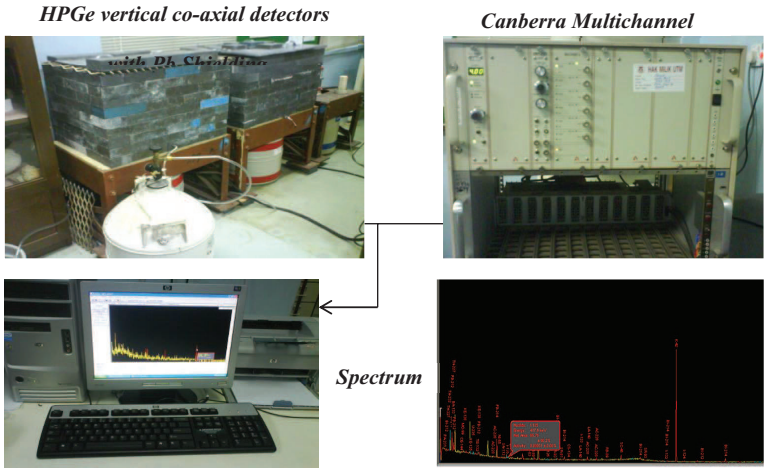

Figure 3.11 Set of Gamma Spectrometer (Counting and Analysis)

Table 3.5: The decay Isotopes, Gamma-ray Energy and Gamma disintegration

Radioactive Series	Decaying Isotopes	Gamma-ray Energy (keV)	Percentage of Gamma Disintegration (%)
Uranium	^{214}Pb (for ^{238}U decay series) ^{214}Bi (for ^{238}U decay series)	352.0 609.4	35 43
Thorium	^{208}Tl (for ^{232}Th decay series) ^{228}Ac (for ^{232}Th decay series)	583.1 911.1	30 29
Kalium	K	1460.8	100

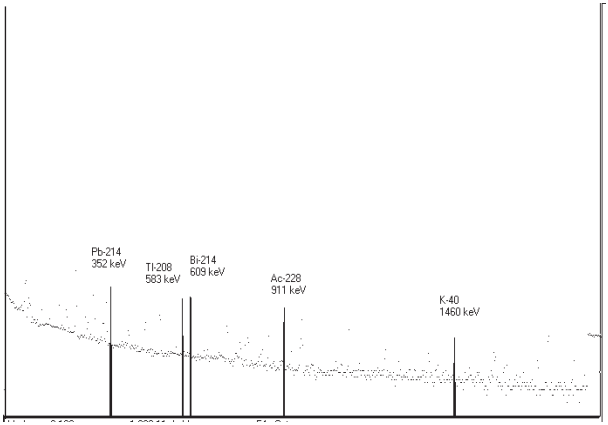

Figure 3.12 Gama energy spectrums of isotopes of natural occurring radionuclides

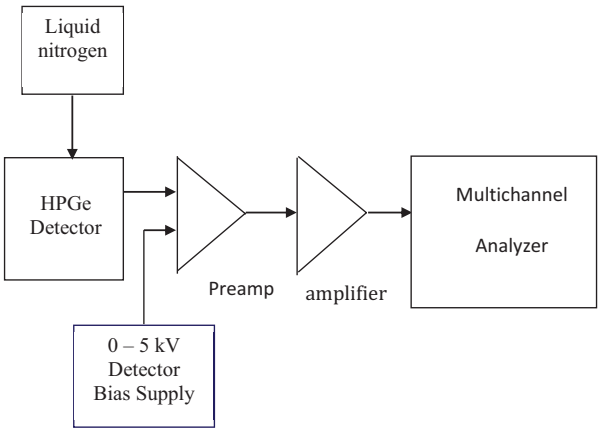

Figure 3.13 Block diagram of the HPGe detector spectrometer.

3.3.4 Standard Sample Preparation for Gamma Spectrometry

The IAEA standard sample Thorium Ore (S-14) and Lake Sediment (SL-2) were used as reference materials and mixed with SiO_2 in Marinelli beakers. The uranium and Thorium contents from S-14 are 29 ppm and 610 ppm respectively. A weight of 20.00 g from Sample IAEA S-14 was thoroughly mixed with 100.00 g of SiO_2 in a Marinelli beaker (Coded as S-14). After mixing with SiO_2, the uranium and thorium concentrations are 4.63 ppm and 97.3 ppm respectively. The IAEA standard sample SL-2 was used to calculate the specific activity of potassium (K). It has a specific activity of 240 Bq kg^{-1}. Another Marinelli beaker contains a weight of 74.18 g of SL-2 was mixed with 100.00 g of SiO_2 (Coded as SL-2). This provides background for standard samples. The IAEA standard samples used in this study are presented in Table 3.6. Figure 3.14 presents the prepared standard samples used for this study. The calculation of IAEA standard samples used is shown in Appendix B.

Table 3.6: IAEA standard samples used in this study

Standard Sample Code	**Concentrations**		
	U (ppm)	**Th (ppm)**	**K (Bq kg^{-1})**
S-14 (Thorium ore)	29	610	-
SL-2 (Late sediment)	-	-	240

Figure 3.14 Standard Sample (IAEA) for S-14 (Thorium ore) and SL-2 (Lake sediment) prepared for gamma analysis

3.3.5 Measurement of Gamma-ray Radioactivity from Dei-Dei, Kubwa, Gosa and Lugbe Borehole Rock Samples

A total of thirty one (31) samples collected were dried under the ambient temperature of 25-29^{o}C for some weeks and sealed back into the plastic sock in Nigeria. It was crushed to powder and passed through 250μm sieve mesh with the help of sieve shaker. The fine powdered samples were homogenized, and carefully weighed using an electronic balance with a sensitivity of 0.01g. The powdered samples were sealed in standard 500 mL Marinelli beakers and labelled accordingly with an indelible marker. The samples were sealed and stored for four weeks to achieve secular equilibrium between radium and its progeny (Alnour *et al* 2012; Ibrahim, 1993, Maxwell *et al* 2013a; Maxwell *et al.* 2013b).

Under the conditions of secular equilibrium, ^{232}Th concentration was determined from the average concentration of ^{208}Tl using the 583 keV peak and ^{228}Ac by using the 911 keV peak. ^{238}U was determined from the average concentrations of the ^{214}Pb by using the 352 keV peak and ^{214}Bi by using the 609 keV peak (Hamby and Tynybekov, 2002; Alnour *et al.,* 2012; Maxwell *et al.* 2013a; Maxwell *et al.* 2013b). The 1460 keV peak was used to determine the concentration of K. Each sample was put into a shielded HPGe detector and measured for 21600 s. The background gamma-ray spectrum of the detection system was determined with an empty Marinelli beaker under identical conditions, and was subtracted from the spectra of each sample. The specific activity was determined by comparing with IAEA standard samples S-14 (Thorium ore) and SL-2 (Lake Sediment). The samples prepared for gamma-ray counting are shown in Figure 3.15.

Figure 3.15 Prepared samples for Gamma counting after 4 Weeks secular equilibrium

3.3.7 Calculation of the Concentration of ^{238}U, ^{232}Th and K

Calculations of count rates for each detected photopeak and radiological concentrations (activity per unit mass) of detected radionuclides depend on the establishment of secular equilibrium in the samples. Due to smaller life-time of the radionuclides in the decay series of ^{238}U and ^{232}Th, the ^{238}U concentration was determined from the average concentrations of the ^{214}Pb at 352 keV and ^{214}Bi at 609 keV in the sample, and that of ^{232}Th was determined from the average concentrations of ^{208}Tl at 583 keV and ^{228}Ac at 911 keV decay products (Hamby and Tynybekov, 2000). Thus, an accurate radiological concentration was determined. The concentration of K was based on 1460 keV peak.

The concentration of uranium, thorium and the specific activity of potassium in the rock samples were calculated using the formula stated in Appendix C.

3.4 Neutron Activation Analysis (NAA) Method

The NAA method was used to compare the results for uranium and thorium measured by direct method (gamma spectrometry). Comparison of the results was discussed in Section 4.4.1. The results obtained will serve as verification of the direct method for this work.

3.4.1 Sample Preparation for NAA

Few samples were prepared and sent to Nuclear Malaysia Agency (NMA) for irradiation using TRIGA MARK II reactor. Approximately 0.15-0.2 g from each sample was prepared in a polyethylene vial, labelled and sealed. Each sample has

duplicates to ensure quality of the analytical technique, completely homogegenized to check errors that can happen during sample preparation.

A uranium-thorium standard solution of 100 ppm U and 98 ppm Th was used. Approximately, 0.1000 g (ml) U-Th solution was mixed with small amount of Silica (Si_2O-IAEA) in a vial (2.5 ml) and placed in an oven for 4 h at 60 °C until dry; then the vial was labelled and sealed. The details of the results were discussed in Section 4.4.1.

3.4.2 Sample Irradiation

Each batch of sample together with the reference standard sample and an empty vial (blank) was attached with Au wire and Zr foil monitor to determine the neutron flux parameters simultaneously with the sample. However, the Au wire also used to correct flux differences between each sample and standard or blank sample.

Each batch of sample together with the reference standard sample were irradiated for 6 h simultaneously at a neutron flux of 2.15 x 10^{12} n $cm^{-1}s^{-1}$ at PUPATI TRIGA MARK II reactor (Auu, 1998) operated at 750 kW power. After approximately 3 days radioactive decay (to allow interfering activities to decay away) of the samples, blank and reference standard sample were counted for 3600 s on the gamma detection system.

3.4.3 Calculation of Element Concentration

The procedure generally used to calculate the concentration (i.e., ppm of element) in the unknown sample is to irradiate the unknown sample and a comparator standard containing a known amount of the element of interest together

in the reactor. If the unknown sample and the comparator standard are both measured on the same detector, then one needs to correct the difference in decay between the two. One usually corrects the measured counts (or activity) for both samples at the end of irradiation using the half-life of the measured isotope. The equation used to calculate the mass of an element in the unknown sample relative to the comparator standard is

$$\frac{A_{samp}}{A_{std}} = \frac{m_{samp}(e^{-\lambda T_{dsamp}})}{m_{std}(e^{-\lambda T_{dstd}})} \tag{3.6}$$

where

A_{samp} = activity of the sample

A_{std} = activity of the standard sample

m_{std} = mass of the standard sample

m_{samp} = mass of the sample

λ = decay constant for the isotope

T_d = decay time.

When performing short irradiation, the irradiation decay and counting times are normally fixed for all the samples and standards such that the time factors cancel. Thus the above equation simplifies into

$$C_{samp} = \frac{C_{std}\ W_{std}}{W_{samp}} \tag{3.7}$$

where

C_{samp} = concentration of the sample

C_{std} = concentration of the standard

W_{std} = weight of the standard sample

W_{samp} = weight of the sample

3.4.4 Determination of the Concentration of ^{238}U and ^{232}Th.

The concentration of ^{238}U and ^{232}Th are based on the photopeaks of ^{239}Np at 277.9keV and ^{233}Pa at 311.9 keV obtained from NAA respectively. The concentrations were determined in parts-per million (ppm) units. The half-life and the energy lines are shown in Table 3.7. ^{233}Pa peak at 311.9 keV has an interference peak of ^{239}Np at 315.7 keV.

Table 3.7: Nuclides formed by neutron capture, Adams and Dam, (1969)

Element	Isotope	Production	Half-life (days)	Energy (keV)
Uranium	^{239}Np	^{238}U (n, γ, β^-)	2.34	277.9
Thorium	^{233}Pa	^{232}Th (n, γ, β^-)	27.4	311.9

3.5 X-ray analysis of the major oxides in the rock samples from the study area

A total of thirty-one (31) samples were chemically analysed in Environmental Analysis Laboratory, Department of Water and Environmental Engineering, Faculty of Civil and Environmental Engineering, Universiti Tun Hussein ONN Malaysia on 15th of July, 2013 for the major oxides such as SiO_2, Al_2O_3, Fe_2O_3, CaO, MgO, MnO, K_2O, Na_2O, P_2O_5, TiO_2, CO_2, SO_3, BaO and ZrO_2 using X-ray fluorescence (XRF) technique attached to Geo quant M software. Certified reference material soil (CRM) provided by Institute of Geophysical and Geochemical Exploration (Langfang, China) coded: GBW07406 (DC73324) has been used to standardised the XRF fluorescence analysis system; reference material date of certification: 1986;

modification: 2003 and expiration: 2013. It is mainly used in geology, mineral reconnaissance, agriculture and related fields for carrying out chemical analysis as calibration samples and for monitoring the quality of measurements.

The reference material was used for checking of the consistency of the recommended values in relation to the time of the calibration. Raw material (rock samples/soul samples) was dried in an oven at 105^{o}C for 24 hours and crushed at 350 rpm (rotation per minute) for 5 to 10 minutes. The crushed samples were passed through a sieve mesh of 50 µm. 7 g of sieved sample was added to 3 g of lico wax (as binding agent) and were further dried, homogenised and pulverised, and then compressed into pellets with the help of machine (Model PE Man) to pelletize the mixture at about 8 x 10^4 N (80 kN). The geometry differences, particle size effects and inhomogeneity problems could have been eliminated. From the certified reference material, two samples were taken and measured several times to check the time correlation and standard values recovery. The pellet samples were subjected to XRF chamber (Model: Bruker Pioneer S4 WDXRF) machine to get the percentage composition of elements in the soil samples for about 45 minutes each. The block diagram of the Bruker S4 pioneer (WDXRF) and the complete setup of Bruker Pioneer S4 WDXRF are shown in Figure 3.16 and 3.17, respectively. Both the prepared samples and standard reference material soil, GBW07406 (DC73324) for X-ray analysis are shown in Figure 3.18. The results are discussed in Section 4.5.

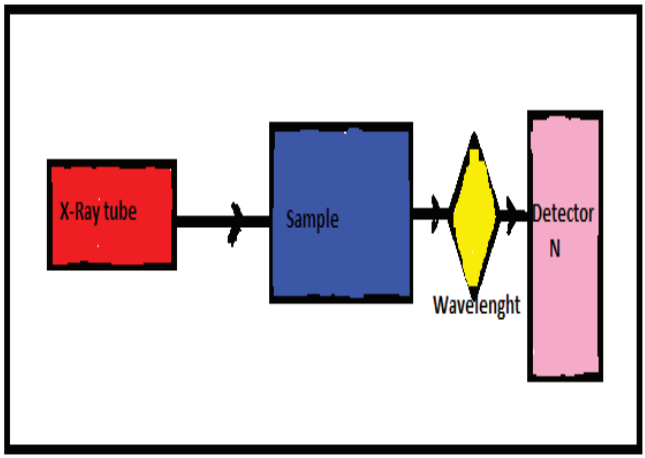

Figure 3.16 Block diagram of bruker pioneer S4 WDXRF

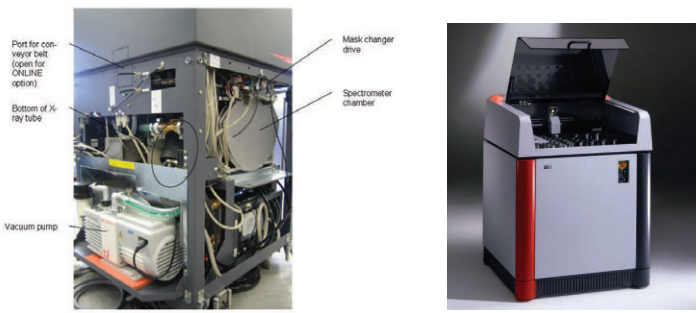

Figure 3.17 Bruker Pioneer S4 WDXRF side panel and complete setup

Figure 3.18 Prepared rock samples for X-ray analysis and the standard reference material

3.6 ICP-MS Experimental and Analytical Method for Groundwater Samples

3.6.1 Materials and Reagents for Inductively Coupled Plasma Mass Spectroscopy (ICP-MS)

This study was to determine the radioactivity level and toxic elements in groundwater used for human consumption on an extended area in four satellite towns, Dei-Dei, Kubwa, Gosa and Lugbe boreholes, thus, compare with public water supply (water board collected at Area 10 Garki Tap water) and hand dug well from Dei-Dei, 500 m away from Dei-Dei borehole point, all in Abuja, Northcentral Nigeria. Samples were collected from the boreholes of varying depths, 70 m at Dei-Dei, 60 m at Kubwa, 50 m at Gosa, 40 m at Lugbe, 14 m Hand dug well at Dei-Dei (500 m away) from the 70 m borehole point of Dei-Dei and public water supply for this work. Water samples were collected in high density polyethylene containers at the site in Nigeria previously washed in a solution of 10 % nitric acid for 15 minutes, followed by repeated rinsing with distilled water and finally rinsing with ultrapure water (resistivity of about 18 MΩ cm^{-1}). The collection containers were kept in

sealed polyethylene bags before the collection of samples. Borehole water samples were stabilized with 5 ml of nitric acid in each litre of water in order to prevent it from attacking to the wall of the container. The minimum detectable concentration was 0.01 µg L^{-1}, corresponding to 124 µBq L^{-1} (Tarvainen et al., 2001).

For accurate determination of elemental compositions in groundwater samples, a solution analytical method was used; a multi-standard calibration method was applied using Elan 9000 instrument that performs analysis at parts-per-trillion and lower. The samples were collected at each borehole point and hand-dug well as shown in Figures 3.19 (a) and (b) respectively to know if depth contributes to low or high activity concentrations of radionuclides in groundwater. In addition to the samples, public water supply was collected to compare with the groundwater resources from the study area. Both the groundwater samples, hand-dug well and public water supply collected from the study area are shown in Figure 3.20.

(a) (b)

Figure 3.19 Collection of borehole water sample and hand-dug well at Dei-Dei

Figure 3.20 The water samples collected from Dei-Dei, Kubwa, Gosa and Lugbe boreholes, hand-dug well and public water supply in Abuja, Nigeria.

The prepared water samples for the ICP-MS analysis is shown in Figure 3.21, and labeled according to locations and site numbers, on the bodies of the plastic bottles. The details of the results analysed using ICP-MS spectrometry are discussed in Section 4.6.

Figure 3.21 Water samples prepared for ICP-MS analysis

3.6.2 Sample analysis using ELAN 9000 instrument and technique

Measurement of ^{238}U, ^{232}Th and ^{40}K including toxic elements using ICP-MS was performed at the Universiti Tun Hussein Onn Malaysia Environmental and Soil Science Laboratory. The results are reliable because of the duplicates of which were comparable to each other. The ELAN 9000 instrument measures at parts-per-trillion level and even below. The resolution characteristics allows for proper adjustment of the resolution for each mass, while maintaining nominal resolution across the mass range, reducing the ambiguity in spectral and enhancing the limits of detection. The uniqueness of the Lens feature optimizes the lens voltage for individual element. The increase in analyte signals due to this powerful system reduces the matrix ambiguity during the multi-element operation, thereby improving the sensitivity. The method of sample introduction uses an integrated peristaltic pump to drastically minimise sample uptake time.

The new method of ICP-MS for determining multi-element analysis and ideal for groundwater, since the vast majority of target compounds can be detected below 0.1 mg L^{-1} (Adrian, 2007; Thomas, 2004). In this study, the analysis of radionuclides and other heavy metals was based on ISO standard 17025 (European Standard EN ISO/IEC 17025:2000). The samples and all the parameters used were stored in an encrypted, checksum-protected dataset, in order to protect from losing the information analyzed. The powerful quality-control system sets the limits, parameters and standards based on U.S. EPA (EPA 200.8) or other quality-control guidelines.The ELAN 9000 instrument used to perform the analyses is shown in Figure 3.22.

Figure 3.22 The ICP-MS ELAN 9000 instrument

3.7 Conceptual Model

To validate the formulated conceptual model and to answer the research questions from view point of Nuclear Geophysics/geochemistry attributes in Figure 3.23

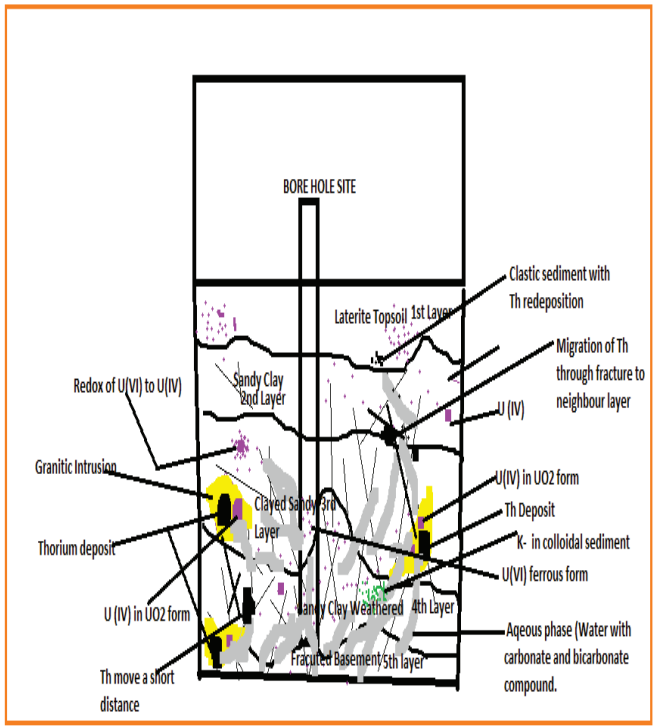

Figure 3.23 Conceptual Model of radionuclides behaviour in subsurface water rock interaction.

The model was developed for the idea of behaviour of natural occurring radioactive element in subsurface water rock interaction. In this work, few of these research questions are to be answered to know where to improve from the basic

ideas. Deposit of U (IV) in the form of UO_2 in the host rock in subsurface geologic formation, what are the ideas for the questions hereunder?

1. What causes uranium to oxidize to soluble form?
2. In subsurface media, what keeps uranium in aqueous phase to form many chemical species?
3. Why the reaction of U (IV) in aqueous phase is a function of pH, oxidation-reduction potential and complexity lingand?
4. What is the effect of temperature on U (IV) in the soil?

CHAPTER 4

RESULTS AND DISCUSSION

4.1 Introduction

This chapter presents the discussions of the field work of geophysical data acquisitions and groundwater depth location using VES, structural studies of the subsurface lineaments and fracture trend using SRTM, modeling of flow in a homogeneous isotropic media using Matlab, experimental results for gamma ray measurements using HPGe spectrometry, geochemical characteristics of rock samples using XRF analysis, radiological and toxic elements concentration in groundwater using ICP-MS analysis.

4.2 Vertical Electrical Sounding (VES) Measurements

In this work, the objective of VES was to determine the subsurface resistivity distribution by making measurements on the ground surface. The search for groundwater was carried out through the use of electrical methods of near surface geophysical survey. The Schlumberger configuration in vertical electrical sounding (VES) was used to obtain field data. VES probes the vertical in resistivity of the subsurface, thereby indicating the presence of fluid and ionic concentration in the

subsurface materials, (Reynolds, 2011). It was also applied to determine the depth to bedrock, delineate the various units that constitute the overburden (regolith), determine the degree of fracturing of the bedrock; all of which would helpe in making the choice for a feasible site for constructing a successful borehole. VES data for this work were obtained using the Allied OmegaC2 Terrameter as shown in Figure 3.3. The field data obtained was presented as curve of apparent resistivity values against half of the current electrode separation (AB/2) in metres on a log-log scale. The VES data obtained were analyzed using the WINRESIST 2004 Version computer software to improve the quality of the interpretation by iteration and modeling to goodness of fit. The practical field data acquisition using Schlumberger array of VES method is shown in Figure 3.4. From these measurements, the true resistivity of the subsurface can be estimated. The ground resistivity is related to various geological parameters such as the mineral and fluid content, porosity and degree of water saturation in the rock. The resistivity measurements are normally made by injecting current into the ground through two current electrodes (A and B in Figure 3.2), and measuring the resulting voltage difference at two potential electrodes (M and N). From the current (I) and voltage (V) values, an apparent resistivity (ρ_a) value is calculated. The mathematical expression of apparent resistivity determination discussed in Section 3.2 was derived from Equation 3.4.

Resistivity meters normally give a resistance value, $R = {}^{V}/_{I}$, so in practice the apparent resistivity value is calculated as stated in Equation 3.4. To determine the true subsurface resistivity, an inversion of the measured apparent resistivity values using a computer program must be carried out. Instrument readings (current and voltage) are generally reduced to "apparent resistivity" values. The apparent resistivity is the resistivity of the half-space which would produce the observed instrument response for a given electrode spacing. Apparent resistivity is a weighted average of soil resistivities over the depth of investigation. For VES, a log-log plot of apparent resistivity versus electrode separation is obtained. This is sometimes referred to as the "sounding curve. The theoretical response is then compared with the observed field response and differences between observed and theoretical were noted. The hypothetical earth model is then adjusted to create a response which more

nearly fits the observed data. When this iterative process is automated it is referred to as "iterative inversion" or "optimization

4.2.1 Vertical Electrical Sounding (VES) data analysis and interpretation

The resistivity variation with layers, electrodes spacing and lithological descriptions of the subsurface information from the VES at Dei-Dei are shown in Table 4.1.

Table 4.1: Summary of results obtained from Dei-Dei VES

VES No	Electrode spacing AB/2 (m)	Electrode spacing MN/ (m)	Resistance (Ω)	Resistivity (Ω-m)	Lithology	Remark
VES 1 Dei-Dei	1	0.25	25.47	320.0	Sandy clay topsoil	Good yield
	2	0.25	5.970	300.3		
	3	0.25	2.370	267.7		
	9	0.5	0.071	100.5	Weathered basement	
	15	1.0	0.384	271.4		
	20	1.0	0.159	200.1		
	25	1.0	0.148	291.3		
	32	1.0	0.1121	360.7	Fractures overlay fresh basement	
	50	2.5	0.2031	638.1		

Table 4.1 shows the field data obtained from Dei-Dei borehole which gives remark of feasible borehole of good yield. The data were used to plot apparent resistivity versus electrode spacing to obtain a VES profile plot as shown in Figure 4.1. The VES revealed that the area consists of three major geoelectrical layers. The first geolectric layer correspond to the topsoil made of sandy clay with resistivity values ranging from 267.7 to 230.0 Ω-m and thickness ranging from 0.5 to 9.7 m. The weathered basement was encountered at about 10 m depth. The second layer

consists of weathered basement with resistivity ranging from 100.5 to 291.3 Ω-m with thickness ranges from 9.7 to 59 m. The third layer consist of fractures which overlaid the fresh basement at about 73 m or greater with resistivity ranging from 360 to 638.1 Ω-m. The VES recommends about 70 m to be drilled in Dei-Dei area.

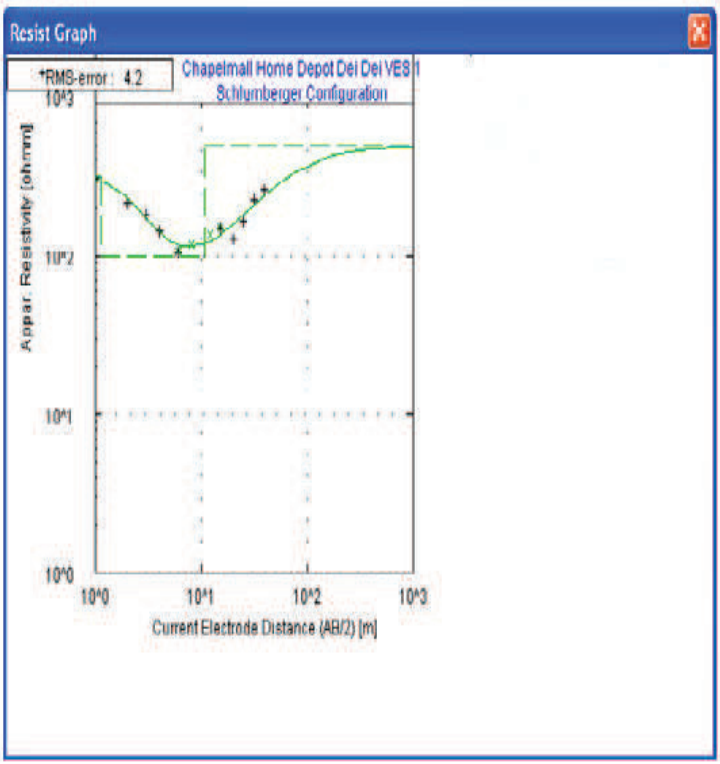

(+ = experimental, x = calculated)

Figure 4.1 1D profile plot of VES 1 for Dei-Dei Site

At Kubwa, the resistivity variation with layers, electrodes spacing and lithological descriptions of the subsurface information from the VES are shown in Table 4.2.

Table 4.2: Summary of results obtained from Kubwa VES.

VES No	Electrode spacing AB/2 (m)	Electrode spacing MN/ (m)	Resistance (Ω)	Resistivity (Ω-m)	Lithology	Remark
VES 2 Kubwa	1	0.25	55.58	698.1	Sandy clay topsoil	
	2	0.25	15.70	788.9	Weathered basement	Good yield
	4	0.25	3.623	728.4		
	15	0.5	1.132	800.3		
	20	1.0	0.639	802.1		
	32	1.0	0.262	842.1		
	50	2.5	0.311	976.0	Fresh basement	
	65	2.5	0.230	1219.8		

Table 4.2 gives remark of feasible borehole of good yield. The data were used to plot apparent resistivity versus electrode spacing to obtain a VES profile plot as shown in Figure 4.2. The VES 2 reported similar aquifer characteristics as VES 1 with good yield inferred, but varies with layers and resistivity values as shown in Table 4.2. The first geoelectric layer consists of sandy clay topsoil with thickness of about 0.5 to 1.2 m and resistivity values range from 698.1 to 788.9 Ω-m. The weathered basement was encountered at the depth of about 3.2 m as the second layer. It has thickness ranges from 3.2 to 32.0 m with resistivity values ranges from 728.4 to 842.2 Ω-m. The third layer which is fresh basement overlaid by fractured layers at about 32.0 to 65.0 m thick with a resistivity values ranges from 976.0 to 1219.8 Ω-m. The VES recommends drilling at about 60 m to the aquifer bearing formation.

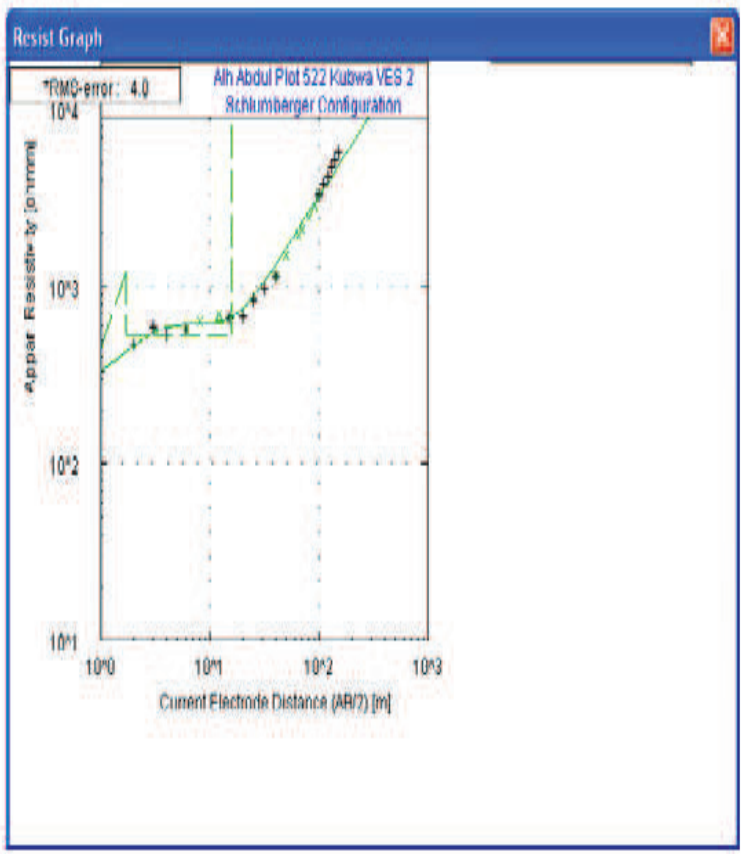

(+ = experimental, x = calculated)

Figure 4.2 1D profile plot of VES 2 for Kubwa

The resistivity variation with layers and lithological descriptions of the subsurface information from the VES 3 are shown in Table 4.3 for Gosa area. VES 3 indicates complicated subsurface and basement information from the remark as it shows low yield. It shows almost similar aquiferous features as VES 1 and VES 2 in

terms of weathered basements, but differs in low yield to dry aquifer even after drilling up to 50 m depth estimated.

Table **4.3:** Summary of results obtained from Gosa VES.

VES No	Electrode spacing AB/2 (m)	Electrode spacing MN/ (m)	Resistance (Ω)	Resistivity (Ω-m)	Lithology	Remark
VES 3 Gosa	1	0.25	28.19	354.1	Laterite topsoil	Low yield to dry well
	2	0.25	9.139	459.3	Micaceous sandy clayey weathered	
	3	0.25	2.372	477.0		
	6	0.5	1.569	354.8	Unweathered basement	
	15	1.0	0.285	201.6		
	32	1.0	0.069	222.1		
	40	2.5	0.113	226.2		
	50	2.5	0.071	221.5	Fresh basement	

The data were used to plot apparent resistivity versus electrode spacing to obtain a VES profile plot as shown in Figure 4.3. The results obtained from the sounding revealed the first layer, laterite topsoil with thickness ranges from 0.8 to 3.3 m and resistivity ranges from 354.1 to 459.3 Ω-m.The second layer; weathered basement has resistivity ranges from 459.3 to 477.0 Ω-m with thickness ranges from 3.3 to 40.2 m. The unweathered basement was noted to have resistivity ranges from 254.8 to 226.2 Ω-m with thickness ranges from 42.2 m to 50 m. Since the resistivity values are lower than the weathered zone in other area which is supposed to be a good promising aquifer features, hence, reported low to dry well when drilled up to 50 m. In this location, low yield was experienced in several boreholes which were inferred to be the presence of dense intrusive bodies which may have shattered the aquifer thereby become devoid of water from the zone. The profile plot of the apparent resistivity versus electrode spacing in Figure 4.3 recommends drilling at about 50 m in the area.

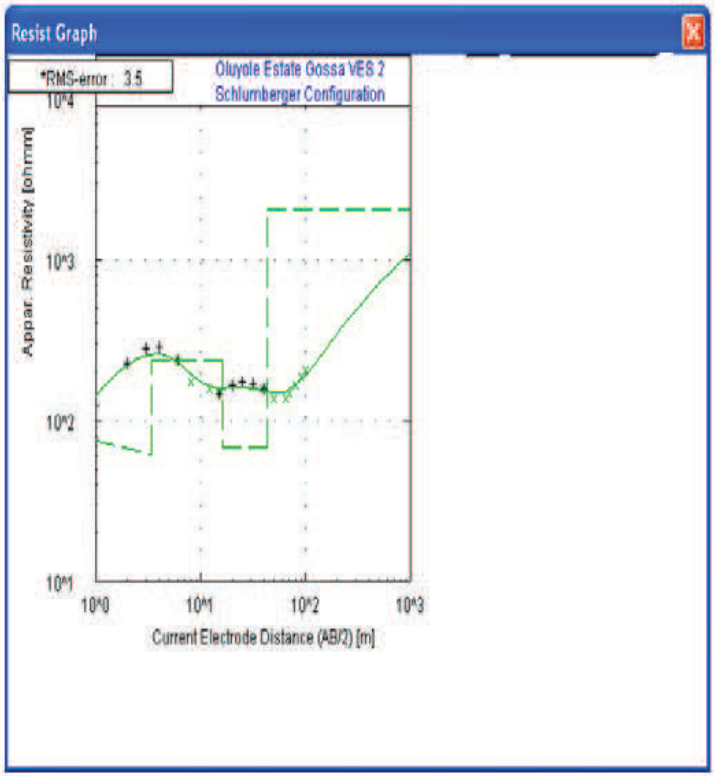

(+ = experimental, x = calculated)

Figure 4.3 1D profile plot of VES 3 for Gosa

The resistivity variation in layers of the subsurface formation from the VES carried out for aquifer characterisation at Lugbe is shown in Table 4.4. The VES in the region revealed three major geoelectrical layers overlaying fresh basement.

Table 4.4: Summary of results obtained from Lugbe VES

VES No	Electrode spacing AB/2 (m)	Electrode spacing MN/ (m)	Resistance (Ω)	Resistivity (Ω-m)	Lithology	Remark
VES 4 (Lugbe)	1	0.25	28.85	362.4	Sandy clayey topsoil	Good yield
	2	0.25	5.909	297.0	Weathered basement	
	4	0.25	1.471	296.6		
	8	0.5	0.249	100.1		
	15	1.0	0.399	282.3		
	20	1.0	0.235	294.5	Fractured basement overlay fresh basement	
	40	2.5	0.149	300.1		
	50	2.5	0.111	348.5		
	65	2.5	0.070	372.3		

VES 4 shows the same promising good aquifer yield as VES 1 and VES 2 respectively as presented in Table 4.4. The profile plot of apparent resistivity against electrode spacing as shown in Figure 4.4 reveals the first layer which is sandy clayey topsoil with thickness ranges from 0.6 to 1.7 m and resistivity ranges from 297.0 to 362.4 Ω-m.The second layer reported resistivity ranges from 100.1 to 300.1 Ω-m with thickness varying from 1.7 to 6.4 m as weathered basement. An interesting observation here is that the fractured basement overlies the fresh basement at the depth ranging from 15 to 20 m with varying resistivity at about 294.5 to 372.3 Ω-m. This indicates that the aquifer is can be tapped closer to the surface than other areas. The profile plot of the apparent resistivity versus electrode spacing recommends drilling at about 40 m at Lugbe.

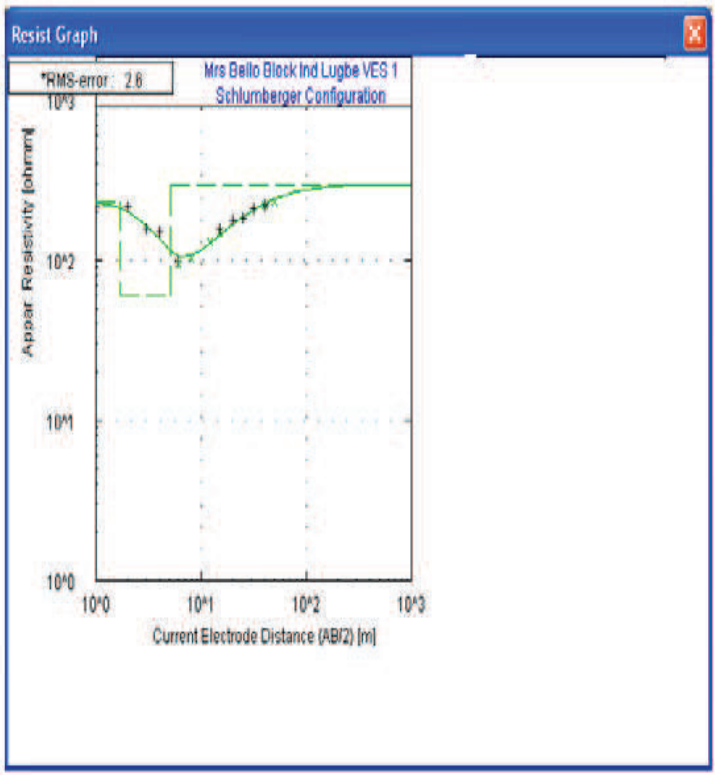

(+ = experimental, x = theoretical)

Figure 4.4 1D profile plot of VES 4 for Lugbe Site

4.2.2 Interpretation of Two-Dimensional (2D) Cross-sections of VES Layers Across the Survey Area

The two-dimensional (2D) geoelectrical sections were then generated by combining any two VES data falling along the distinct trends of each location. Figure

4.5 shows 2D lithological characterizations obtained from VES data combination around Dei-Dei to Kubwa and Gosa to Lugbe. In Dei-Dei area, SW-NE is assumed by area VES 1 and VES 2 around the Dei-Dei to Kubwa axis. A similar trend (WSW-ENE) in the Gosa area, VES 3 and 4 respectively, falls within Gosa to Lugbe. It is observed from Figure 4.5(a) that the weathered zone is thin around Gosa and become considerably thicker around Lugbe. This explains why groundwater condition is less problematic around Lugbe. In the Dei-Dei to Kubwa area as shown in Figure 4.5(b), the top layers which correlate with the weathered layers exhibit considerable thickness. Although the interested weathered layers thin out towards Western part of Dei-Dei area, it is still much thicker than that obtained around VES 3, Gosa area.

.

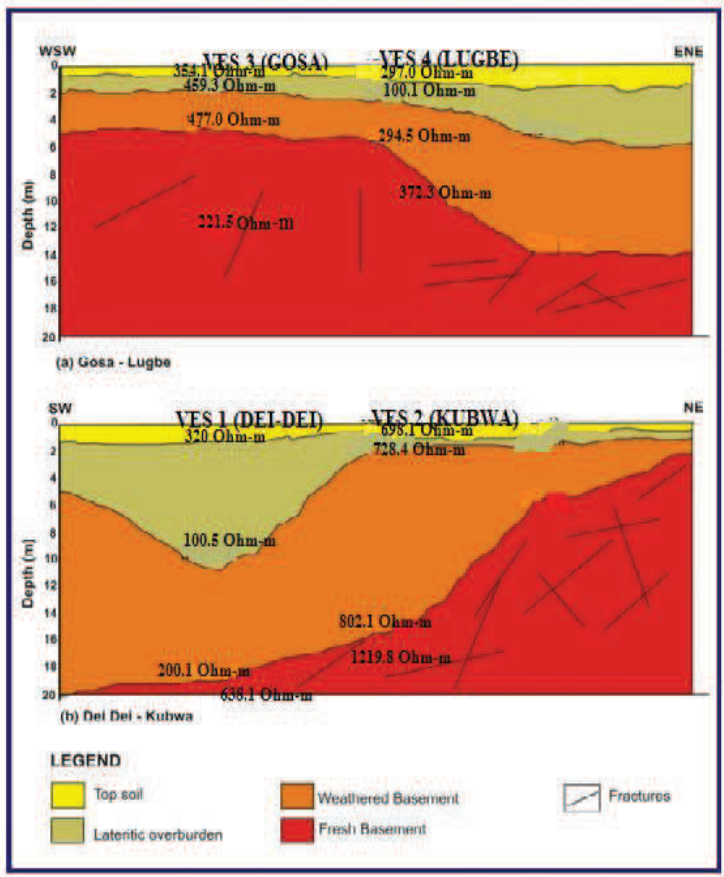

Figure 4.5 2D cross-sections of interpreted VES depths across the survey area with fractures

In view of this complicated report in VES 3, Gosa area, which is densely populated area and seeking for groundwater supply, which is part of this project work; a geophysical technique to integrate with the conventional VES method was needed for adequate delineation of subsurface structures that control the groundwater system in the area. For the purpose of further investigation of Gosa aquifer

characterisation, integration of Shuttle Radar Topography Mission Imagery data with VES was used. The detailed methodology is discussed in Section 3.2.

4.2.3 SRTM Data Analysis and Interpretation.

The introduction of SRTM in this research was to delineate the structures that control the groundwater system in the area due to the complicated basement terrain information obtained using only VES method especially in VES 3 location. The information from VES method seems to have limitation over VES 3 subsurface basement terrain groundwater which is part of this research to collect groundwater samples in the area (Gosa). The detailed method of integrating the VES data with SRTM is discussed in Section 3.2.3.

A total of 88 interpreted lineaments were digitized on screen and displayed on the lineament map of the study area as shown in Figure 4.6. Visual interpretation of the lineament distribution shows that the eastern part of the structural map which falls within the Abuja Municipal Council, has higher concentration of lineaments than the Western part. Moreover it was observed that many of the lineaments around VES 3, Gosa, are not intersecting, whereas those in Dei-Dei, Kubwa and Lugbe parts are intersecting, thereby showing higher promise of fractured basement aquifer potential (Maxwell *et al.,* 2014). This may explain why the boreholes in the VES 1, VES 2 and VES 4 from Figure 4.6 are productive, whereas the VES 3 is not productive or rather low yield or dry well. It is observed from the rose diagram, Figure 4.7 that the dominant fracture trends (NNE-SSW and N-S) coincide with the dominant Pan-African trend in the Basement Complex of Nigeria, (Ajibade *et al*., 1987; Caby, 1989; Dada, 2008). This indicates that the fractures are regional in scale; hence their intersections can form large zones of brecciation with more pronounced porosity and permeability, which are desirable in regions where boreholes need to intersect significantly groundwater, (Maxwell *et al.,* 2014).

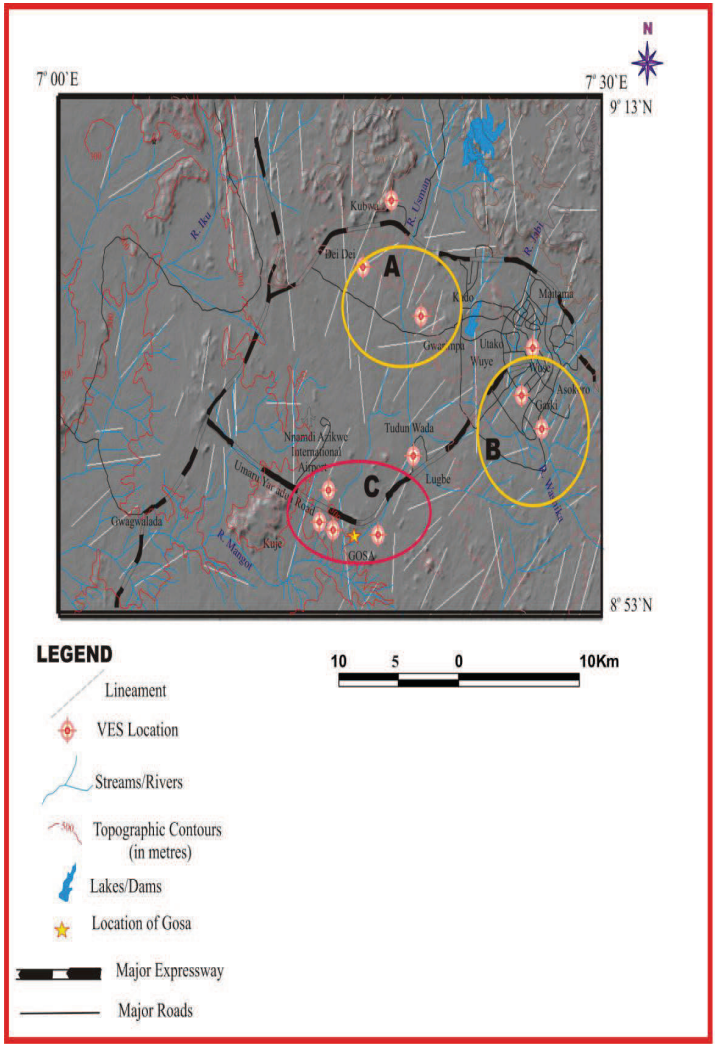

Figure 4.6 Lineament Map draped on Hillshaded SRTM-DEM image of the study area. Yellow ellipses show zones of higher fracture density and interception, red ellipse shows the Gosa area with low fracture density and no interception

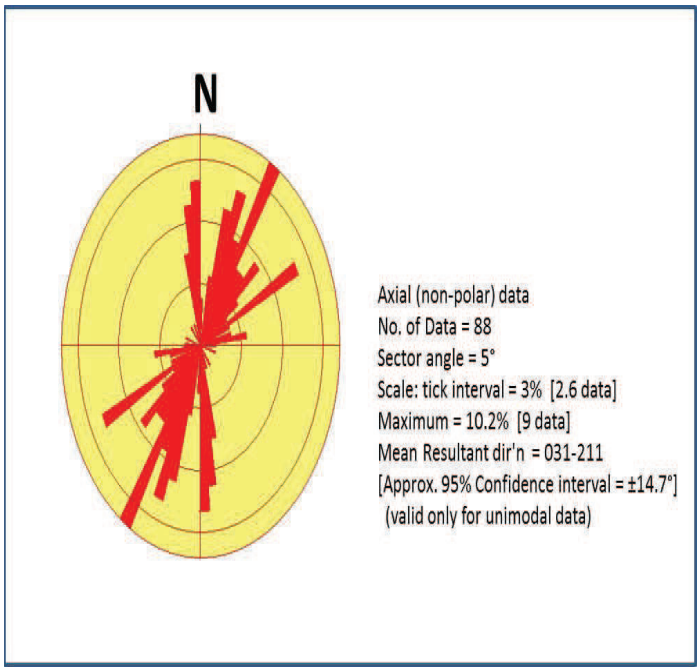

Figure 4.7 Rose diagram showing the distribution of fracture orientations in the study area

4.2.4 Compatibilty of VES and SRTM

The similarity in the VES sections suggests a relatively homogenous aquiferous setting for the area. However, after subsequent intensive investigations, it was found that this was not the case, a total of four (4) boreholes that were drilled for this study, three had good water yield with the static water level ranging from 2 – 6.7 m approximately below ground level (bgl), while one borehole around Gosa area were low to dry well. Geoelectrical surveys indicated the existence of both weathered and fractured basement, which ideally could form good aquifers in the study area.

The regolith over the unweathered basement is, however, clayey, and so does not constitute a good aquiferous material as indicated in borehole (Figure 4.8(b) compared to Figure 4.8(a) in Dei-Dei. These observations agree with previous works in the Basement Complex of Central Nigeria (e.g, Olorunfemi and Okankune 1992; Okogbue and Omonona, 2013). Okogbue and Omonona, (2013) identified three aquifer potential types in the Mopa-Egbe basement area of central Nigeria. They include relatively high (> 2.0 L s^{-1}), medium (1.0 – 2.0 L s^{-1}) and low (< 1.0 L s^{-1}) productivity types. The high productivity aquifers constitute the weathered layer aquifer and weathered/fractured aquifer.

Omeje, *et al.* (2013) attempted to map aquiferous zones around the Gosa area, using only VES data. The study inferred that the groundwater problems around the area were as a result of the presence of dense intrusive bodies. This differs remarkably with results from the integration of VES and SRTM, which suggests that in addition to the absence of thick weathered overburden, low fracture densities and absence of interconnected fractured zones most probably constitute the reasons for unsuccessful boreholes in VES 3 location, Gosa area (Figure 4.5 and 4.6), (Maxwell *et al.,* 2014).

In order to overcome the challenges of drilling dry wells around the study area, structural data generated from hill-shaded SRTM data, in combination with VES data, constitute a powerful tool for delineating potential aquifers in basement rocks especially in areas where the weathered overburden constitute poor aquifers. Figure 4.6 shows the spatial distribution of lineaments (fractures) digitized from enhanced SRTM data. It is observed that in most parts of the study area, large scale fractures exist, many of which extends for distances in excess of 2 km. These regional features would usually undergo intense brecciation at points of intersection, resulting in widespread shattering of unweathered rocks which leads to enhanced porosity and permeability, (Maxwell *et al.,* 2014). This porosity and permeability could serve as pathway for mobility of radionuclides and toxic elements seeping to the groundwater system.

Figure 4.8 Lithological logs of representative boreholes drilled in (a) Dei-Dei with good water yield and (b) Gosa with no water yield

Schematic representation of four well logs, from Dei-Dei, Kubwa, Gosa and Lugbe are shown in Figures 4.9, 4.10, 4.11 and 4.12 respectively. They correlate well with the interpreted VES data and revealed the absence of thick weathered basement around VES 3, Gosa borehole area.

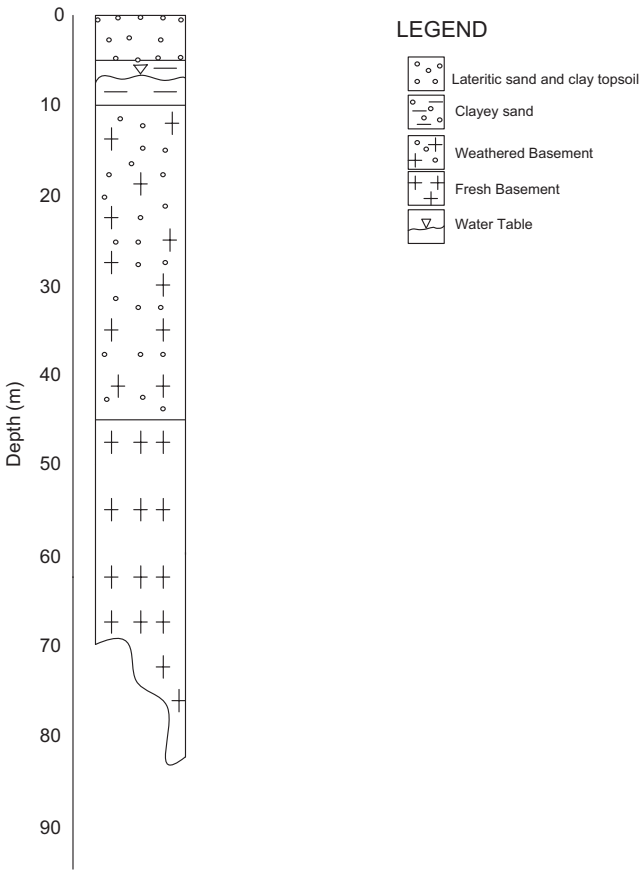

Figure 4.9 Lithologic log of representative borehole drilled around Dei-Dei areas, 70 m, (lat: 9^{o} 6’52’’ N and long: 7^{o} 15’39’’ E).

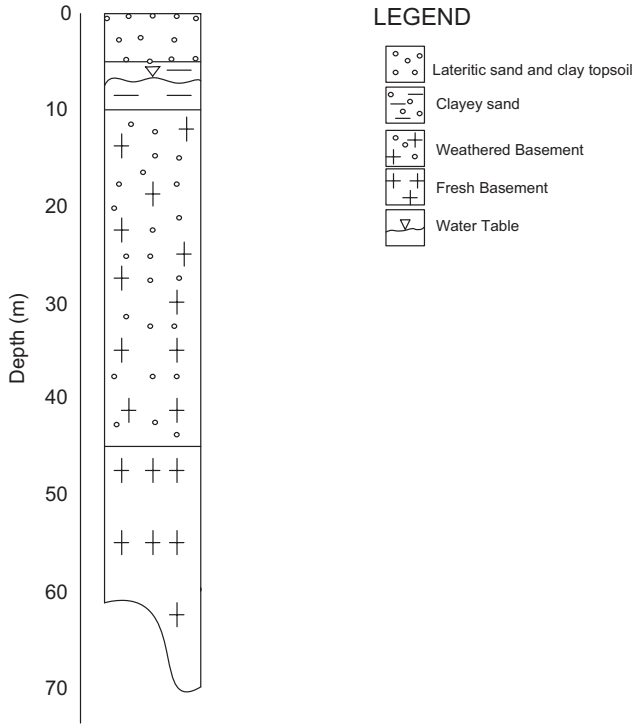

Figure 4.10 Lithologic log of representative borehole drilled around Kubwa areas, 60 m, lat 9^{o} 6'16.7" and long: 7^{o} 16'26.0" E).

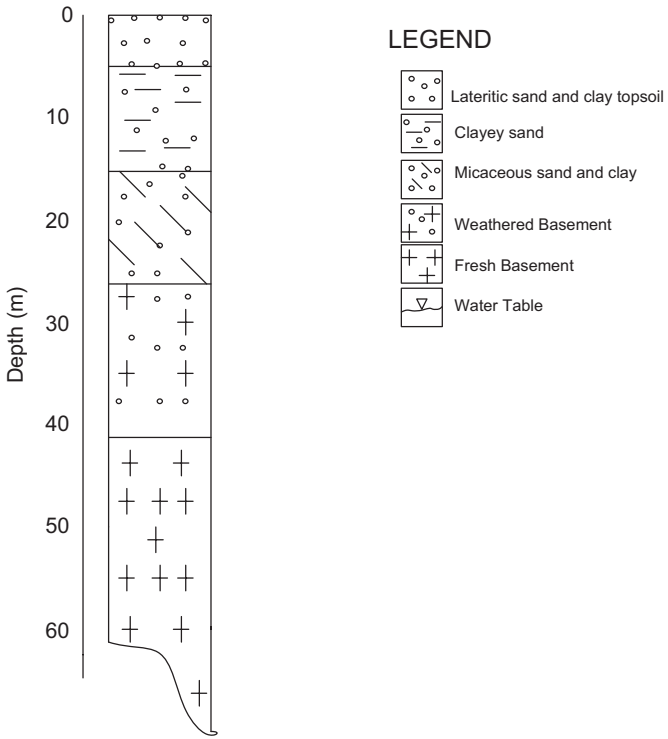

Figure 4.11 Lithologic log of representative borehole drilled around Gosa areas, 50 m, (lat: 8° 56'45.6" and long: 7° 13'26.2" E)

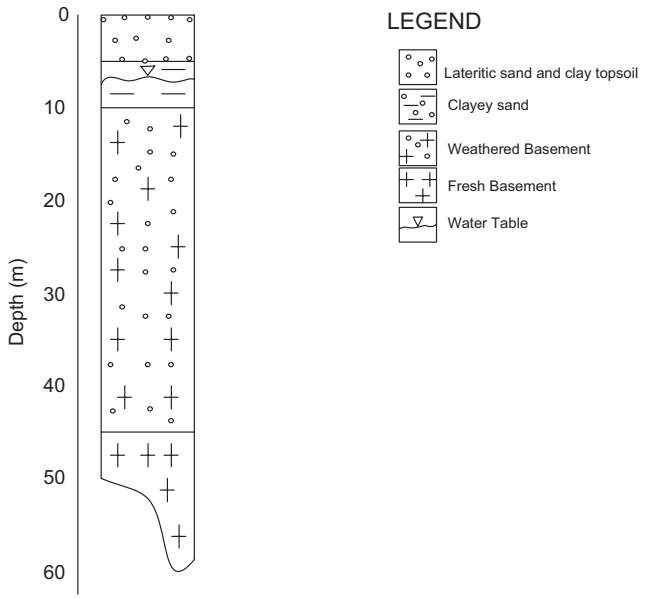

Figure 4.12 Lithologic log of representative borehole drilled around Lugbe areas, 40 m, (lat: 8° 59'2.3" N and long: 7° 23'7.8"E)

4.3 Interpretation of Mathematical Model of Flow in Homogeneous Isotropic Medium

The objective of this mathematical model is to determine the density of water and the volumetric water content as functions of the spatial variables and of time. Thus, to verify that the density of water as well as the control volume varies with time due to the water pressure variation to be modeled using a computer package (MatLab 2009a). This will help to demonstrate the variations of flow equation in porous media as shown in Appendix F. If the hydraulic head is obtained by in-situ measurements, Darcy's law is sufficient to describe the groundwater flow. The input and output discharges at the level of the Representative Elementary Volume, REV,

for limited volumes of the porous media or for the whole system can be computed based on the hydraulic gradients and the parameters of the porous medium and the fluid. Equation (xiv) discussed in Appendix F was used to model and verify the variation in control volume with time due to the water pressure as shown in Figure 4.13

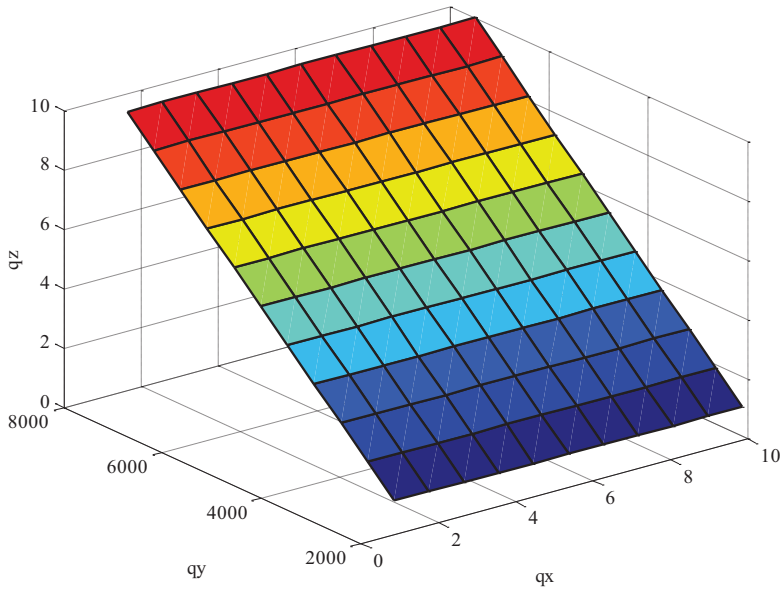

Figure 4.13 Modeling of groundwater flow in homogeneous isotropic medium

In Figure 4.13, the groundwater is thought of as an infinitesimally small cube, Representative Elementary Volume (REV) which follows from the principles of equilibrium that pressure on every side of this unit of groundwater must be equal. As this is the case, it will not move on the direction of the resultant force. Thus, the pressure in this case is said to be isotropic, i.e it acts with equal magnitude in all

directions. The water density and the volumetric water content are functions of the spatial variables and of time: $\rho = \rho(x, y, z, t); \theta = \theta(x, y, z, t)$.

Density of water as well as the control volume varies in time due to the water pressure variation; still, the lateral deformations of the control volume are ignored, and only the vertical deformation is taken into account. In a given control volume, aside from sources or sinks, mass cannot be created or destroyed, the conservation of mass states that for increment of time (Δt), the difference between mass flowing in across the boundaries, the mass flowing out across the boundaries and the source within the volume, is the change in storage as in Equation 4.1.

$$\frac{\Delta M_{stor}}{\Delta t} = \frac{\Delta M_{in}}{\Delta t} - \frac{\Delta M_{out}}{\Delta t} - \frac{M_{gen}}{\Delta t} \tag{4.1}$$

4.3.1 Prediction of Different Scenarios Pertaining Groundwater Flow in a Closed Media of the Model using Darcy's Law

The objective of the prediction is to calculate the Darcy's velocity, volume of water that flows through the media and average linear velocity of the groundwater flow between two closest boreholes, i.e Dei-Dei to Kubwa and Gosa to Lugbe respectively. The method is based on Henry Darcy's work, 1856 to be calculated as follows:

Darcy's law is used to predict the velocity, V, conductivity term, K, head term, h and distance l.

$$V = -K\left(\Delta h/_{\Delta L}\right) \tag{4.2}$$

This is Darcy's velocity (or Darcy's flux) which is defined as the flow per unit cross sectional area of the porous media. In a porous media, the water must flow through the pores, around the solid particles, at a speed greater than the flux. This speed is called the average linear groundwater velocity, V_a and is calculated by $/\emptyset$, where V is the Darcy's velocity (or flux) and $\emptyset$ is porosity of the media. The parameters such as the hydraulic head, pressure head and hydraulic gradient are determined to arrive at a predicted value of the V, q and V_a. The hydraulic head, pressure head and hydraulic gradient are calculated from Figure 4.14 and Figure 4.15 as follow:

Across Dei-Dei to Kubwa:

1) Hydraulic Head $= \Delta h = h_2 - h_1$ (4.3)

   where,

   $h_1 =$ Water rise in the casing at Dei-Dei borehole

   $h_2 =$ Water rise in the casing pipe at Kubwa borehole

   $Z_1 =$ Aquifer thickness at Dei-Dei

   $Z_2 =$ Aquifer thickness at Kubwa, etc

2) Pressure head = $h_p = h_1 - Z_1 = h_2 - Z_2$ (4.4)

3) Hydraulic gradient = $h_g = {\Delta h}/{L}$ (4.5)

For the hydraulic head, pressure head and hydraulic gradient across Dei-Dei to Kubwa is shown in Figure 4.14 using Darcy's law:

1) Hydraulic Head $= \Delta h = h_2 - h_1 = 4.3 - 4.8 = -0.5$ m

2a) Pressure head = $h_{p_1} = h_1 - Z_1 = 4.8 - 2.3 = 2.5$ m

b) Pressure head = $h_{p_2} = h_2 - Z_2 = 4.3 - 1.6 = 2.7$ m

3) Hydraulic gradient = $h_g = {\Delta h}/{L} = {-0.5 \text{ m}}/{7015.1 \text{ m}} = 7.1 \, x \, 10^{-5}$

In this work, the hydraulic conductivity and porosity values for silt, sandy, clay and clayey sand of 10^{-5} as reported elsewhere (Fetter,1994) will be used.

L = 7015.1 m = horizontal difference between Dei-Dei and Kubwa

A = (0.4 x 5.2) m^{-2} = 2.08 m^{-2} = diameter of boreholes (0.2 m each) x ($h_{p_1} + h_{p_2}$)

$\emptyset$ = 40 % 0r 0.4 = average Porosity for sediment size from 0.002- 2.0 mm (Fetter, 1994)

$K = 1$ x 10^{-5} m s^{-1} = hydraulic conductivity for silt, sand and clayey sand (Loxnachar, 1999)

$\Delta h = h_2 - h_1 = 4.3 - 4.8 = -0.5$ m = hydraulic head

$h_g = {\Delta h}/{L} = {-0.5 \text{ m}}/{7015.1 \text{ m}} = -7.1 \ x \ 10^{-5}$ = hydraulic gradient

therefore,

$V = -(10^{-5})$ X $(-7.1 \ x \ 10^{-5}) = 7.1 \ x \ 10^{-10} =$ Darcy's velocity (or Darcy's flux)

$q = (7.1 \ x \ 10^{-10})$ X 2.08 = 1.5 X 10^{-9} $m^3 s^{-1}$ = volume of water flowing through the media.

Average linear velocity, V_a is given across Dei-Dei to Kubwa to be

${V}/{\emptyset} = {1.5 \text{ X } 10^{-9} \text{ m}^3 s^{-1}}/{0.4}$

Therefore,

$V_a = 3.75$ X 10^{-9} $m^3 s^{-1}$

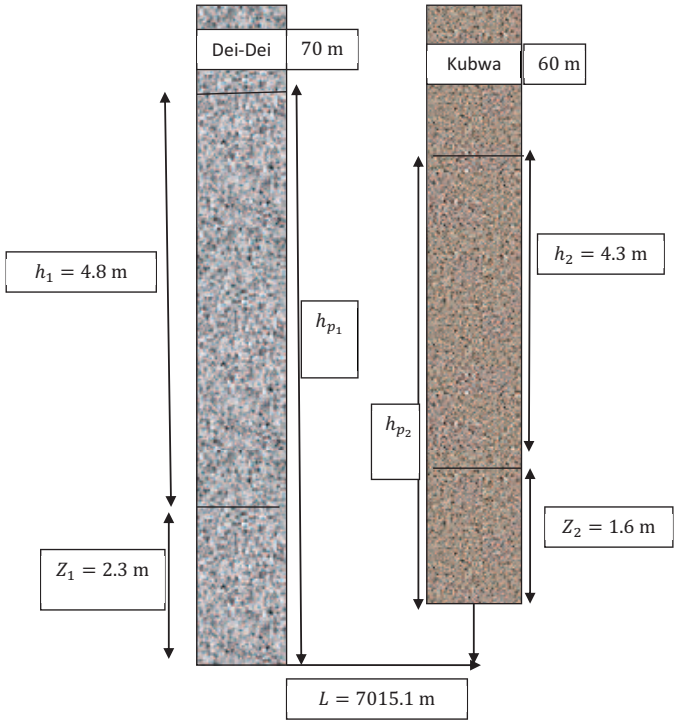

Figure 4.14 Determination of hydraulic head, pressure head and hydraulic gradient of the groundwater flowing across Dei-Dei to Kubwa

Across Gosa to Lugbe using Darcy's law:

1) Hydraulic Head $= \Delta h = h_2 - h_1 = 5.2 - 1.8 = 3.4$ m

2 a) Pressure head = $h_{p_1} = h_1 - Z_1 = 1.8 - 0.9 = 0.9$ m

b) Pressure head = $h_{p_2} = h_2 - Z_2 = 5.2 - 2.9 = 2.3$ m

3) Hydraulic gradient = $h_g = {}^{\Delta h}/_{L} = {}^{3.4\text{ m}}/_{5211.2\text{ m}} = 6.5\ x\ 10^{-4}$

$L = 5211.2$ m = horizontal difference between Gosa to Lugbe

A = (0.4 x 3.8) m^{-2} = 2.08 m^{-2} = Diameter of boreholes (0.2 m each) x ($h_{p_1} + h_{p_2}$)

$\emptyset$ = 40 % 0r 0.4 = average porosity for sediment size from 0.002- 2.0 mm (Fetter, 1994)

$K = 1$ x 10^{-5} m s^{-1} = hydraulic conductivity for silt, sand and clayey sand (Loxnachar, 1999)

$\Delta h = h_2 - h_1 = 5.2 - 1.8 = 3.4$ m = hydraulic head

$h_g = {\Delta h}/_{L} = {3.4 \text{ m}}/_{5211.2 \text{ m}} = 6.5\ x\ 10^{-4}$ = hydraulic gradient

therefore,

$V = -(10^{-5})$ X $(6.5\ x\ 10^{-4}) = 6.5\ x\ 10^{-9} =$ Darcy's velocity (or Darcy's flux)

$q = (6.5\ x\ 10^{-9})$ X $2.08 = 1.35$ X 10^{-8} $m^3 s^{-1}$ = volume of water flowing through the media.

Average linear velocity, V_a is given across Gosa to Lugbe to be

${V}/_{\emptyset} = 1.35$ X 10^{-8} ${m^3 s^{-1}}/_{0.4}$

therefore,

$V_a = 3.4$ X 10^{-8} $m^3 s^{-1}$

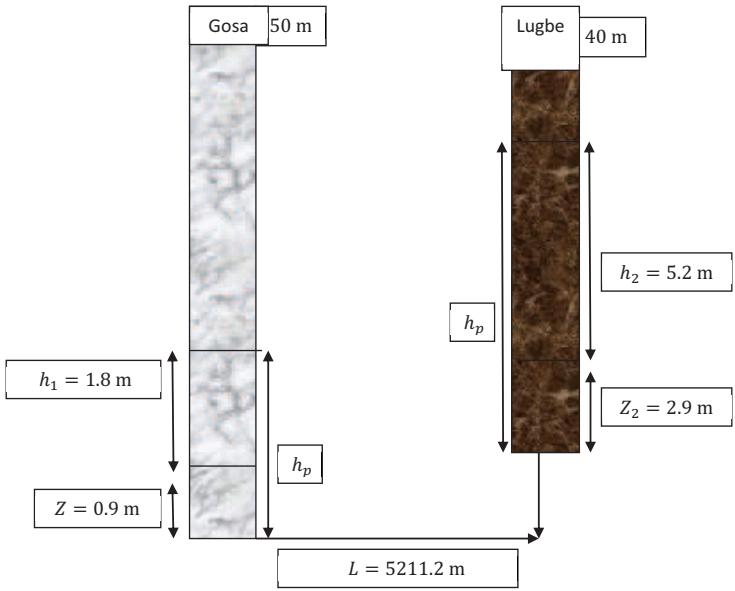

Figure 4.15 Determination of hydraulic head, pressure head and hydraulic gradient of the groundwater flowing across Lugbe to Gosa

From the above groundwater flow evaluation, it is shown that the average linear velocity obtained from the calculations across Gosa to Lugbe is higher than that of Dei-Dei to Kubwa. It can be concluded that the groundwater at Lugbe recharges the Gosa area where low yield was found whereas Dei-Dei groundwater recharges that of Kubwa considering the hydraulic heads across the two pairs of drilled holes in different locations. It was noted that the flow in subsurface structures at Gosa to Lugbe reported higher volume of water than that flows across Lugbe to Gosa than the corresponding Dei-Dei to Kubwa which flows from higher depth to lower depth and may be attributed to greater large scale fractures interconnected at Lugbe borehole layers.

4.4 Measurements of ^{238}U, ^{232}Th and ^{40}K in Subsurface Layers of Dei-Dei, Kubwa, Gosa and Lugbe Boreholes

The objective of these measurements was to determine the concentrations of ^{238}U, ^{232}Th and ^{40}K in different layers of the groundwater bearing formation, thus, to infer the layer that constitutes the higher activity level and the geologic rock type. Initially, the concentrations of ^{238}U and ^{232}Th of few selected samples were measured using High Purity Germanium Gamma Spectrometry (HPGe) in Nuclear Laboratory, Faculty of Science, Universiti Teknologi Malaysia for verification with neutron activation analysis. The details of the gamma ray method used are discussed in Section 3.4. The few samples were selected for neutron activation analysis (NAA) in Malaysian Nuclear Agency (MNA) for verification of the present work. The closest three out of the few selected samples were S1L7, S3L4 and S4L1 respectively. The details of the NAA processes discussed in Section 3.4.

4.4.1 Verification of ^{238}U, ^{232}Th Using Neutron Activation Analysis (NAA)

Few samples were prepared and sent to Malaysian Nuclear Agency for irradiation using PUSPATI TRIGA MARK II reactor. Each sample about 0.2 g was prepared in a polyethylene vial and labelled accordingly. Each sample has duplicates to ensure quality of the analytical technique. A uranium-thorium standard solution of 100 ppm U and 98 ppm Th was used. Approximately, 0.1000 g (ml) U-Th solution was mixed with small amount of Silica (SiO_2-IAEA) in a vial (2.5 ml) and placed in an oven for 4 hours at 60 °C until dry; then the vial was labelled and sealed.

This technique was adopted in this work in order to verify the results obtained using gross gamma method (HPGe GRS). The results of NAA method from Malaysian Nuclear Agency (MNA) and gross gamma method using HPGe gamma ray spectrometry are comparable as shown in Table 4.5. The results of the NAA and direct method analysis for ^{238}U and ^{232}Th for three samples are in good agreement,

except for sample S1L7 for ^{238}U where the concentration of the sample is lower than the detection limit. For ^{238}U, the average difference is 4.85 % whereas 8.8 % was the average difference for ^{232}Th. Based on the strong agreement between NAA and direct method results; further analysis was conducted using HPGe gamma ray spectrometry in this present work.

Table 4.5: Comparison between NAA and gross gamma method

Sample	NAA	Gross gamma method	^{238}U % Difference	NAA	Gross gamma method	^{232}Th % Difference
ID	^{238}U (ppm)	^{238}U (ppm)	^{238}U	^{232}Th (ppm)	^{232}Th (ppm)	^{238Th}
S1L7	<0.5	3.00 ± 0.3	-	22.90 ± 1.1	19.00 ± 2.0	21.0
S3L4	2.40 ± 0.1	2.46 ± 0.2	-2.4	15.90 ± 0.8	18.60 ± 2.0	-14.5
S4L1	2.20 ± 0.1	2.05 ± 0.2	-7.3	11.60 ± 0.2	11.83 ± 1.0	-2.0

4.4.2 Activity concentrations of ^{238}U, ^{232}Th and ^{40}K in Subsurface Rock Samples from Dei- Dei, Kubwa, Gosa and Lugbe Boreholes Layers

The objective of this measurement is to determine the activity concentration of ^{238}U, ^{232}Th and ^{40}K in different layers and the possible geological features that attribute to higher activity level in each subsurface structure. In addition, the activity concentrations of the rock samples from the four different borehole sites will be compared and also to the previous work reported in other countries.

The measurements were done on the rock samples collected from different subsurface layers drilled with the help of 30 ton capacity Rig machine coupled with high pressure air compressor made by INGERSOL with 25 ton capacity. The rocks were made from clay and sand, and the medium was heterogeneous as the thickness of the different layers differed in the boreholes. The cutting method of drilling by technical procedure (TP 8.0,Rev. 15, 2003) was used. The identification of

boundaries between layers with noticeably different particle sizes using visual manual logging method and record the thickness as layer changes. Layer thickness change may range from less than one metre to tens of metres. Distinct layers with clearly marked on plastic sock with an indelible felt-tipped pen, using a single entry for each layer on the plastic poly bag for easy identification.

A total of 31 rock samples were collected from the four boreholes in different locations of the study area. In addition, the samples were labeled using borehole number and depth drilled on each polyethylene bag as discussed in Section 3.2.5.

Measured concentrations of K, nuclides from ^{232}Th series (^{208}Tl, ^{228}Ac) and ^{238}U series (^{214}Pb and ^{214}Bi) in investigated rock samples for each location are discussed in Section 4.4.3. The details of sample preparations for gamma analysis are discussed in Section 3.3.

4.4.3 Activity Concentration of ^{238}U, ^{232}Th and ^{40}K in Dei-Dei Borehole Rock Samples

In Dei-Dei borehole area, eleven (11) different layer samples were collected lithologically. The samples were labeled accordingly as S1L1 to S1L11 up to below ground the level of about 70 m. The objective is to determine the layer that constitutes the higher activity level and the source rock in subsurface formation. The measurement was done using HPGe detector, all the details of sample preparation, analysis and calculations for gamma ray analysis are presented in Section 3.3 and 3.3.7 respectively.

The activity concentrations of ^{238}U, ^{232}Th and ^{40}K in each layer from Dei-Dei borehole rock samples, S1L1 to S1L11 were measured as shown in Tables 4.6. ^{238}U activity concentrations were calculated as the arithmetic means of the activities of

^{214}Pb and ^{214}Bi isotopes and ^{208}Tl and ^{228}Ac isotopes for ^{232}Th. The concentrations of K in (%) was determined from the value obtained in Bq kg^{-1}, ^{232}Th and ^{238}U (ppm) in measured samples were calculated using conversion factors given by IAEA, 1989, and the values obtained are presented in Table 4.6 in Bq kg^{-1}. For all rocks Th/U ratio was calculated.

Table 4.6: Activity concentrations of ^{238}U, ^{232}Th (ppm); K (%) and (Bq kg^{-1}) in Dei-Dei borehole layers

Sample	Concentration			Activity concentration (Bq kg^{-1})			Th/U Ratio
	^{238}U (ppm)	^{232}Th (ppm)	K (%)	^{238}U	^{232}Th	^{40}K	
S1L1	2.7 ± 0.3	13.0 ± 1.0	0.8 ± 0.1	33.8 ± 3.2	52.8 ± 4.1	253.5 ± 31.3	4.7 ± 0.6
S1L2	2.2 ± 0.2	11.0 ± 1.0	1.3 ± 0.2	26.6 ± 2.6	44.7 ± 4.1	416.3 ± 50.1	5.1 ± 0.7
S1L3	2.2 ± 0.2	13.0 ± 1.0	3.8 ± 0.5	27.3 ± 2.6	52.8 ± 4.1	1195. 7±150.2	5.9 ± 0.7
S1L4	2.2 ± 0.2	14.0 ± 1.0	1.9 ± 0.2	26.7 ± 2.6	56.8 ± 4.1	601.0 ± 75.1	6.5 ± 0.8
S1L5	3.0 ± 0.3	18.0 ± 1.0	2.6 ± 0.3	36.9 ± 3.6	73.1 ± 4.1	801.3 ± 100.2	6.0 ± 0.7
S1L6	2.8 ± 0.3	16.0 ± 1.0	2.7 ± 0.3	34.3 ± 3.3	65.0 ± 4.1	829.5 ± 103.3	5.8 ± 0.7
S1L7	3.0 ± 0.3	19.0 ± 1.0	3.4 ± 0.4	37.1 ± 3.6	77.1 ± 4.1	1073.6± 134.6	6.3 ± 0.9
S1L8	1.4 ± 0.1	11.0 ± 1.0	2.8 ± 0.4	17.5 ± 1.7	44.7 ± 4.1	873.3 ± 109.6	7.8 ± 1.0
S1L9	2.8 ± 0.3	24.0 ± 2.0	3.2 ± 0.4	34.0 ± 3.2	97.4 ± 8.1	998.5 ± 125.2	8.7 ± 1.1
S1L10	2.0 ± 0.2	19.0 ± 2.0	3.5 ± 0.4	25.1 ± 2.5	77.1 ± 8.1	1101.8 ±137.7	9.4 ±1.4
S1L11	2.5 ± 0.2	24.0 ± 2.0	3.2 ± 0.4	31.4 ± 2.5	97.4 ± 8.1	1011.0± 137.7	9.5 ± 1.1
			Mean	30.1± 2.9	67.2± 5.2	832.3± 105.0	6.9 ± 0.9

Data presented in Table 4.6 shows that radioactive equilibrium between progenies in ^{232}Th series for all rock samples can be assumed. Some measured rocks are characterized by very high values of activity concentrations of ^{232}Th. The highest activity value for ^{232}Th refers to the sample from the depth to the bottom of aquifer bearing formation (S1L11), with the activity concentration of 97.4 ± 8.1 Bq kg^{-1}. Activity concentrations of ^{232}Th in the investigated rocks varies in the range from 44.7 ± 4.1 Bq kg^{-1} to 97.4 ± 8.1 kg^{-1} in the Borehole layers with a mean value of 67.2± 5.2 Bq kg^{-1}. Lower activity value of ^{232}Th of 44.7 ± 4.1 Bq kg^{-1} was noted in site one layer two (S1L2). Noted activity concentrations were compared with average activity concentrations of ^{232}Th in the continental crust i.e. 44 Bq kg^{-1} and in the soil i.e. 37 Bq kg^{-1} (Eisenbud and Gesell, 1997). The highest measured value of ^{232}Th

activity concentration exceeds the average activity concentration refers to the continental crust almost twice in S1L11, site one layer eleven (Maxwell et al., 2013a).

In the same Dei-Dei borehole rock samples, the highest activity concentration values of ^{238}U refer to the samples collected from the S1L7 with the values of 37.1 ± 3.6 Bq kg^{-1}. Distinctly lower value was obtained from S1L8 with a value of 17.5 ± 1.7 Bq kg^{-1}. ^{238}U concentration varies in the range from 17.5 ± 1.7 Bq kg^{-1} to 37.1 ± 3.6 Bq kg^{-1} respectively with a mean value of 30.1± 2.9 Bq kg^{-1} in Dei-Dei. For comparison, the arithmetic mean of the activity concentrations of ^{238}U from lower Silesia equals to 35 Bq kg^{-1} which is higher than the present work of 30.1± 2.9 Bq kg^{-1}. ^{238}U activity concentrations in granite from SzKlarska poreba (Karkonosze granite) vary in the wide range from 15 to 119 Bq kg^{-1} whereas in aplite and in mica schist from SzKlarska Poreba ^{238}U activity concentrations are 66 ± 6 Bq kg^{-1} and 54 ± 9 Bq kg^{-1} respectively (Przylibski, 2004). Comparing the activity concentrations of ^{238}U with the average activity concentrations of ^{238}U reported for the continental crust i.e. 36 Bq kg^{-1} and for soil i.e. 22 Bq kg^{-1} (Eisenbud and Gesell, 1997) with the present work, the average value of 30.1± 2.9 Bq kg^{-1} for ^{238}U is lower.

As shown in Table 4.6 for Dei-Dei borehole, ^{40}K activity concentrations for all the rock samples are greater than 200 Bq kg^{-1}. In first and second layers, the activity concentrations of the radionuclide do not differ much, but the lowest value was noted in first layer, S1L1 with a value of 253.5 ± 31.3 Bq kg^{-1},whereas the highest value refers to the sample layer three (S1L3) with a value of 1195.7 ± 150.2 Bq kg^{-1} respectively. The range varies from 253.5 ± 31.3 Bq kg^{-1} to 1195.7 ± 150.2 Bq kg^{-1} in Dei-Dei borehole with a mean value of 832 ± 103 Bq kg^{-1}. In contrast with the range of the average activity concentrations of ^{40}K reported for the continental crust i.e. 850 Bq kg^{-1} and for soil i.e. 400 Bq kg^{-1} (Eisenbud and Gesell, 1997), it can be seen that measured activity concentrations associated with K decay are distinctly higher than the average concentration of this isotope in the continental crust for all samples. The percentage is higher in layer three (S1L3) for about 3.82%. The plot of activity concentration of ^{232}Th, ^{238}U and K versus sample ID in Dei-Dei

is presented in Figure 4.16 indicating almost 100 % increase of ^{232}Th activity with depth (Maxwell et al., 2013a).

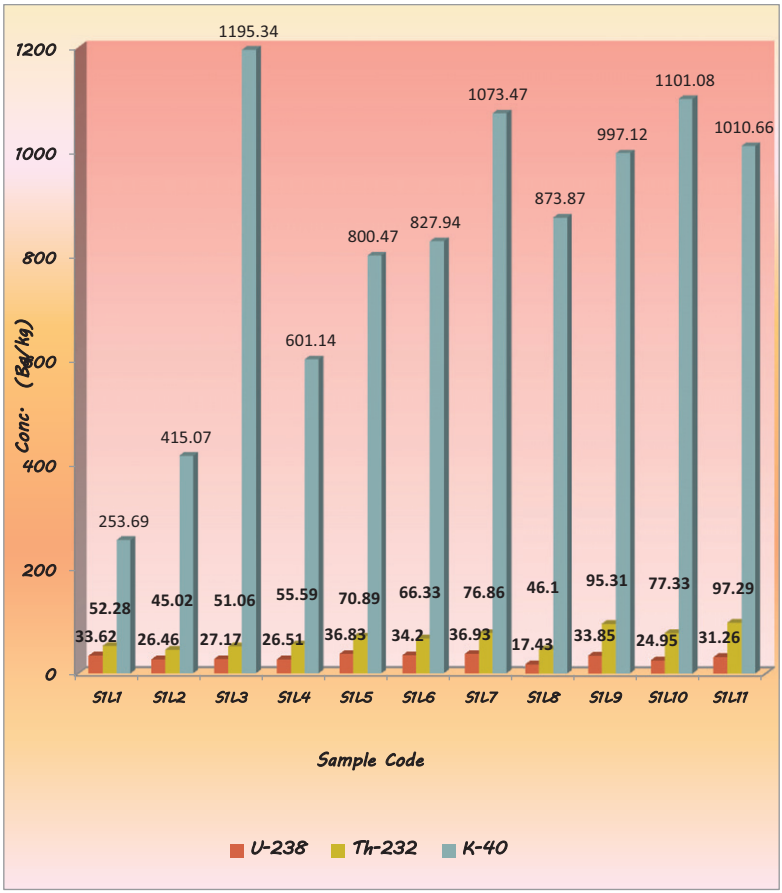

Figure 4.16 Activity concentration of ^{238}U, ^{232Th} and ^{40}K versus sample ID in Dei-Dei borehole, Abuja.

4.4.4 Th/U Ratio in Rock Samples from Dei-Dei Borehole

The Th/U ratio varies ranging from 4.7 ± 0.6 to 9.5 ± 1.1 as shown in Table 4.6. The highest value refers to layer eleven (S1L11) with a value of 9.45 ± 1.1 whereas the lowest value was noted in the sample collected from first layer(S1L1) with a value of 4.7 ± 0.6 and rock type shows laterite top soil (Maxwell et al., 2013a). Obtained Th/U ratios are very high, higher than data published in literature relating to rocks of Karkonosze-Irera block. For example, in hornfel from Death Bend area, Th/U ratio equals to 3 and Th/U concentration ratio in rocks in the environs of Swieradow Zdroj varies between 1.5 and 3.2 (Malczewski *et al.*, 2005), is low compared to 9.5 ± 1.1 obtained in the present study by a factor of 3.

Th/U concentration ratio given by (Eisenbud and Gesell, 1997) for the continental crust equals to 1.2 and for granite is 1.8. Cited values are distinctly lower than Th/U concentration ratio obtained from the investigated rock samples from Dei-Dei borehole site. In addition, the value of Th/U ratio in the present work is greater than the measured value in granite from Szklarska Poreba that is equals to 3.2 (Plewa and Plewa, 1992). Obtained results suggest that very high content of ^{232}Th and high content of ^{238}U in investigated rock samples were related to being rocks formed due to thermal metamorphism and metasomatic processes (Maxwell et al. 2013a). These processes seem to be responsible for high level of radioactivity of rocks in the area. The highest value of Th/U concentration ratio refers to the deepest layer up to 70 m, S1L11. The lowest values of Th/U ratio concentrations was measured in rock sample collected at the laterite top soil to the depth of about 6 m thick, this lower value could be assigned to erosion impact on the surface of the soil.

4.4.5 Correlation of Lithologic Variation with the Activity Concentrations of ^{238}U, ^{232}Th and ^{40}K in Borehole Layers at Dei-Dei .

The objective of this correlation for different layers is to determine the rock types and the corresponding activity concentrations of ^{238}U, ^{232}Th and ^{40}K relating with the rock samples being measured with HPGe gamma spectrometry. Details about the correlations are listed in Table 4.7.

Table 4.7: Correlation between the lithologic rock layers and the activity concentration of ^{238}U, ^{232}Th and K (Bq kg^{-1}) in Dei-Dei borehole

Sample ID	Lithology description	Activity concentration (Bq kg^{-1})		
		^{238}U	^{232}Th	^{40}K
S1L1	Sandstone, brownish and ferruginous, interbedded with quartz feldspar	33.8 ± 3.2	52.7 ± 4.1	253.5 ± 31.3
S1L2	Coarse sand with clay, bright red.	26.6 ± 2.6	44.6 ± 4.1	415.3 ± 50.8
S1L3	Slightly micaceous Sandy clay, brownish pebbly, fine to coarse feldspar.	27.3 ± 2.6	52.8 ± 4.1	1195.6 ±151.2
S1L4	Fin to coarse sandy clayey and gravel	26.7 ± 2.6	56.8 ± 4.1	601.0 ± 75.1
S1L5	Sand. Brown, clayey at the top, fine to coarse	36.9 ± 3.6	73.1 ± 4.1	801.2 ± 100.2
S1L6	Light grey coarse sand, granite gravel	34.3 ± 3.3	65.0 ± 4.1	829.5 ± 103.3
S1L7	Silty sand feldspar, blackish to grey	37.1 ± 3.6	77.1 ± 4.1	1073.6 ± 134.6
S1L8	Grey silty sand, low grade	18.5 ± 1.7	44.7 ± 4.1	873.3 ± 109.6
S1L9	Greyish to Purple silty sand	34.0 ± 3.2	97.4 ± 8.1	998.5 ± 125.2
S1L10	Sand, fine to coarse, pebbly blackish to grey	25.1 ± 2.5	77.1 ± 8.1	1101.8 ±137.7
S1L11	Sand, fine to medium-grained, blackish to grey becoming whitish from 69m	31.4 ± 2.5	97.4 ± 8.1	1011.0 ± 137.7

The data presented in Table 4.7 shows that the highest value for ^{40}K refers to the sample layer three (S1L3). Correlating the ^{40}K activity concentration with the lithology in S1L3, it could be observed that the highest ^{40}K activity value corresponds to slightly micaceous sandy clay, brownish pebble, fine to coarse feldspar. The geologic types that constitute such high activity level are inferred to be the cross-bedding of undifferentiated Pan-African granite and biotite-homblende granodiorite as shown in Appendix B. The lowest value noted in S1L1 is due to sandstone, brownish and ferruginous, interbedded with quartz feldspar. The presence of ferrugenous composition in the host rock samples could have masked off the activity of ^{40}K thereby reporting low activity level in the rock sample.

Correlation between lithologic rock layers and activity of ^{232}Th in Dei-Dei borehole presented in Table 4.7 shows the highest value in S1L11 and noted that the rock sample from that layer is made of sand, fine to medium-grained, blackish to grey becoming whitish from the depth of 69 m to 70 m. It could be that the activity concentration of natural radionuclides in rocks are connected to radionuclides in groundwater which reacts with soil and bedrock and release quantities of dissolved components, depending on the mineralogical and geochemical composition of the rock. The redox conditions and the residence time of groundwater in the soil and bedrock may also contribute to such higher value in Dei-Dei borehole. The geologic type is inferred to be Pan-African granite (undifferentiated). The lower value reported in S1L2 constitute coarse sand interbedded with clay, bright red. This low activity level could be caused by the deformed and fractured characteristic of the layer formation due to tectonic activity in the area.

The correlation of rock samples from the subsurface layers and measured activity concentration of ^{238}U in Dei-Dei borehole indicates that the highest values refer to the samples collected from the S1L5 and S1L7 respectively as shown in Table 4.7. It can be observed that the major rock minerals were sand, brown clayey at the top, fine to coarse for S1L5 and silty sand feldspar, blackish to grey were the major rock lithology for S1L7 respectively. Such lithologic rock type could be inferred to Pan-African granite with some fractions of biotite homblende metamorphosed together in the samples. Distinctly lower value was noted in S1L8

with lithologic description of grey silty sand, low grade which could support oxidization of ^{238}U in aqueous phase since the aquiferous zone of the water bearing formation extended to the layer; and the disperse the activity to neighbouring layers, S1L7 and S1L9, respectively (Maxwell *et al*., 2013). The geology could be weathered Pan-African granite.

4.4.6 Activity Concentration of ^{232}Th, ^{238}U and ^{40}K in Kubwa Borehole Rock Samples

In Kubwa borehole source, a total of nine (9) different layer samples were collected lithologically. The samples were labeled accordingly ranging from S2L1 to S2L9 below ground level up to about 60 m. The activity concentrations of ^{238}U, ^{232}Th and ^{40}K in each layer from Kubwa borehole rock samples, S2L1 to S2L9 were measured and presented in Tables 4.8.

Table 4.8: Activity concentrations of ^{238}U, ^{232}Th (ppm); K (%) and (Bq kg^{-1}) in Kubwa borehole layers

Sample	Concentration			Activity concentration (Bq kg^{-1})			Th/U Ratio
	^{238}U (ppm)	^{232}Th (ppm)	K (%)	^{238}U	^{232}Th	^{40}K	
S2L1	4.2 ± 0.4	21.0 ± 2.0	0.38 ± 0.1	51.7 ± 5.0	85.3 ± 8.1	118.9 ± 15.7	5.01 ± 0.7
S2L2	1.9 ± 0.1	8.0 ± 1.0	1.27 ± 0.2	23.0 ± 1.2	32.5 ± 4.1	397.5 ± 50.1	4.30 ± 0.6
S2L3	2.6 ± 0.3	14.0 ± 1.0	1.94 ± 0.3	32.6 ± 3.7	56.8 ± 4.1	607.2 ± 78.3	5.30 ± 0.7
S2L4	3.2 ± 0.3	9.0 ± 1.0	2.03 ± 0.3	39.0 ± 3.7	36.5 ± 4.1	635.4 ± 81.4	2.85 ± 0.4
S2L5	1.2 ± 0.1	10.0 ± 1.0	1.63 ± 0.2	15.7 ± 1.2	40.6 ± 4.1	510.2 ± 62.6	8.40 ± 1.1
S2L6	2.8 ± 0.3	17.0 ± 1.0	2.25 ± 0.3	34.3 ± 3.7	69.0 ± 4.1	704.3 ± 87.6	6.12 ± 0.8
S2L7	3.5 ± 0.3	19.0 ± 2.0	2.22 ± 0.3	42.7 ± 3.7	77.1 ± 8.1	694.9 ± 84.5	5.49 ± 0.8
S2L8	3.3 ± 0.3	19.0 ± 2.0	2.36 ± 0.3	40.3 ± 3.7	77.1 ± 8.1	738.7 ± 93.9	5.83 ± 0.8
S2L9	2.5 ± 0.2	17 ± 1.0	2.40 ± 0.3	31.1 ± 2.5	69.0 ± 4.1	751.2 ± 93.9	6.75 ± 0.7
			Mean	34.4± 3.2	60.5± 5.4	573.1± 72.0	5.56± 0.7

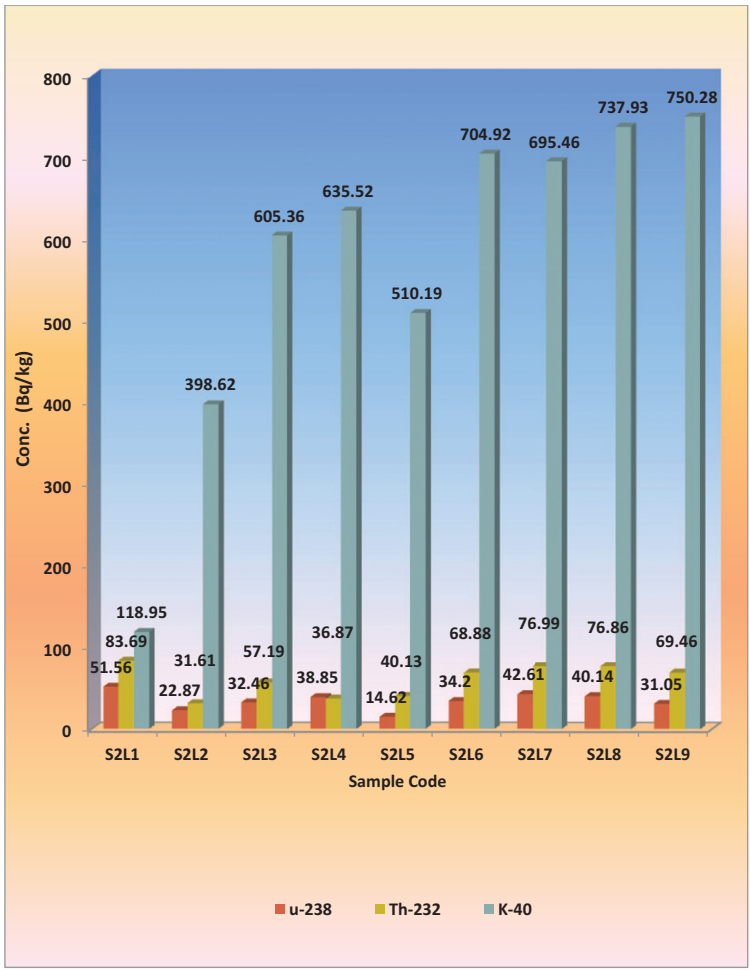

Figure 4.17 Activity concentration of ^{238}U, ^{232Th} and ^{40}K versus sample ID in Kubwa borehole, Abuja

Data presented in Table 4.8 is the elemental concentration and activity concentrations of ^{238}U, ^{232}Th and ^{40}K from Kubwa borehole samples. Table 4.8 shows that the higher activity concentration of ^{232}Th refers to sample layer one (S2L1) with the value of 85.3 ± 8.1 Bq kg^{-1}. Sample collected from second layer (S2L2) has value of 32.5 ± 4.1 Bq kg^{-1} and is distinctly lower. It was observed that S2L7 and S2L8 activity concentrations of ^{232}Th reported similar activity level with values of 77.1 ± 8.1 and 77.1 ± 8.1 Bq kg^{-1} respectively. This closeness in activity values may be attributed to metamorphism process of Pan-African events. The activity concentrations of ^{232}Th varies from 32.5 ± 4.1 to 85.3 ± 8.1 Bq kg^{-1} with a mean value of 60.5 ± 5.4 Bq kg^{-1}in Kubwa borehole. Noted activity concentrations were compared with average activity concentrations of ^{232}Th in the continental crust as reported by (Eisenbud and Gesell, 1997). The measured value of ^{232}Th activity concentration in (S2L1) exceeds the average activity concentration compared to the continental crust almost twice, (Maxwell et al., 2013a).

Measured rocks are characterized by radioactivity of ^{238}U in Kubwa borehole. The highest value refers to the sample collected from S2L1, (51.7 ± 5.0 Bq kg^{-1}). Distinctly lower value was obtained from S2L5 with a value of 15.7 ± 1.2 Bq kg^{-1} as shown in Table 4.8. ^{238}U concentration in Kubwa borehole varies ranging from 15.7 ± 1.2 Bq kg^{-1} to 51.7 ± 5.0 Bq kg^{-1} respectively, with a mean value of 34.4± 3.2 Bq kg^{-1}. Comparing the range of 15 ± 1 Bq kg^{-1} to 52 ± 5 Bq kg^{-1} of ^{238}U in the present study with ^{238}U activity concentrations in granite from SzKlarska poreba (Karkonosze granite) varying widely from 15 to 119 Bq kg^{-1}, they are within the normal range. Przylibski, (2004) reported 66 ± 6 Bq kg^{-1} and 54 ± 9 Bq kg^{-1} for ^{238}U with a mean value of 35 Bq kg^{-1} from lower Silesia. Comparing the mean value of the present work, 34 Bq kg^{-1} with Przylibski, (2004), they are in good agreement. Measured activity concentrations of ^{238}U were compared with the average activity concentrations of ^{238}U reported by Eisenbud and Gesell (1997) in continental crust; the average activity concentrations of ^{238}U in the present study are higher except in samples S2L2, S2L3, S2L5 and S2L9 respectively, (Maxwell et al., 2013a).

As shown in Table 4.8, ^{40}K activity concentrations for all the rock samples are greater than 100 Bq kg^{-1}. The activity concentrations of ^{40}K did not differ much,

but the lowest value was noted in first layer (S2L1) with a value of 118.9 ± 15.7 Bq kg^{-1}, whereas the highest value refers to the sample layer nine (S2L9) with a value of 751.2 ± 93.9 Bq kg^{-1} . The range varies between 118.9 ± 15.7 Bq kg^{-1} to 751.2 ± 93.9 Bq kg^{-1} in Kubwa borehole with a mean value of 573.1± 72.0 Bq kg^{-1}. Compare to the range of the average activity concentrations of ^{40}K reported by Eisenbud and Gesell, (1997), it can be seen that the measured activity concentrations associated with ^{40}K decay are distinctly lower than the average concentration reported in the continental crust for some samples from Kubwa Borehole. In Figure 4.17 for Kubwa borehole samples, it can be observed that ^{40}K increases with depth compared to Dei-Dei borehole samples as shown in Figure 4.16. They strongly agree with the distinct increase of ^{40}K with depth below ground level. It may be due to the process of deposition of sediments in the subsurface layers within the region which might differ in other areas.

4.4.7 Th/U Ratio in Rock Samples from Kubwa Borehole

The Th/U ratio varies in the range from 2.85 ± 0.4 to 8.40 ± 1.1. The highest value refers to sample layer five (S2L5) with a value of 8.40 ± 1.1 whereas the lowest value was noted in the sample collected from fourth layer (S2L4) with a value of 2.85 ± 0.4 as shown in Table 4.8. Obtained Th/U concentration ratios are higher in the present work compared to data published in literature concerning rocks of Karkonosze-Irera block, by Malczewski *et al*., (2005) and Eisenbud and Gesell (1997) from the investigated rock samples at Kubwa borehole (Maxwell et al.,2013b).

4.4.8 Correlation of Lithologic Variation and the Activity Concentration of ^{238}U, ^{232}Th and ^{40}K in Borehole Layers at Kubwa .

The objective of this correlation of different layers is to determine the relationship between rock type and the corresponding activity concentrations of ^{238}U, ^{232}Th and ^{40}K with the rock samples being measured with HPGe gamma ray spectrometry. Details of the correlations are listed in Table 4.9.

Table 4.9: Correlation between the lithologic rock type and the activity concentration of ^{238}U, ^{232}Th and ^{40}K (Bq kg^{-1}) in Kubwa borehole

Sample ID	Lithology description	Activity concentration (Bq kg^{-1})		
		^{238}U	^{232}Th	^{40}K
S2L1	Brownish ash sandy clay gravely interbedded.	51.8 ± 4.9	85.3 ± 8.1	118.9 ± 15.7
S2L2	Clay with bright red.	22.9 ± 1.2	32.5 ± 4.1	397.5 ± 50.1
S2L3	Sandy clay micaceous, brownish with feldspar.	32.6 ± 3.7	56.8 ±4.1	607.2 ± 78.3
S2L4	Fin to coarse sandy clayey and gravel smoky	39.0 ± 3.7	36.5 ± 4.1	635.4 ± 81.4
S2L5	Clay sandy, fine grain size, darkish ash feldspar	14.7 ± 1.2	40.6 ± 4.1	510.2 ± 62.6
S2L6	Silty clay, interbedded, bright ash to glacy feldspar.	34.3 ± 3.7	69.0 ± 4.1	704.3 ± 87.6
S2L7	Fine to coarse ashy sandy clay.	42.7 ± 3.7	77.1 ± 8.1	694.9 ± 84.5
S2L8	Fine to coarse sand, greyish.	40.3 ± 3.7	77.1 ± 8.1	738.7 ± 93.9
S2L9	Micaceous - gravely sandy, fine-medium coarse darkish to grey.	31.1 ± 2.5	69.0 ± 4.1	751.2 ± 93.9

Comparison of the lithological layer variations and the activity concentrations of ^{238}U, ^{232}Th and ^{40}K in Kubwa area as shown in Table 4.9, it can be noted that brownish ash sandy clay, gravely interbedded, constituted the highest activity value for ^{238}U and ^{232}Th as in S2L1 which is inferred to be porphyroblastic gneisse and

biotite homblende granidiorite geologically. On the other hand, micaceous - gravely sandy, fine-medium coarse darkish to grey reported higher activity of ^{40}K as in S2L9, which could be felsinc sediments of migmatite gneiss intrusion.

4.4.9 Activity Concentration of ^{232}Th, ^{238}U and ^{40}K in Gosa Borehole Rock Samples.

In Gosa borehole, a total of six (6) different layer rock samples were collected lithologically. The samples were labeled accordingly from S3L1 to S3L6 to depth below ground level up to about 50 m. A summary of the average activity concentrations of ^{238}U, ^{232}Th and ^{40}K in each layer from Gosa borehole rock samples labelled S3L1 to S3L6 were measured and the values are presented in Tables 4.10.

Table 4.10: Activity concentrations of ^{238}U, ^{232}Th (ppm), K (%) and (Bq kg^{-1}) in Gosa borehole layers

Sample ID	Concentration			Activity concentration (Bq kg^{-1})			Th/U Ratio
	^{238}U (ppm)	^{232}Th (ppm)	K (%)	^{238}U	^{232}Th	^{40}K	
S3L1	2.1 ± 0.2	11.8 ± 1.0	1.4 ± 0.2	25.3 ± 2.5	48.0 ±4.1	438.2± 56.3	5.8±0.7
S3L2	1.9 ± 0.2	16.2 ± 1.0	1.6 ± 0.2	23.0 ± 2.5	65.9 ±4.1	497.7 ± 62.6	8.7± 1.1
S3L3	1.8 ± 0.2	16.5 ± 1.0	1.5 ± 0.2	22.6 ± 2.5	67.0 ±4.1	472.6 ± 56.3	9.0± 1.1
S3L4	2.5 ± 0.2	18.6 ± 2.0	2.6 ± 0.3	30.4 ± 2.5	75.5±8.1	820.1± 103.3	7.6± 1.0
S3L5	2.2 ± 0.2	12.9 ± 1.0	2.2 ± 0.3	27.7 ± 2.5	52.5± 4.1	698.0± 87.6	5.8± 0.7
S3L6	2.3 ± 0.2	16.7 ± 1.0	1.6 ± 0.2	27.9 ± 2.5	68.0± 4.1	513.3± 65.7	7.4± 0.8
			Mean	26.1± 2.5	62.8± 4.8	573.3± 73.0	7.4± 0.9

In Table 4.10 of Gosa data, it can be observed that the activity concentration of ^{238}U ranged from 22.6 ± 2.5 to 30.4 ± 2.5 Bq kg^{-1}; ^{232}Th varied from 48.0 ± 4.1 to 75.5 ± 8.1 Bq kg^{-1} and ^{40}K varied from 438.2 ± 56.3 to 820.1 ± 103.3 Bq kg^{-1}. The mean values are 26.1 ± 2.5 Bq kg^{-1}; 62.8± 4.8 Bq kg^{-1} and 573.3 ± 73.0 Bq kg^{-1} for ^{238}U, ^{232}Th and ^{40}K respectively. Sample layer four (S3L4) has the highest

activities for ^{238}U, ^{232}Th and ^{40}K with values of 30.4 ± 2.5 Bq kg^{-1} , 75.5 ± 8.1 Bq kg^{-1} and 820.1 ± 103.3 Bq kg^{-1} respectively in a single layer. The lowest values of ^{238}U, ^{232}Th and ^{40}K were observed in different layers. The lower activity of ^{238}U was noted in site three layer three (S3L3) with a value of 22.6 ± 2.5 Bq kg^{-1} whereas site three layer one (S3L1) reported the lowest activities for ^{232}Th and ^{40}K with values of 48.0 ± 4.1 Bq kg^{-1} and 438.2 ± 56.3 Bq kg^{-1} respectively (Maxwell *et al*., 2013b). The average activity concentration for ^{238}U reported in continental crust is 36 Bq kg^{-1} and for soil is 22 Bq kg^{-1}, for ^{232}Th, the value for continental crust is 44 Bq $kg^{-1}$and for soil is 37 Bq kg^{-1} and for ^{40}K, the value for continental crust is 850 Bq kg^{-1} and in soil 400 Bq kg^{-1}. At Gosa borehole, the activity for ^{238}U is close to the report by Eisenbud and Gesell, (1997), whereas the highest value for ^{232}Th is 76 Bq kg^{-1} which exceeds the value for continental crust by a factor of 1.7. In the case of ^{40}K, it is 820.1 ± 103.3 Bq kg^{-1} lower compared to 850 Bq kg^{-1} reported by Eisenbud and Gesell, (1997). In Figure 4.18, it can be observed that the ^{238}U, ^{232}Th and ^{40}K reported higher in a single sample layer four (S3L4) which may have been as a result of deformed nature of sample layer three (S3L3) by distributing its activities to the neighbouring layer four downward (S3L4), (Maxwell et al., 2013b).

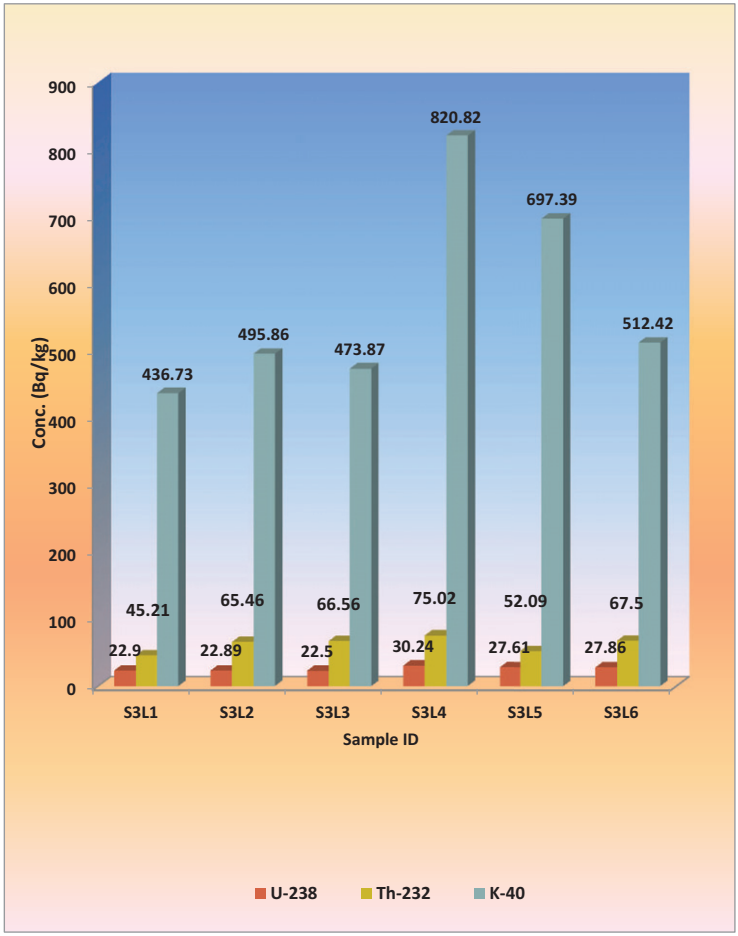

Figure 4.18 Activity concentration of ^{238}U, ^{232Th} and ^{40}K versus sample ID in Gosa borehole, Abuja

4.4.10 Th/U Ratio in Rock Samples from Gosa Borehole

The Th/U ratio in Gosa borehole ranged from 5.55 ± 0.7 to 9.02 ± 1.1 as shown in Table 4.10. Sample layer three (S3L3) reported the highest Th/U ratio of 9.02 ± 1.1 whereas Sample S3L1 and S3L5 have the lowest Th/U ratio of 5.77 ± 0.7. Th/U ratio given by Eisenbud and Gesell (1997) for the continental crust equals to 1.2 and for granite is 1.8. At Gosa borehole, the Th/U ratio is 7 and 5 times higher than the average values for continental crust and granite respectively. For example, in hornfel from Death Bend area, Th/U is 3 and Th/U ratio in rocks in the environs of Swieradow Zdroj varies between 1.5 and 3.2 respectively, (Malczewski, 2005). In comparison with the present work at Gosa, the Th/U ratio of 9.02 exceeds the report from Malczewski (2005) by 3 times (Maxwell et al., 2013b).

4.4.11 Correlation of Lithologic Variation and the Activity Concentrations of ^{238}U, ^{232}Th and ^{40}K in Borehole Layers at Gosa

The objective of correlating different layers is to determine the rock type and the corresponding activity concentrations of ^{238}U, ^{232}Th and ^{40}K being measured with HPGe gamma ray spectroscopy at Gosa borehole layers. Details of the correlations are listed in Table 4.11.

Table 4.11: Correlation between the lithologic rock type and the activity concentration of ^{238}U, ^{232}Th and ^{40}K (Bq kg^{-1}) in Gosa borehole.

Sample ID	Lithology description	Activity concentration (Bq kg^{-1})		
		^{232}U	^{232}Th	^{40}K
S3L1	Sandy clay, reddish brown laterite top soil.	25.3 ± 2.5	48.0 ± 4.1	438.2 ± 56.3
S3L2	Sandy clay, fine to medium, reddish to yellow.	23.0 ± 2.5	65.9 ± 4.1	497.7 ± 62.6
S3L3	Clay sandy feldspar Yellowish brown pebbly	22.6 ± 2.5	67.0 ± 4.1	472.6 ± 56.3
S3L4	Micaceous clayey, grey to black	30.4 ± 2.5	75.5 ± 8.1	820.1 ± 103.3
S3L5	Sandy shinny greyish to black feldspar.	27.7 ± 2.5	52.5 ± 4.1	698.0 ± 87.6
S3L6	Fine medium shinny, qartz interbed, greyish ash feldspar	27.9 ± 2.5	68.0 ± 4.1	513.3 ± 65.7

Correlating the lithological arrangement of the layers with the corresponding activity concentrations of ^{238}U, ^{232}Th and ^{40}K to determine the rock type with the highest activity level are shown in Table 4.11 for Gosa borehole. It is noted that micaceous clayey, grey to black rock constituted the highest activity value which is inferred to be porphyroblastic gneisse and biotite homblende granodiorite geologically for ^{238}U, ^{232Th} and ^{40}K in the same sample layer four (S3L4). The sandy clay, fine to medium, reddish to yellow and clay sandy feldspar Yellowish brown pebbly in S3L2, S3L3 and S3L1 constituted the lower activity values for ^{238}U and ^{40}K respectively in Gosa area. This may be due to the presence of intrusion of basic and altrabasic minerals in a minor quantity that would have turned sandy clay to yellowish at a reasonable depth.

4.4.12 Activity Concentrations of ^{232}Th, ^{238}U and ^{40}K in Lugbe Borehole Rock Samples

A total of five (5) samples were collected from the subsurface layers at Lugbe and labeled accordingly for easy identifications which are from S4L1 to S4L5 below ground level up to the depth of about 40 m. The objective is to determine the source rock that gave the highest activity level of radionuclides in the subsurface formation at Lugbe.

A summary of the average activity concentrations of ^{238}U, ^{232}Th and K in each subsurface layer from Lugbe borehole rock samples, S4L1 to S4L5 were measured are presented in Tables 4.12. ^{238}U activity concentrations were calculated as the arithmetic means of the activities fot ^{214}Pb and ^{214}Bi isotopes and ^{208}Tl and ^{228}Ac isotopes for ^{232}Th. The concentrations of ^{40}K (%), ^{232}Th and ^{238}U (ppm) in measured samples were calculated using conversion factors given by IAEA, 1989 are as shown in Table 4.12 in Bq kg^{-1}. For all rocks Th/U ratio was calculated.

Table 4.12: Activity concentrations of ^{238}U, ^{232}Th (ppm), K (%) and (Bq kg^{-1}) in Lugbe borehole layers.

Sample ID	Concentration			Activity concentration (Bq kg^{-1})			Th/U Ratio
	^{238}U (ppm)	^{232}Th (ppm)	K (%)	^{238}U	^{232}Th	^{40}K	
S4L1	1.8 ± 0.2	11.2±1.0	3.2± 0.4	22.6 ± 2.5	45.5± 4.1	1011.0±128.3	6.1± 0.9
S4L2	1.5 ± 0.1	10.7±1.0	3.1± 0.4	18.0 ± 1.2	43.6± 4.1	970.3±122.7	7.4± 0.9
S4L3	1.7 ± 0.2	12.0 ±1.0	2.9± 0.4	21.5 ± 2.5	48.6± 4.1	907.7±115.8	6.9± 1.0
S4L4	1.8 ± 0.2	12.2±2.0	2.8± 0.4	21.9 ± 2.5	49.6 ±8.1	870.1±110.6	6.9± 1.4
S4L5	1.3 ± 0.1	11.5±1.0	2.6± 0.3	16.1 ± 1.2	46.7 ±4.1	816.9±103.3	8.9± 1.0
			Mean	20.0± 2.0	46.8± 4.9	915.2± 116.1	7.2± 1.0

In Table 4.12, it is noted that the activity concentration of ^{238}U varied from 16.1 ± 1.2 to 22.6 ± 2.5 Bq kg^{-1}, ^{232}Th varied from 43.6 ± 4.1 to 49.6 ± 8.1 Bq kg^{-1}, and ^{40}K varied from 816.9 ± 103.3 to 1011.0 ± 128.3 Bq kg^{-1} with mean values of

20.0 ± 2.0 Bq kg^{-1}, 46.8 ± 4.9 Bq kg^{-1} and 915.2 ± 116.1 Bq kg^{-1} respectively for ^{238}U, ^{232}Th and ^{40}K in Lugbe borehole. In Table 4.12 , rock sample layer one (S4L1) from Lugbe borehole reported the highest activity concentrations for ^{238}U and K with values 22.6 ± 2.5 Bq kg^{-1} and 1011.0 ± 128.3 Bq kg^{-1} respectively. Sample layer four (S4L4) reported highest activity concentration for ^{232}Th with a value 49 ± 4 Bq kg^{-1}. The lowest values were obtained in same sample layer five (S4L5) for ^{238}U and ^{40}K with values 16.1 ± 1.2 Bq kg^{-1} and 816.9 ± 103.3 Bq kg^{-1} for ^{238}U and ^{40}K respectively whereas Sample layer two (S4L2) reported the lowest ^{232}Th with a value of 44 ± 4 Bq kg^{-1} (Maxwell et al., 2013b). The average activity concentration for ^{238}U in Lugbe borehole rock samples is 20 Bq kg^{-1}, 47 Bq kg^{-1} for ^{232}Th and 915 Bq kg^{-1} for ^{40}K. The average activity concentrations for ^{238}U reported in continental crust is 36 Bq kg^{-1} and for soil is 22 Bq kg^{-1}, for ^{232}Th, continental crust is 44 Bq kg^{-1} and for soil is 37 Bq kg^{-1} and for K, continental crust is 850 Bq kg^{-1} and for soil 400 Bq kg^{-1}, Eisenbud and Gesell (1997). Compared the values of the present work from Lugbe borehole rock samples to Eisenbud and Gesell (1997), the activity concentration of ^{238}U and ^{232}Th are within the range but for ^{40}K, it is 1.2 times higher than the report by Eisenbud and Gesell (1997). The 19.22 % decrease in activity concentration of ^{40}K with depth is noted at a glance in Figure 4.19. This decrease in activity concentrations of ^{40}K with depth could be attributed to the chemical weathering and magma flow which may have deposited felnsic sediments with depth during the cooling in the metamorphic processes in the area, , (Maxwell et al., 2013b).

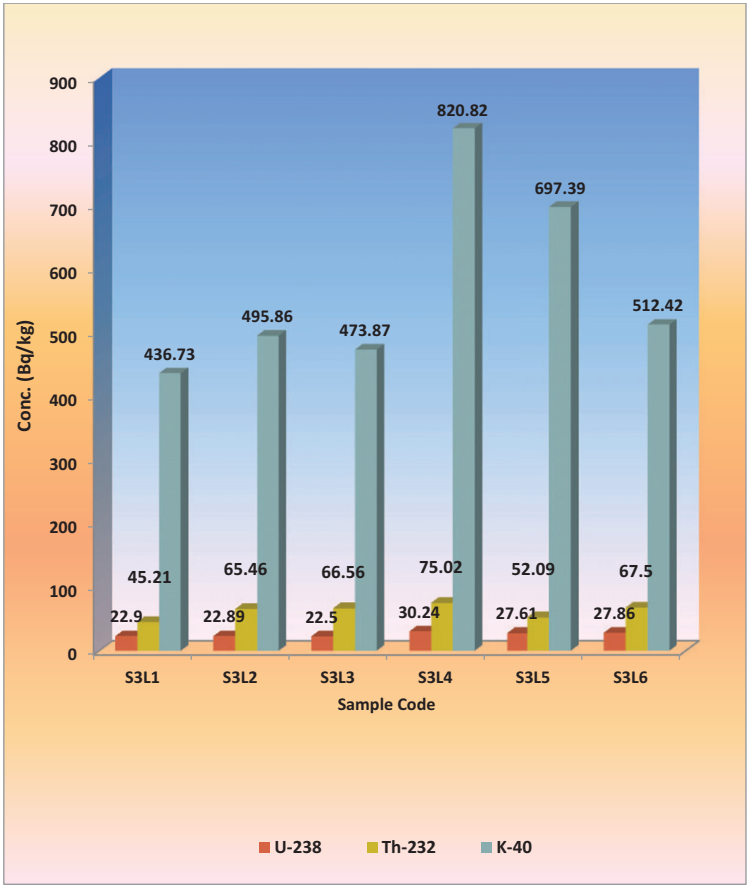

Figure 4.19 Activity concentration of ^{238}U, ^{232}Th and ^{40}K versus sample layers ID in Lugbe borehole, Abuja

4.4.13 Th/U Ratio in Rock Samples from Lugbe Borehole

The Th/U ratio ranged from 6.13 ± 0.8 to 8.85 ± 1.0 as shown in Table 4.12. The highest Th/U ratio of 8.85 ± 1.0 was obtained from sample layer five (S4L5) and lowest Th/U ratio from sample layer one (S4L1) is 6.13 ± 0.8. Th/U ratio given by Eisenbud and Gesell (1997), for the continental crust is 1.2 and for granite is 1.8. The Th/U ratio in the present work has a value 7 and 4 times higher than the average value for the continental crust and granite respectively (Maxwell *et al*. 2013b). For example, in hornfel from Death Bend area, Th/U is 3 and Th/U ratio in rocks in the environs of Swieradow Zdroj varies between 1.5 and 3.2, (Malczewski, 2005), comparing with the present study, it is twice compared the value reported by Malczewski (2005).

4.4.14 Correlation of Lithologic Variation and the Activity Concentrations of ^{238}U, ^{232}Th and ^{40}K in Borehole Layers at Lugbe

The purpose of this correlation of different layers in Lugbe subsurface rock samples is to determine the geology rock type and the corresponding activity concentrations of ^{238}U, ^{232}Th and ^{40}K being measured with HPGe gamma ray spectroscopy. Details of the correlations are listed in Table 4.13. Table 4.13 presented the lithologies and the corresponding activity concentrations of each subsurface layer. It can be observed that the topsoil, S4L1 that comprises laterite, yellowish brown in colour reported the highest activity concentration of ^{238}U and K. The geology of that location that could constitute such activity level is inferred to be intercalation of biotite-homblende graniodiorite and porphryblastic gneisses. It can be noted from Figure 3.3, the geologic map of the study area that a glaring fracture cuts across the terrain of Lugbe toward other areas in NE-SW trend, hence, could enhance the mobility of oxidized ^{238}U in aqueous phase and K in feldspatic sediments thereby re-depositing at the near surface. The highest value of ^{232}Th was noted in sample layer four (S4L4).

Table 4.13: Correlation between the lithologic rock type and the activity concentration of ^{238}U, ^{232}Th and ^{40}K (Bq kg^{-1}) in Lugbe borehole

Sample ID	Lithology description	Activity concentrations (Bq kg^{-1})			
		^{238}U	^{232}Th	^{40}K	Th/U Ratio
S4L1	Laterite topsoil, yellowish brown	22.6 ± 2.5	45.5 ± 4.1	1011.0± 128.3	6.1±0.9
S4L2	Sandy clay, fine to coarse, brownish yellow.	18.3 ± 1.2	43.6 ± 4.1	970.3± 122.1	7.4±0.9
S4L3	Clayey sandy, brownish ash, fine grain feldspar	21.5 ± 2.5	48.6 ± 4.1	907.7± 115.8	6.9±1.0
S4L4	Sandy maicaceous, grey, interbedded with quatz feldspar	21.9 ± 2.5	49.6 ± 8.1	870.1 ± 109.6	6.9±1.4
S4L5	Fine to coarse, ashy to grey	16.1 ± 1.2	46.7± 4.1	816.9 ± 103.3	8.9±10

4.4.15 Comparison of Activity Concentration of ^{232}Th, ^{238}U and K in Subsurface Layers from Dei-Dei, Kubwa, Gosa and Lugbe Boreholes

The objective of this comparison is to verify if the same geologic rock type can reflect similar activity concentrations of ^{238}U, ^{232}Th and K in the study areas. Secondly, to determine the source rock of the radionuclides in each location of the borehole area which will encourage the professionals in groundwater developments the identify regions that are safer for groundwater based drinking water exploration.

The findings of this study showed that the activity concentrations of ^{238}U in Dei-Dei reported the highest value in layer seven (S1L7) whereas in Kubwa, is in layer one (S2L1). The higher value in topsoil is due to soil type and the mobility characteristics of ^{238}U in subsurface sediment (Maxwell et al., 2013a). In Gosa borehole rock samples, the activity concentration of ^{238}U reported higher in layer

four (S3L4), whereas in Lugbe borehole samples, sample layer one (S4L1) reported the highest value. The lowest value of ^{238}U in Dei-Dei is noted in layer eight (S1L8) whereas in Kubwa borehole, it was noted in fifth layer (S2L5). The lowest value of ^{238}U in Gosa reported in layer three (S3L3) whereas in Lugbe, it was noted in layer five (S4L5), it may be due to low distribution of acidic felsic intrusion in the subsurface sediment, (Maxwell et al., 2013b). In all the samples, the highest ^{238}U activity value was noted at Kubwa borehole sample; in sample layer one at the topsoil with porphyroblastic gneisse and biotite homblende granodiorite as the geological formation.

The activity concentrations of ^{232}Th in Dei-Dei was noted higher in layer eleven (S1L11) whereas in Kubwa and Gosa boreholes, it was noted in sample layer one (S2L1 and S3L1) respectively. In Lugbe borehole, the activity concentration of ^{232}Th was noted in layer four (S4L4). The lowest values of ^{232}Th in Dei-Dei was noted in layer two (S1L2) and in Kubwa, the lowest value was in (S2L2). Both layers (S1L2 and S2L2) may appear to have the same deposition of inter sedimentation and could have the same geologic rock type, but differ in ^{238}U due to its oxidation characteristics, (Maxwell et al., 2013a). The lowest value of ^{232}Th in Gosa was noted in layer one (S3L1) whereas the lowest value in Lugbe reported in layer two (S4L2). In Gosa, the sample layer one (S3L1) may have been affected by the same geological attributes associated with ^{232}Th mineral composition during Pan-African Orogeny event, (Maxwell et al., 2013b). The highest value of ^{232}Th was recorded in Dei-Dei sample layer eleven (S1L11) which geologically could be migmatite gneiss complex intruded into the fractured basement terrain aquifer bearing rock.

The activity concentration of ^{40}K in Dei-Dei is higher in layer three (S1L3) and in Kubwa was noted in ninth layer (S2L9). The contradicting result here is the lowest values of ^{40}K was noted in first layers of both Dei-Dei and Kubwa (S1L1 and S2L1), which may be attributed to low colloidal sediments in the near surface of both Dei-Dei and Kubwa boreholes. In Gosa borehole, the highest activity concentration of ^{40}K was noted in layer four (S3L4) whereas in Lugbe borehole, the highest value was noted in sample layer one (S4L1). The lowest value of ^{40}K in Gosa and Lugbe were found in layer one and layer five (S3L1 and S4L5) respectively. The highest

value of ^{40}K in the four boreholes was noted in Dei-Dei in sample layer three (S1L3) which geologically was attributed to biotite granitic intrusion (Maxwell *et al.*, 2013a).

In these comparisons, few significant results were found as follows:

1) In S1L2 and S2L2 reporting low activity values of ^{232}Th in the same topsoil from Dei-Dei and Kubwa boreholes and was attributed to the same deposition or sedimentation processes which may be due to similar geologic rock type, (Maxwell et al., 2013a)
2) In that similar layer the activity level of ^{238}U in S1L2 and S2L2 varies due to ^{238}U oxidation characteristics (Maxwell et al., 2013a).
3) Another scenario was that S1L2 and S2L2 reported the lowest activity of ^{232}Th whereas S1L1 and S2L1 reported the lowest activity of ^{40}K which was attributed to low felsinc sediments in the layers, (Maxwell et al., 2013a).
4) In Gosa borehole, the activity concentrations of ^{238}U, ^{232}Th and ^{40}K reported to be higher in a single layer (S3L4). Such similar homogeneity of activity concentrations reporting higher value in a single layer, S3L4 from the structural/ tectonic point of view could be due to that the area underwent complex polyphase deformation shown by tectonometamorphic phase that is caused by granitic intrusions, (Maxwell et al., 2013b).
5) In Lugbe borehole, the variations in activity concentrations of radionuclides may be due to the oxidation of ^{238}U and the colloidal sediments containing carbonate and bicarbonate constituents that keep ^{238}U and ^{40}K mobile, (Maxwell et al., 2013b).
6) It could be noted in Figures 4.16 and 4.17 that the activity concentrations of ^{40}K increases with depth in Dei-Dei and Kubwa, (Maxwell et al., 2013b); whereas at Lugbe, Figure 4.19, its apparently decreases 100 % with depth, (Maxwell et al., 2013b). It may be caused by the variation in sediment distribution in subsurface aqueous phase due to large scale fractures by dissolution of its concentration from higher deposit to lower deposit region. It could be observed that the situation of ^{40}K increase with depth in Dei-Dei and Kubwa boreholes differ from Gosa and Lugbe borehole which may be

attributed to the sequence of sedimentation deposit of felsinc intrusions which depends on the fracture trend in the basement terrain of Abuja and its environs.

4.4.16 Comparison of Th/U Ratios in Rock Samples from Dei-Dei, Kubwa , Gosa and Lugbe Boreholes

The Th/U ratio in Dei-Dei with highest value refers to layer eleven (S1L11), whereas the lowest value was noted in the sample collected from first layer, laterite top soil, S1L1. In Kubwa, the Th/U ratio with highest value refers to layer five (S2L5), whereas the lowest value was noted in the sample collected from fourth layer, S2L4. At Gosa borehole, sample S3L3 has the highest Th/U ratio and sample S4L5 at Lugbe borehole reported higher value. These two layers (S3L3 and S4L5) indicated whether enrichment or relative depletion of radioisotopes may have occurred, as given in Tables 4.10 and 4.12 respectively (Maxwell *et al*., 2013c). The lowest Th/U ratio at Gosa borehole was noted in Sample S3L5 whereas at Lugbe borehole, it was Sample layer one (S4L1) as shown in Table 4.10 and 4.12 respectively. Dei-Dei reported higher Th/U ratio and presumed to be due to rock samples being connected to where rocks were formed from thermal metamorphism and metasomatic processes that occurred, (Maxwell et al., 2013a).

4.4.17 Comparison of Activity Concentration of ^{232}Th, ^{238}U and ^{40}K in Topsoil of the Study Area (Dei-Dei, Kubwa, Gosa and Lugbe)

The objective of this comparison was to detect the area that reports higher activity concentrations of ^{238}U, ^{232}Th and ^{40}K in order to recommend for environmental assessment of radiological impact on inhabitants in the region.

The activity concentrations of the topmost layers of the four borehole rock samples were presented in Figure 4.20. As it can be observed that the activity of ^{40}K

is reported to be higher in Lugbe (S4L1). Also, ^{238}U and ^{232}Th noted to be higher in Dei-Dei and Kubwa respectively (S1L1 and S2L1). The two areas may require environmental assessment of background radiation.

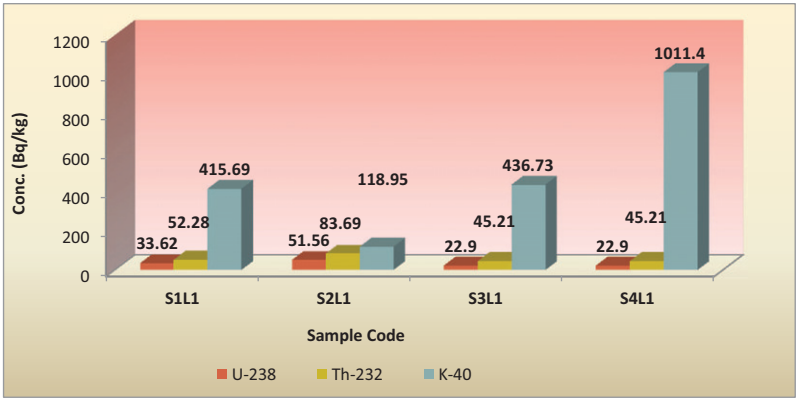

Figure 4.20 The activity Concentration of ^{238}U, ^{232}Th and ^{40}K in topsoils of the four boreholes (Dei-Dei, Kubwa, Gosa and Lugbe)

In Figure 4.20, which comprises S1L1 (Dei-Dei topsoil), S2L1 (Kubwa topsoil), S3L1 (Gosa topsoil) and S4L1 (Lugbe topsoil) indicated that the natural radionuclides are not uniformly distributed, thus, the knowledge of the natural radioactivity on topsoil in the study area is important for their management and consequently on the possible radiation exposure to the population. This knowledge is essential for the development of guide report for environmental assessment recommendation if found to be higher than the permissible limit. The goal of evaluating the topsoil is to determine radium equivalent (Ra_{eq}), the air absorbed dose rate (D_c), the annual effective dose rate (AEDR) and the external hazard index (H_{ex}), thus, to determine the environmental exposure to the people within the study area.

Dose rate: In the study area Equation (4.6) was used to calculate the external gamma dose rate D_c in air from natural radionuclides for samples from topsoil, UNSCEAR, 2000

$$D_c = 0.462\ A(^{238}U) + 0.604\ A(^{232}Th) + 0.0417\ A(^{40}K) \quad (4.6)$$

where, D_c is the absorbed dose rate at 1 m from the ground, $A(^{238}U)$, $A(^{232}Th)$ and A(K) are the activity concentrations of ^{238}U, ^{232}Th and ^{40}K in Bq kg^{-1} of the samples respectively.

Radium equivalent: Radium equivalent was calculated according to the Equations (4.7), UNSCEAR, 2000.

$$Ra_{eq} = A_{Ra} + 1.43\ A_{Th} + 0.077\ A_K \quad (4.7)$$

Radiation hazard: The gamma ray radiation hazards due to the specified radionuclides were assessed by external radiation hazard and was calculated using Equation (4.8), UNSCEAR, 2000

$$H_{ex} = A_{Ra}/370 + A_{Th}/259 + A_K/4810 \leq 1 \quad (4.8)$$

where, $A_{Ra} \sim A_U$, A_{Th} and A_K are the average activity concentrations of ^{238}U, ^{232}Th and ^{40}K in Bq kg^{-1}, respectively. For the radiation hazard to be acceptible, it is recommended that the Ra_{eq} activity is lower than the value of 370 Bq kg^{-1}, while the H_{ex} be less than unity.

Annual Effective Dose Rate: The annual effective dose rate (AEDR) in units of μSv y^{-1} was calculated by the following formula as shown in Equation (4.9)

$$AEDR = D_c\ (nGy\ h^{-1})\ x\ 8760\ h\ x\ 0.7\ Sv\ Gy^{-1}\ x\ 10^{-3} \quad (4.9)$$

To estimate the AEDR, the conversion coefficient from absorbed dose rate in air to effective dose (0.7 Sv Gy^{-1}) , UNSCEAR, 2000 was used.

The values obtained from the calculated dose rate, radium equivalent, external radiation hazard and annual effective dose rate due to the topsoil samples from Dei-Dei, Kubwa, Gosa and Lugbe borehole samples are presented in Table 4.14.

Table 4.14: Calculated dose rate, radium equivalent,external radiation hazard and annual effective dose rate of the topsoil samples from Dei-Dei, Kubwa, Gosa and Lugbe

Location	Sample ID	Lithology	Dc (nGy h^{-1})	Ra_{eq} (Bq kg^{-1})	Hex	AEDR (µSv y^{-1})
Dei-Dei	S1L1	Sandston	58	126	0.35	355.7
Kubwa	S2L1	Sandy clay	80	180	0.49	490.6
Gosa	S3L1	Sandy clay	59	124	0.34	361.8
Lugbe	S4L1	Laterite	81	160	0.45	496.7

The results of the dose rate, radium equivalent activity, external radiation hazard and annual effective dose rate due to topsoil of the sampling sites are shown in Table 4.14. The calculated dose rate was higher at Lugbe with a value of 81 nGy h^{-1} which is attributed to lateritic topsoil interbedded with gravel as the formation of the surface area. The low dose rate was determined on the sandstone at Dei-Dei topsoil with a value of 58 nGy h^{-1} . The higher radium equivalent activity of 180 Bq kg^{-1} was reported at Kubwa whereas Gosa reported a distinctly lower value of 124 Bq kg^{-1}. The external radiation hazard index of 0.49 was noted at Kubwa and lower value of 0.34 was reported at Gosa. The external hazard index of 0.49 did not exceed the recommended value. All the lower values found at Gosa area may be due to the absence of interconnectivity of fractures reported earlier in this study from geologic interpretation as shown in Figure 4.6. The highest annual effective dose rate (AEDR)

of 496.7 μSv y^{-1} was noted at Lugbe and lower value was noted at Dei-Dei with a value of 355.7 μSv y^{-1}. The annual effective dose rate (AEDR) determined, 496.7 μSv y^{-1} is about 35 % of the recommended value by the International Commission on Radiological Protection, ICRP (1991), as the recommended effective dose equivalent for members of the public. In Table 4.15, the values obtained were compared to values reported in other countries and the world standard, thus, within the normal range except the reports at Kubwa and Lugbe which were higher than the world standard by a factor of 1.3 and above.

Table 4.15: Calculated dose rate, radium equivalent activity, external radiation hazard and annual effective dose rate compared with other studies

Location	Dc ($nGyh^{-1}$)	Ra_{eq} ($Bq\ kg^{-1}$)	H_{ex}	AEDR ($\mu Sv\ y^{-1}$)	Reference
Dei-Dei, North Central Nigeria	58	126	0.35	71	Current study
Kubwa , North Central Nigeria	80	180	0.49	98	Current study
Gosa, North Central Nigeria	59	124	0.34	72	Current study
Lugbe, North Central Nigeria	81	160	0.45	99	Current study
Port Harcourt, Nigeria	46	92	0.27	57	Aviwiri, G. O., 2005
Abeoluta, Ogun State, South Western, Nigeria	84	172	0.48	103	Okedeyi, A.S. et al., 2012
Izmir,Turkey	86	132	0.52	106	Cam, N. F. et al., 2010
Kinta District, Malaysia	212	483	1.31	260	Lee et al., 2009
Pontian District, Malaysia	61	136	0.37	238	Saleh et al., 2013
World	60	127	0.35	74	UNSCEAR, 2000

4.4.18 Comparison of activity concentration of ^{232}Th, ^{238}U and K in Dei-Dei, Kubwa, Gosa , Lugbe and other Countries

The purpose of this comparison was to correlate the values of the results of the present work and the previous work published elsewhere. Comparison of the activity concentrations of ^{238}U, ^{232}Th and K in the present study with previous studies are presented in Table 4.16. Most of the reports were not from sequential subsurface layers as this present study, but they are all from soils and rocks. The results of present work show good agreement with those reported in previous studies. In general, all results existed within the range of values given in UNSCEAR, (UNSCEAR, 1998).

Table 4.16: Summary of Activity Concentration of radioisotopes in topsoil samples in Dei-Dei, Kubwa, Gosa and Lugbe boreholes in Abuja and other Parts of the World (UNSCEAR, 1998)

Region/ Country	^{232}Th (Bq kg^{-1})		^{238}U (Bq kg^{-1})		K (Bq kg^{-1})	
	Range	Mean	Range	Mean	Range	Mean
Dei-De1 Abuja, Nort Central Nigeria[a]	53 ± 4	53	34 ± 3	34	236 ± 32	236
Kubwa Abuja, Northcental,Nigeria[a]	84 ± 7	84	52 ± 5	52	119 ± 15	119
Gosa Abuja, Nort Central Nigeria[a]	48 ± 4	48	25 ± 2	25	438 ± 56	438
Lugbe Abuja, Northcental,Nigeria[a]	46 ± 4	46	23 ± 2	23	1011± 128	1011
Ikogosi-Ekiti,South western Nigeria[b]	1- 108	82	4 -111	58	40-2437	1203
Malaysia[c]	63 -110	82	49 – 86	66	170-430	310
China[c]	1 - 360	41	2 - 690	84	9-1800	440
India[c]	14-160	64	7 - 81	29	38-760	400
Japan[c]	2-88	28	2 - 59	29	15-990	310
United State[c]	4 -130	35	4 - 140	35	100-700	370
Egypt c	2 - 96	18	6 - 120	37	29-650	320
Greece[c]	1 - 190	20	1 - 240	25	12-1570	360
Portugal[c]	22 -100	51	26 - 82	49	220-230	840
Russia[c]	2 - 79	30	0 - 67	19	100-400	520
Spain[c]	2-210	33	-	-	25-1650	570
World[d]	7-50	45	16 -116	33	100-700	420

a- Present study; b- O.S Ajayi (1999); c- UNSCEAR (1998); d- UNSCEAR (2000)

4.5 Geochemical Characteristics of Rock Sample from Dei-Dei, Kubwa, Gosa and Lugbe Using X-ray Fluorescence Analysis

The main objective of this geochemical characteristic investigation is to study the effect of mineral elements on rock samples from Dei-Dei, Kubwa, Gosa and Lugbe borehole samples and to compare with the GBW07406 (DC73324) reference material, hence, to know their effect on activity concentration of ^{238}U, ^{232}Th and K and on the variations of layers activity levels. The details of the sample preparation and methods are discussed in Section 3.5.

Thirty-one (31) samples were chemically analysed in Environmental Analysis Laboratory, Department of Water and Environmental Engineering, Faculty of Civil and Environmental Engineering, Universiti Tun Hussein ONN Malaysia. The purpose of the analysis was to determine the major oxides such as SiO_2, Al_2O_3, Fe_2O_3, CaO, MgO, MnO, K_2O, Na_2O, P_2O_5, TiO_2, CO_2, SO_3, BaO and ZrO_2 in the samples using X-ray Fluorescence (XRF) technique attached to Geo-quant M software. Certified reference material soil (CRM) provided by Institute of Geophysical and Geochemical Exploration (Langfang, China) coded: GBW07406 (DC73324) has been used as the standard for the XRF fluorescence analysis system; reference material date of certification: 1986; modification: 2003 and expiration: 2013. It is mainly used in geology, mineral reconnaissance, agriculture and the related fields to carry out chemical analysis as calibration samples and for monitoring the quality of measurements. The studied layers, for Dei-Dei with eleven samples are S1L1 to S1L11, for Kubwa with nine samples are S2L1 to S2L9, for Gosa with six samples S3L1 to S3L6 and Lugbe rock samples are S4L1 to S4L5.

4.5.1 Interpretation of Major Oxides in Dei-Dei Borehole Rock Samples

At Dei-Dei, the chemical composition of the collected samples is shown in Table 4.17. The samples can be differentiated according to their SiO_2, CaO, Fe_2O_3,

Al_2O_3, TiO_2, Na_2O, FeO, MnO, K_2O, MgO and P_2O_5 content. The different composition at Dei-Dei borehole samples could be attributed to the hydrothermal alteration and metasomatism process. i.e; the area was subjected to surface and subsurface processes of alteration. At Dei-Dei, the subsurface processes are represented by hydrothermal alteration caused by the mobility of some major oxides, which leads to enrichment in SiO_2, Fe_2O_3 and depletion of Al_2O_3. The surface processes include the effect of meteoric water, responsible for the elements such as uranium from high to low physiographic features. The higher activity concentration of ^{238}U in both S1L5 and S1L7 in Dei-Dei may be the effect of high percentage compositions of SiO_2 and the depleted Al_2O_3 present in the layers. In the same way, ^{232}Th was reported to be higher in S1L11 which could be attributed to the presence of Fe_2O_3 and the higher percentage composition of SiO_2 and Al_2O_3. It may be that the percentage increase in Fe_2O_3 and Al_2O_3 with a decrease in SiO_2 composition in rock sample promotes the activity level of K as in S1L3 that recorded the highest K activity concentration. In comparison with the standard reference material provided by Institute of Geophysical and Geochemical Exploration (Langfang, China) coded: GBW07406 (DC73324) as shown in Table 4.18, the results suggests good agreement with the certified values for some of the major oxides at Dei-Dei borehole.

Table 4.17: Mineral content (%) of different layer rock samples in Dei-Dei borehole

Oxides	S1L1	S1L2	S1L3	S1L4	S1L5	S1L6	S1L7	S1L8	S1L9	S1L10	S1L11	mean	SD	SE
SiO_2	43.3	45.5	47.9	59.3	64.6	66.1	62.7	60.8	54.9	52	55.2	55.66	7.80	2.35
CaO	1.1	1.91	2.2	2.09	0.8	0.65	0.78	0.37	0.45	0.76	0.38	1.04	0.69	0.21
Fe_2O_3	23	20.2	19.2	9.32	7.06	6.39	6.55	9.32	12.5	11.8	10	12.30	5.86	1.77
Al_2O_3	30.1	28.2	27.1	20.3	19.2	18.2	20	17.5	19.1	21.9	23.3	22.26	4.35	1.31
TiO_2	1.51	1.5	1.3	1.06	0.59	0.45	0.92	2.02	1.92	2.34	1.83	1.40	0.60	0.18
Na_2O	2.7	2.12	1.02	0.7	0.41	0.39	0.44	0.31	0.32	0.38	0.36	0.83	0.82	0.25
FeO	7	6.7	4.1	3.5	3.33	3.3	3.2	2.2	1.63	0.72	0.48	3.29	2.11	0.64
MnO	1.21	1.11	1.3	0.16	1.93	1.69	0.07	0.16	0.44	1.38	1.44	0.99	0.66	0.20
K_2O	1.16	2.54	2.44	3.71	4.58	5.27	5.72	6.04	6.33	7	6.6	4.67	1.95	0.59
MgO	0.51	0.03	0.21	0.011	0.2	0.09	0.1	0.06	0.02	0.1	0.03	0.12	0.14	0.04
P_2O_5	0	0	0	0.09	0.26	0.35	0.27	0	0	0	0	0.09	0.14	0.04

*ND: Not detected

The mean M, standard deviation, SD and standard errors, SE were calculated according to Samat and Evans, 1992. Considering the experimental data presented in Table 4.17. Let n be the number of measured samples. If the set of major oxides (mineral contents) of sample data are presented as shown in Table 4.17, the mean (M) of the data can be calculated using Equation 4.10.

$$M = \frac{X_1+X_2+X_3+\cdots X_n}{n} \tag{4.10}$$

Standard deviation: The standard deviation describes the distribution by telling whether the individual scores are clustered close together or scattered over a wide range. It is also the measures of how well any individual score represents the sample by providing a measure between a score and the sample mean. Standard deviation in this work can be identified by the symbol, δ_{est}. The standard deviation of each oxide in this work was calculated using Equation 4.11.

$$\delta_{est} = \sqrt{\frac{\Sigma(X_1-M)^2}{n-1}} \tag{4.11}$$

Standard error: The standard error describes the distribution of sample means. When the sample contains n results, the standard error (in the estimate) of the mean, and this is a factor of $\sqrt{n}$ smaller than the standard deviation. It is identified by a symbol, δ_{SE}. The standard error value of each oxide in this study was calculated using Equation 4.12.

$$\delta_{SE} = \frac{\delta_{est}}{\sqrt{n}} \tag{4.12}$$

In Table 4.17, the highest mean value for all the mineral contents measured at Dei-Dei borehole was SiO_2 with a value of 55.66 ± 2.35 % and P_2O_5 reported the lowest value of 0.09 ± 0.04 % in the same borehole.

4.5.2 Interpretation of Major Oxides in Kubwa Borehole Rock Samples

In Kubwa physico-chemical analysis, nine rock samples were analyzed for the major oxides with SiO_2 reporting the largest weight which may be due to the high content of clay fraction which increases with depth due to decrease in organic carbon content with depth as shown in Table 4.18. The increase in composition of Al_2O_3 may extensively contribute to the high activity level of ^{238}U and ^{232}Th in rock minerals of S2L1 at Kubwa borehole sample. The presence of CaO in S2L9 with low composition of Al_2O_3 could serve to increase in activity level of ^{40}K in the analyzed sample in Kubwa rock samples.

Table 4.18: Mineral content (%) of different layer rock samples in Kubwa borehole

oxides	S2L1	S2L2	S2L3	S2L4	S2L5	S2L6	S2L7	S2L8	S2L9	mean	SD	SE
SiO_2	43.1	45.4	45.6	39.6	58	63.8	62.8	63.4	60.8	53.61	9.96	3.00
CaO	0.21	5.55	0.87	0.82	7.23	6.63	7.03	6.74	7.54	4.74	3.13	0.94
Fe_2O_3	23.4	17.4	19.3	27.9	9.68	6.43	6.67	6.47	7.13	13.82	8.33	2.51
Al_2O_3	29.7	23.3	25.8	21.7	15.9	14.6	14.7	14.3	15.3	19.48	5.78	1.74
TiO_2	1.99	2.99	2.99	3.92	1.61	1.14	0.99	1.17	1.5	2.03	1.03	0.31
Na_2O	0.43	0.59	1.02	1.3	1.93	2.44	2.44	2.4	2.29	1.65	0.82	0.25
FeO	1.37	2.81	3.21	1.41	1.26	1.62	0.73	0.42	0.28	1.46	1.00	0.30
MnO	0.2	2.47	1.58	2.02	2.31	1.59	1.37	1.34	1.71	1.62	0.66	0.20
K_2O	0.8	2.1	2.81	2.79	2.21	2.38	2.83	2.96	2.68	2.40	0.67	0.20
MgO	0.1	0.31	0.01	0.2	0.12	0.13	0.01	0.08	0.04	0.11	0.10	0.03
P_2O_5	ND	0.33	0.25	0.44	0.29	0.26	0.24	0.37	ND	0.31	0.07	0.02

*ND: Not detected.

In Table 4.18, the mean, standard deviation and standard error of the mineral contents were calculated using equations (4.10), (4.11) and (4.12) respectively. The highest mean value of oxides measured was SiO_2 with a value of 53.61 ± 3.00 % at Kubwa borehole and lower value of 0.31 ± 0.02 % was obtained from P_2O_5 in the same borehole samples.

4.5.3 Interpretation of Major Oxides in Gosa Borehole Rock Samples

In Gosa, the S3L6 in Table 4.19 reported the highest activity concentrations of both ^{238}U and ^{232}Th which could be refer to the higher percentage composition of SiO_2 and Fe_2O_3 in the presence of P_2O_5. It could be that P_2O_5 could increase the activity of radionuclides at low composition of Al_2O_3 in rock samples. In Gosa area, it could be observed that Al_2O_3 decreases appreciably with depth as it is in other areas, Dei-Dei and Kubwa respectively. The sample layer four (S3L4) with high percentage of SiO_2 and Al_2O_3 with addition of high composition of K_2O percentage in the sample may have contributed to high activity concentration of ^{40}K in the rock sample obtained in that layer.

Table 4.19: Mineral content (%) of different layer rock sample in Gosa borehole

oxides	S3L1	S3L2	S3L3	S3L4	S3L5	S3L6	mean	SD	SE
SiO_2	45.2	53.4	51.8	57.2	71.8	54.6	55.67	8.87	2.67
CaO	0.22	3.3	0.1	0.78	1.58	1.7	1.28	1.19	0.36
Fe_2O_3	19	8.35	9.05	7.58	6.8	23.5	12.38	7.06	2.13
Al_2O_3	29.1	33.7	34.6	27.1	11.5	11.7	24.62	10.46	3.15
TiO_2	1.2	0.73	0.78	0.71	1.38	0.81	0.94	0.28	0.09
Na_2O	2.41	3.87	1.32	0.74	1.37	1.1	1.80	1.16	0.35
FeO	1	0.12	1.53	1.03	1.1	0.87	0.94	0.46	0.14
MnO	1.14	0.03	0.14	0.17	0.13	1.88	0.58	0.76	0.23
K_2O	0.8	2.54	0.78	3.88	3.13	2.09	2.20	1.25	0.38
MgO	0.99	0.78	0.84	1.24	1.21	1.42	1.08	0.25	0.08
P_2O_5	ND	ND	ND	ND	ND	0.26	0.02	0.08	0.02

*ND: Not detected

In the same way, the mean, standard deviation and standard error of mineral contents in Table 4.19 were calculated using Equations (4.10), (4.11) and (4.12) respectively. The highest mean value of 55.67 ± 2.67 % was from SiO_2 and a mean value of 0.02 ± 0.02 % obtained for P_2O_5 as shown in Table 4.19 reported the lowest mineral content in the area.

4.5.4 Interpretation of Major Oxides in Lugbe Borehole Layers

Table 4.20 shows that the activity concentrations of ^{238}U and ^{40}K reported to be higher in rock sample S4L1 from Lugbe borehole may be due to the high percentage composition of SiO_2, Al_2O_3 and K_2O associated with low level of Fe_2O_3 constituent in the rock sample. ^{232}Th that reported the highest activity concentration in S4L4 rock sample in Lugbe borehole rock samples could be due to the absence of MgO in presence of SiO_2 and Al_2O_3 in addition to low composition of Fe_2O_3.

Table 4.20: Mineral content (%) of different layer Rock Samples in Lugbe borehole

oxides	S4L1	S4L2	S4L3	S4L4	S4L5	mean	SD	SE
SiO_2	56.3	56.1	62.8	63.5	64	60.54	3.99	1.20
CaO	0.93	1.23	4.4	4.9	5.25	3.34	2.09	0.63
Fe_2O_3	10.4	8.89	5.4	5.07	4.99	6.95	2.52	0.76
Al_2O_3	22.8	22.6	17.6	16	15.7	18.94	3.51	1.06
TiO_2	1.38	1.21	0.82	0.74	0.66	0.96	0.31	0.09
Na_2O	0.24	0.46	2.27	2.96	3.21	1.83	1.39	0.42
FeO	0.14	2.1	2.57	4.22	2	2.21	1.46	0.44
MnO	0.17	0.01	ND	ND	0.02	0.04	0.07	0.02
K_2O	6.15	4.62	4.71	4.63	4.28	4.88	0.73	0.22
MgO	0.83	1.01	0.91	1.04	0.85	0.93	0.09	0.03
P_2O_5	ND	ND	0.4	0.45	0.43	0.26	0.23	0.07

*ND: Not detected

At Lugbe borehole, the mean, standard deviation and standard error of mineral contents in rock samples as shown in Table 4.20 were calculated using equations (4.10), (4.11) and (4.12) respectively. The highest mean value of 60.54 ± 1.78 was obtained from SiO_2 at Lugbe borehole whereas a lower mean value of 0.04 ± 0.02 was reported from MnO as shown in Table 4.20.

4.6 Measurement of Activity Concentrations of ^{238}U and Toxic Elements in Groundwater Sample from Dei-Dei, Kubwa, Gosa and Lugbe

This study proposed to investigate the quality of groundwater used for human consumption without treatments in Dei-Dei, Kubwa, Gosa and Lugbe area of Abuja where the public water supply is inadequate due to the population growth recently. The results obtained from the four boreholes were compared with the public water supply (water board) and hand-dug well, 1 km away from the 70 m borehole sample point at Dei-Dei. There are lack of data on the radiological and chemical effect of radionuclides and other toxic metals in borehole drinking water supply in the study locations. Four hydrogeologically motivated boreholes were drilled for this work to monitor the radioactivity and toxicity in groundwater based drinking water as recommended elsewhere, (Maxwell et al., 2013a; Maxwell et al, 2013b). Samples were collected from the boreholes at varying depths, 70 m at Dei-Dei, 60 m at Kubwa, 50 m at Gosa and 40 m at Lugbe below ground level. 14 m below ground level Hand dug well (1 km away) at the same location in Dei-Dei borehole and Water Board (public water supply) from Area 10 Garki Abuja were collected to compare with the four boreholes. The samples were labeled as shown in Table 4.21 for easy identifications:

Table 4.21: The borehole water samples, Water Board and hand-dug well, symbols and locations for ICP-MS analysis

Sample number	Symbol	Location
1	SW1	Dei-Dei borehole
2	SW2	Kubwa borehole
3	SW3	Gosa borehole
4	SW4	Lugbe borehole
5	SWB	Water Board
6	SWH	Hand-dug well from Dei-Dei

Water samples were collected in high density polyethylene containers at the borehole site from the study area in Nigeria. They were previously washed in a solution of 10 % nitric acid for 15 minutes, followed by repeated rinsing with

distilled water and finally rinsing with ultrapure water (resistivity of about 18 MΩ cm^{-1}). Before the sample collection, the prepared collection containers were kept in sealed polyethylene bags. Borehole water samples were stabilized with 5 ml of nitric acid in each litre of water. For accurate determination of elemental compositions in groundwater samples, a solution analytical method was used; a multi-standard calibration method was applied using Elan 9000 instrument that performs analysis at parts-per-trillion and lower (ICP-MS). The details of the method were discussed in Section 3.6.

Table 4.22 presents the activity concentrations of ^{238}U that were determined in groundwater samples taken from the study area. The data in Table 4.22 were converted to μBq L^{-1} using the conversion factor of 15 μg L^{-1} (0.19 Bq L^{-1}), (WHO, 2003). The activity concentrations of ^{238}U in the water supplies for drinking and domestic purposes were found to be higher at Lugbe borehole with a value of 2736 μBq L^{-1} whereas lower value of 443 μBq L^{-1} was reported at Gosa borehole. Activity concentration of 1824 μBq L^{-1} was noted for Water Board sample whereas 2430 μBq L^{-1} was reported in hand-dug well water sample. It was observed that the activity concentration of ^{238}U radionuclide in groundwater based drinking water at Lugbe borehole was higher than that of Dei-Dei, Kubwa and Gosa. Comparing the activity level in Lugbe borehole with the Water Board, Lugbe borehole was higher by a factor of 1.5. Interestingly, the hand-dug well with activity level of 2430 μBq L^{-1} at a depth of about 14 m collected 1 km away from Dei-Dei borehole was closer to the activity level of 2698 μBq L^{-1} found at Dei-Dei borehole water sample. The activity concentration of ^{238}U in Lugbe borehole was higher than all the values obtained in other samples; probably, the ^{222}Rn content in the water may not have way to escape to the surrounding compared to other boreholes and the surface water that serves the Water Board. In addition, the Water Board in Abuja which is the public water supply in the region noted higher than the borehole drilled at Gosa and Kubwa. This may be attributed to solubility and high content of heavy metals in the public water supply which was identified from ICP-MS analysis. The variation of the activity levels depend on the activity of ^{222}Rn in water. The reason for higher solubility of ^{238}U in some groundwater samples may be due to the chemical composition of Abuja groundwater. Compared to water from hand-dug well, bedrock waters are more

alkaline, contain more bicarbonate and change towards the sodium type especially at greater depth. In such waters, ^{238}U can form soluble complexes (Jang, Dempsey, & Burgos, 2006).

The activity concentration of ^{238}U in Gosa borehole may not have been in +VI (uranyl oxidation state) due to non-interconnectivity of fractures that would have allowed +IV (uranous state) to oxidize to +VI by enhancing the activity level in the borehole sample at Gosa. The Gosa borehole condition and radionuclide contamination may have been affected by the geology of the area such as insufficient fractures, joints and fissures that creates favourable condition for water-rock interaction and thorough mineral contacts with groundwater system. At Kubwa borehole, the lower value compared to hand-dug well and Water Board could be attributed to the tectonic impact that resulted in subsurface deformation and large scale fractures that could serve as pathway for ^{222}Rn escape to the surface, thus, decrease the activity of ^{238}U in groundwater sample from Kubwa borehole.

Table 4.22: Results of activity concentrations of ^{238}U in Dei-Dei, Kubwa, Gosa, Lugbe, Water Board and Hand Dug Well from Abuja, Nigeria and various countries

Location	**Concentration ^{238}U ($\mu g\ L^{-1}$)**	**Activity Concentration ^{238}U ($\mu Bq\ L^{-1}$)**	**Reference**
Dei-Dei	0.213 ± 0.00	2698	Present Study
Kubwa	0.067 ± 0.00	849	Present Study
Gosa	0.035 ± 0.00	443	Present Study
Lugbe	0.216 ± 0.01	2736	Present Study
Water Board	0.144 ± 0.00	1824	Present Study
Hand-dug well	0.192 ± 0.00	2430	Present Study
Slovavenia	0.5	6333	Kobal *et al.,* 1990
Brazil	0.08	1013	Almeida *et al.,* 2004
Germany	1.15	14567	Guns *et al.,* 1987
China	1.4	17733	Zhou *et al.,* 2004
Finland	1.6	20,267	Salonen and Huikuri 2002, Juntunen 1999, Makelainen *et al*., 2002

Table 4.22 summarizes the concentrations of ^{238}U in groundwater in the study area and compared to other work published elsewhere, (Kobal *et al*., 1990; Almeida *et al*., 2004; Guns *et al.,* 1987; Zhou *et al.,* 2004; Salonen and Huikuri,2002; Juntunen, 1999; Makelainen *et al.,* 2002). It was noted that the concentrations of ^{238}U in this present work are distinctly lower than other works reported in other countries except the work reported in Brazil, 0.08 µg L^{-1}, Almeida *et al.,* 2004, which is distinctly lower than the values noted in Dei-Dei; Kubwa ,Gosa, Lugbe, Water bored and hand-dug well, 0.213 ± 0.00 µg L^{-1} , 0.067 ± 0.00 µg L^{-1} , 0.035 ± 0.00 µg L^{-1} , 0.216 ± 0.01 µg L^{-1} , 0.144 ± 0.00 µg L^{-1} and 0.192 ± 0.00µg L^{-1} respectively as shown in Table 4.22. The concentration of ^{238}U was lower at Gosa compared to water board and Hand dug well whereas the concentration at Lugbe and Dei-Dei boreholes were higher than both water board and hand-dug well in contrast. The highest concentration was noted in Lugbe with a value of 0.216 ± 0.01 µg L^{-1} which may be due to the uranous state (+IV) deposit in the host aquifer bearing rock that may have been oxidized form of uranyl condition (+VI). This could be the influence of tectonic activity resulting into dissolution of rock minerals in groundwater system around Lugbe basement groundwater channel. It could be observed that the concentration of 0.216 ± 0.01 µg L^{-1} found at Lugbe borehole was closer to the value of 0.5 µg L^{-1} reported at Slovavenia, Kobal *et al.,* 1990. The closeness of the reported value in Brazil, 0.08 µg L^{-1} to the present study, especially the value obtained at Gosa borehole with a value of 0.035 ± 0.00 µg L^{-1} may be due to the geology soil type of aquifer bearing rocks. The activity concentration of ^{238}U in groundwater based drinking water was found to be higher at Lugbe borehole with a value of 2736 µBq L^{-1} and lower value of 443 µBq L^{-1} as reported at Gosa borehole. Comparing with the Water Board and hand-dug well, 1824 and 2430 µBq L^{-1}, the activity level of 2736 µBq L^{-1} at Lugbe borehole is higher.

4.6.1 Accumulation of Radionuclide (^{238}U) in Humans and Recommendations for the Maximum Permissible Limit

The objective of the estimation of radionuclide accumulation was to know the level of exposure to the inhabitants of the study area that depend on borehole water by determining the annual effective dose and the life average daily dose. The International Commission on Radiological Protection, ICRP, provides recommendations and guidance on all aspects of protection against ionizing radiation, which are published in the commission's own scientific journal, the Annals of the ICRP, was also referred to in this work. The process of exposure starts through ingestion of groundwater that contains radionuclides; after entering the human body, radionuclides are typically accumulated in the skeleton, liver, kidney and soft tissues. Ingested radionuclides are not entirely retained in the human body. Dose coefficients help to determine the effective dose associated with radiation exposure in assessing the health risk to people. The dose coefficient is expressed in Sv Bq^{-1}, the effective dose equivalent per unit water activity concentration of the radionuclide. The annual effective dose is calculated taking into account the activity concentration of the nuclide (Bq L^{-1}), the dose coefficient (Sv Bq^{-1}) is give as 4.5 x 10^{-8} (ICRP67, 1993; ICRP72, 1996; National Research Council, 1999) and the annual water consumption is given as 731 L L y^{-1}, (WHO, 2004; National Research Council, 1999), from Equation (4.13).

$$AED\ (\text{mSv y}-1) = AC\ (\text{Bq L}^{-1})\ X\ \ DC\ (\text{Sv Bq}^{-1})\ X\ AWC\ L\ y^{-1}\ X\ 1000 \qquad (4.13)$$

where,

AED = Annual effective dose

AC = Activity concentration

DC = Dose coefficient

AWC = Annual water consumption

In the present study, Equation (4.13) was used to determine the annual effective dose of the water samples for ^{238}U radionuclide only in groundwater based drinking water as shown in Table 4.23. The World Health Organisation (WHO) and Environmental Protection Agency (EPA-USA) used the quantity of 2 litres per day water consumption for adults (World Health Organisation, 2004; National Research Council 1999). The annual effective dose reported higher in Lugbe borehole with a value of 9.0 x 10^{-5} mSv $y^{-1}$and lower value of 1.5 x 10^{-5} mSv y^{-1} noted at Gosa borehole as shown in Table 4.28. Compared to Water Board and hand-dug well, with values 6.0 x 10^{-5} mSv y^{-1} and 8.0 x 10^{-5} mSv y^{-1} respectively which were lower than the values obtained at Lugbe and Dei-Dei boreholes, of 9.0 x 10^{-5} mSv y^{-1} and 8.9 x 10^{-5} mSv y^{-1} respectively. In contrast with the previous report of the international standard (Council Directive 98/83/EY, 1998), 0.1 mSv y^{-1}, the highest value of borehole water sample obtained in the study area, Lugbe with a value of 9.0 x 10^{-5} mSv y^{-1} was far below the recommended limit. According to ICRP 69 (1995), uranium gets to the blood through the soft tissues and excretes in urine. It can be excreted in few months whereas the parents could be retained for years. Uranium exchanges with Ca^{2+} accumulate in surface of bone and highly concentrated area of growth. The liver accumulates 1.5 to 2% of which most of it removed in a few weeks. Furthermore, the radioactivity of uranium has chemical toxicity that predominately affects the kidneys (Kurttio *et al.,* 2002; Kuttio *et al.,* 2005). From the reference work done elsewhere, the uranium concentration is limited mainly by chemical toxicity rather than the effective dose (WHO, 2006). In 2003, the World Health Organization proposed a provisional guideline of 15 µg L^{-1} (0.19 Bq L^{-1}). The result of this present study is below the recommended limit and within the range for the standard guideline for drinking water as shown in Table 4.23.

Table 4.23: Comparing the Annual Effective Dose of ^{238}U in the present study and International Standard (WHO, 2003; ICRP 67 1993, ICRP 72 1996, National Research Council 1999)

Location	Activity Concentration of ^{238}U ($\mu Bq\ L^{-1}$)	Annual Effective Dose ($mSv\ y^{-1}$)
Dei-Dei borehole	2698	8.9×10^{-5}
Kubwa borehole	849	2.8×10^{-5}
Gosa borehole	443	1.5×10^{-5}
Lugbe borehole	2736	9.0×10^{-5}
Water Board	1824	6.0×10^{-5}
Hand-dug well	2430	8.0×10^{-5}
WHO, 2003, Council Directive 98/83/EY, 1998	19,000	1.0×10^{-1}

4.6.2 Radiological Risk Assessment of ^{238}U in Groundwater from the Study Area

The objective of the radiological risk assessment was to evaluate the life time cancer risk associated with the intake of a given radionuclide in groundwater. The lifetime cancer risks R, associated with the intake of a given radionuclide were estimated from the product of the applicable risk coefficient, r and the per capita activity intake, I expressed in Equation (4.14).

$$R = r\ x\ I \tag{4.14}$$

According to WHO (2008), the average life expectancy at birth in Nigeria is 45.5 y and, an annual consumption of water for an individual is about 731 L. This brings the lifetime intake of water to 33,215 L. The cancer risk coefficients of uranium 1.13×10^{-9} Bq^{-1} for mortality and 1.73×10^{-9} Bq^{-1} for morbidity respectively were obtained from the literature (EPA, 1999; UNSCEAR, 2000). Using Equation 4.22 and these coefficients, the cancer mortality and morbidity risks of uranium over lifetime consumption of water were calculated and the results are presented in Table 4.24.

Table 4.24: The estimated lifetime cancer mortality and morbidity risk of ^{238}U in the water Samples.

Location	Cancer Mortality Risk	Cancer Morbidity Risk	Reference
Dei-Dei	1.01×10^{-7}	1.55×10^{-7}	Present Study
Kubwa	3.19×10^{-8}	4.88×10^{-9}	Present Study
Gosa	1.67×10^{-8}	2.55×10^{-8}	Present Study
Lugbe	1.03×10^{-7}	1.57×10^{-7}	Present Study
Water Board	6.85×10^{-8}	1.05×10^{-7}	Present Study
Hand-dug well	9.12×10^{-8}	1.40×10^{-7}	Present Study
Odeda, Ogun state, Nigeria	2.54×10^{-4}	3.39×10^{-4}	Amokom & Jibri 2010

In Table 4.24, the cancer mortality risk ranged from 1.67×10^{-8} to 1.03×10^{-7} while for morbidity risk ranges from 4.88×10^{-9} to 1.57×10^{-7}. The highest cancer mortality value was found at Lugbe borehole with a value of 1.03×10^{-7} and lower value reported at Gosa borehole with a value of 1.67×10^{-8}. The highest cancer morbidity of 1.57×10^{-7} was noted at Lugbe whereas lower value of 1.67×10^{-8} reported at Gosa borehole. The cancer risk comparing Lugbe cancer mortality risk of 1.03×10^{-7} to 6.85×10^{-8} and 9.12×10^{-8} values of cancer mortality risks for Water Board and hand-dug well respectively, Lugbe was distinctly higher than the two

values. In contrast with a study reported by Amokom & Jibri, (2010) in Ogun State Nigeria, Lugbe borehole water sample of 1.03×10^{-7} was lower than 2.54×10^{-4} value obtained. For cancer morbidity of 1.57×10^{-7} obtained from Lugbe borehole water sample was higher than 1.05×10^{-7} and 1.40×10^{-7} values obtained for cancer morbidity for Water Board and hand-dug well water samples respectively when compared but lower than the value of 3.39×10^{-4} for cancer morbidity reported in Ogun State Nigeria, (Amokom & Jibri, 2010). The cancer risk at 10^{-7} is low compared to the acceptable level of 10^{-3} for the radiological risk (EPA-USA, 1999). It can be noted that both cancer mortality and morbidity reported is to be high at Lugbe borehole, the aquifer could be affected due to higher deformation of fractures which enabled water to trap at the near surface since the subsurface geology permits the rapid downward movement of water sources from the source.

4.6.3 Chemical Toxicity Risk of ^{238}U in Groundwater from the Study Area

The purpose of the chemical toxicity was to determine the effect of the carcinogenic and non-carcinogenic risks associated with chemical toxicity in the water sample selected for this study. The analysis was done using inductively coupled plasma mass spectroscopy (ICP-MS). The chemical toxicity risk was evaluated using the lifetime average daily dose of ^{238}U through drinking water intake, and compared it with the reference dose (RFD) of 0.6 μg kg^{-1} day^{-1} (EPA-USA, 1999) used as a standard criteria for uranium in several foreign organizations and thereby produce a hazard quotient, Equation (4.15) and the lifetime average daily dose (LADD), Equation (4.16)

$$\text{Hazard quotient} = \frac{LADD}{RFD} \tag{4.15}$$

$$\text{Ingestion } LADD \text{ of drinking water} = \frac{EPC \; x \; IR \; x \; EFx \; ED}{AT \; x \; BW} \tag{4.16}$$

where, *LADD* is lifetime average daily dose (μg kg^{-1} day^{-1}), *EPC* is the exposure point concentration (μg L^{-1}), *IR* is the water ingestion rate (L day^{-1}); *EF* is the

exposure frequency (days year^{-1}), *ED* is the total exposure duration (years), AT is the average time (days) and *BW* is the body weight (kg). Using therefore, *IR* = 2 L day^{-1}, *EF* = 350 days, *ED* = 45.5 y, *AT* = 16,607.5 (obtained from 45.5 × 365) and *BW* = 70 kg (for a standard man). The chemical toxicity risk for uranium over a lifetime consumption was estimated and presented in Table 4.25. The exposure dose ranged from 1 x 10^{-3} to 6 x 10^{-3} µg kg^{-1} day^{-1}. The *LADD*s values were observed to be higher in the Lugbe and Dei-Dei boreholes compared to Kubwa and Gosa boreholes. This could be due to the altrabasic minerals emanated from the deep seated source caused by magmatic and metamorphic processes of granitic intrusions and its interconnectivity with geochemistry and aquifer bearing formation. The lowest value of 1 x 10^{-3} µg kg^{-1} day^{-1} was found in Gosa borehole. Comparing the LADD from Dei-Dei and Lugbe to Water Board and hand-dug well, it can be observed that Dei-Dei and Lugbe boreholes were higher than 4 x 10^{-3} and 5 x 10^{-3} values for Water Board and hand-dug well respectively. By comparing the LADD obtained in this study and the RFD (0.6 µg kg^{-1} day^{-1}) that is an acceptable level, the chemical toxicity risk due to ^{238}U in the water samples were all below the RFD. This shows that there may not be health risks associated with ^{238}U in the water samples which are mainly due to the chemical toxicity risk of ^{238}U.

Table 4.25: The estimated lifetime average daily dose (LADD) of uranium in the water samples.

Location	LADD (µg kg^{-1}day^{-1})	Reference
Dei-Dei borehole	6 x 10^{-3}	present
Kubwa borehole	2 x 10^{-3}	present
Gosa borehole	1 x 10^{-3}	present
Lugbe borehole	6 x 10^{-3}	present
Water Board	4 x 10^{-3}	presnt
Hand-dug well	5 x 10^{-3}	present
RFD (Reference Dose)	6 x 10^{-1}	Ye-shin et al., 2004

The LADD of ^{238}U in drilled borehole of Dei-Dei and Lugbe were higher than Kubwa borehole, Gosa borehole, Hand-dug well and Water-Board. Probably, ^{222}Rn may have escaped so easily from the Kubwa Borehole due to large scale fractures found in the region which may have channel towards the surface. The low activity level in Gosa may be caused by non-interconnectivity of fractures that hampers groundwater yield in the zone reported by Omeje et al., (2014). In addition, the Water Board of Abuja which is the public water supply in the region noted higher than Kubwa and Gosa boreholes which may be attributed to solubility and high content of toxic non-carcinogen metals in the source of the surface water of the public water supply. Compared the Dei-Dei borehole and hand-dug well since both were collected very close to each other but of varying depth, the LADD in Dei-Dei borehole was noted to be higher than the hand-dug well. The higher value in Dei-Dei borehole could be due to the bedrock waters are more alkaline, contain more bicarbonate and change towards the sodium type especially at greater depth (Juntunen 1991, Tarvainen et al., 2001). However, Dei-Dei borehole reported higher value of LADD of ^{238}U than hand-dug well which may have formed soluble complexes in aqueous phase in deeper well, (Langmuire 1978). The low level in hand dug well may be due to ^{222}Rn escapes so easily since the depth is too shallow.

4.6.4 The Elemental Concentrations of Water Samples in Dei-Dei, Kubwa, Gosa , Lugbe, Hand-Dug Well and Public Water Supply

The objective of determining the elemental concentrations was to infer the source of the groundwater pollution in the study area. The concentrations of the elements were determined using ICP-MS analysis in the same water samples. The concentrations in mg L^{-1} of the elements in the study area are presented in Table 4.26.

Table 4.26: Results of elemental concentrations of water analysis in Dei-Dei, Kubwa borehole, Water Board and hand-dug well and comparing with EPA 200.8 and Powel *et al.,*1989

Sample Location	Carcinogenic toxic elements (mg L^{-1})			Non-carcinogenic toxic elements (mg L^{-1})				
	As	Cr	Cd	Pb	Ni	Zn	Mg	K
Dei-Dei borehole	0.002	0.004	0.0001	0.005	0.003	0.02	Nil	Nil
Kubwa borehole	0.0002	0.002	0.00002	0.0002	0.002	0.04	2.11	1.41
Gosa borehole	0.0006	0.0003	0.0003	0.003	0.001	0.032	1.334	1.339
Lugbe	0.002	0.004	0.0001	0.014	0.021	0.277	0.037	0.0006
Water Board	0.001	0.01	0.0002	0.012	0.008	0.04	Nil	Nil
Hand-dug well	0.003	0.001	0.00006	0.002	0.005	0.03	Nil	Nil
U.S EPA 200.8	0.05	0.1	0.005	0.010	0.07	0.07	0.05	-
Powell et al., 1989	-	-	-	-	-	-	-	8.0

Lead is one of the most abundant heavy metals in nature and could be toxic for humans (UNSEAR, 2000). Most important anthropogenic source of lead in the environment is combustion of gasoline with lead. In environmental, lead changes to Pb^{2+} ion or as insoluble lead compounds. Residence time in blood and soft tissues is one month, but in case of livers, it is 50 years (WHO, 1995). Maximum permissible limit for lead in drinking water is 0.01mg L^{-1} (Council Directive 98/83/EC/1998 Quality of Drinking Water). The values obtained in the analysed water samples were well below 0.01mg L^{-1} except Lugbe borehole and Water Board with values 0.014 mg L^{-1} and 0.012 mg L^{-1} respectively which were higher than the standard recommended values (EPA, 200.8).

Cadmium is a metal found in natural deposit such as ores containing other elements. Cadmium is used primarily for metal plating and coating operations, including transportation equipment, machinery backing enamels, photography etc. The major source in drinking water are corrosion of galvanised pipes, erosion of

natural deposit, discharge from metal refineries; runoff from waste batteries and paints. Some people who drink water containing cadmium well in excess of the maximum contaminant level of 0.005 mg L^{-1} or 5 ppb for many years could experience kidney damage (2005 EPA Guidelines for Carcinogenic Risk Assessment). Comparing to the present study from both the groundwater samples and the public water (Water Board), they are below the contaminant level.

Arsenic is widely distributed in the environment because of its natural and anthropogenic sources (Commission Directives 2003/40/CE/May 2003). In surface and groundwater, arsenic is found dissolved in inorganic form (arsenite, arsenic) and organic form (acid-monimetilarsonic MMA-DMA dimetilarsinic acid). Inorganic arsenic is known to have high levels of toxicity, the allowable limits of As in natural mineral water (Commission Directives 2003/40/CE/May 2003) and water for human consumption (Commission 98/83/CE/3 Directives. Nov. 1998) was reduced to 0.05 mg L^{-1} total arsenic. Obtained levels in analyzed water samples were below the acceptable limits.

Accumulation of metal ions in subsurface water is important to be known in order to classify them for quality into standard and for consumption purposes. In this view, the concentrations obtained in four water samples for eight metals toxic assessments were below the acceptable limit. The Dei-Dei borehole, Kubwa borehole, Gosa borehole and Lugbe borehole could be noted that they did not differ much in toxic metal concentration values except in Pb in Gosa and Water Board which reported slightly higher than the recommended limit. In the same way, the concentrations of Zn, Cr, Mg and K reported are below the permissible limit except Mg in Kubwa and Gosa boreholes which noted higher than the permissible limit. Mg and K could only be traced in Kubwa, Gosa and Lugbe boreholes as shown in Table 4.30. It could be that the iron and manganese contents in groundwater in those areas are high and could result in hard water compared to Dei-Dei borehole, hand-dug well and Water Board samples. The carcinogenic risk level of toxic elements (Cr, Cd, As) range from 2.0×10^{-5} to 1.0×10^{-2} and for non- carcinogenic (Pb, Zn, Ni, Mg and K), ranges from 2.0×10^{-4} to 2.11×10^{0} as shown in Table 4.31. Comparing the carcinogenic toxic metals (Cr, Cd, As,) and non-carcinogenic (Pb, Zn, Ni, Mg and K)

in the studied samples, it can be seen that the values of non-carcinogenic risks are much larger than the values of the carcinogenic risk. This indicates apparently that non carcinogenic pollutants in the drinking groundwater are the major health risks in the groundwater in the study area.

The usefulness of determining elemental concentration comes from the fact that the result can be used to create an overview of the sample, thus, the results can be used to determine the origin of the sample in question or identifying sources of pollution. Determination of toxic elemental concentrations can be used in hydro-geochemical studies because of its potential to provide information about the water-rock interaction and in some cases evaluate the groundwater flow.

CHAPTER 5

CONCLUSION

5.1 Summary

The result from the VES survey carried out in the study area indicated the presence of lateritic or sandy topsoil, weathered basement and fractured basement. In Gosa where the groundwater was complicated to explore, the VES indicated the existence of both weathered and fractured basement which ideally could form good aquifers. The major aquiferous zones in the study area are zones of brecciation developed by intersection of regional fractures detectable on hill-shaded SRTM-DEM images. The lineament map generated shows the presence of large scale fractures around Gosa area; the fracture density is low and do not intersect. This demonstrates the usefulness of integrating conventional vertical electrical sounding (VES) survey with structural data derived from enhanced SRTM imagery in a hydrogeologically complicated terrain.

The results of gamma-ray measurements presented in this work give current information about natural radioactivity variation in layers of varying depths. This is the first subsurface radioactive investigation in the region. The higher activity concentrations of radionuclides (^{238}U, ^{232}Th and ^{40}K) in the study area may be due to the accumulation of felsic granitic intrusion which intruded in the subsurface and erratically distributed higher in near surface layers. Such variation or instability of

activity concentration of radionuclides with depth may be a function of lithological, structural, topographic and climatic factors which work synergistically. ^{40}K values in some rock samples activity concentrations were similar in biotite gneiss rock samples; it could be that biotite granitic intrusion that is inferred as the formation in those layers reflect the same activity of potassium in rock's radioactivity measurements (Maxwell *et al.,* 2013a). It was identified from this study that layers in the region may have encountered more effect of tectonic activities that resulted to interbedding of intrusive materials of magmatic and metasediments that enhanced the activity of radionuclides. In addition, the granitic intrusions produced by denudation and tectonism show that the majority of the radionuclides genetically connected with granitic intrusion built into metamorphosed rocks in the closest vicinity of the intrusion. The identification of radioactive source rocks that could constitute higher activity concentrations of ^{238}U, ^{232}Th and ^{40}K in subsurface layers geologically, addressed the professionals in hydrogeology and water resources management: civil engineers, environmental engineers, geologists and hydrologists who are engaged in the investigation, management, and protection of groundwater resources in the region suitable site for drilling hydrogeologically motivated boreholes.

In the study area, the mean annual effective dose from the natural radionuclide (^{238}U) for the users of borehole was estimated to be 5.55×10^{-5} mSv of the annual collective dose. The highest annual effective dose from radionuclide was noted in Lugbe Borehole with a value of 9.0×10^{-5} mSv y^{-1}. The lowest value was reported at Gosa borehole which was geologically attributed to redox condition of ^{238}U due to non-interconnectivity of fractures that serve as pathway for transports of sediments through the groundwater system. The radiological risks of ^{238}U in the water samples were found to be low, typically in magnitude of 10^{-7}. It could be that the human risk due to ^{238}U content in water supplies both from groundwater and public water that will result from ingestion in the area may likely be to the chemical toxicity of ^{238}U as a heavy metal rather than radiological risk. Interestingly, the water board reported distinctly high activity concentration of radionuclide and toxic elements compared to some drilled wells in the study area but below recommended limit. There is a variation of concentrations of heavy metals depending on the chemical composition of the groundwater host rock which was inferred by this study. Characterization in terms of concentrations of the metals in water samples collected

in the study areas contain arsenic of below the permissible limit, so to all other elements. Determination of toxic elements in various types of environmental samples is very important in creating a fingerprint of the sample and thus the results can be used in determining the origin of the sample in question and to identify sources of pollution. However, the analysis of both the carcinogen and non-carcinogen chemicals indicate that non-carcinogenic risk from (Pb, Zn, Ni, Mg, K) are much larger than the values of the carcinogenic risk (Cd, Cr, As) in the studied samples. This indicates apparently that chemical carcinogenic pollutants in the groundwater based drinking water are the major risk inducing chemical parameters in the study area.

This study represents a useful radiometric interpretation data that could be of importance in radio-epidemiological assessment, diagnosis and prognosis of uranium-induced diseases to the population of the inhabitants of Abuja.

5.2 Recommendation and Future Work

In the case of activity concentrations of ^{238}U, ^{232}Th and ^{40}K in subsurface layers in the study area, it is recommended that further research or replicate of the similar method in two different regions but deeper depth of 80 m in each region especially in sedimentary terrain and to compare the results with basement complex region lithologically where this work was carried out.

Taking the whole analysis of the groundwater into consideration, it is recommended that non-carcinogens pollution are the primary pollutants that pose the health risk in the region and it is recommended that the groundwater in Abuja should be treated before consumption to decrease the risk if the means is possible. At the same time, measures of groundwater quality protection and monitoring should be enhanced and new supply source which has lower risk must found.

REFERENCES

Abdullah, K., Sarfaraz, A. and Shadab, K. (2012). Geology and geomorphology of the Manipur Valley using digitally Enhanced satellite image and SRTM DEM in the Eastern Himalaya, India. *Int. J. of Geosc.*, 3,1010 – 1018.

Abdallah, M. A. M. and Morsy, F. A. E. (2013). Persistent organochlorine pollutants and metals residues in sediment and freshwater fish species cultured in a shallow lagoon, Egypt. *Environmental Technology*, *34*(13-16), 2389–2399.

Acworth, R.I. (1987). The development of crystalline basement aquifers in a tropical Environment. *Quarterly Journal of Engineering Geology*, 20, 265 - 272.

Adams, F. and Dams, R. (1969). A compilation of precisely determined gamma transition energies of radionuclides produced by reactor irradiation. *Journal of Radioanalytical Chemistry*, 3, 99-121.

Ahmed, J., Baig, T.,Gul Kazi, A., Qadir Shah, G., Abbas Kandhro, H., Imran Afridi, M., Balal Arain, M., Khan Jamali, Jalbani, N. (2010). Ecotoxicology and Environmental Safety 73, 914–923.

Aieta, E. M., Singley, J. E., Trusell, A.R., Thorbjarnarson, K. W., McGuire, M. J. (1987). Radionuclides in Drinking water: An overview. *Journal of the American Water worksAssociation,* 79 (4), 144-152.

Ajayi, I. R., Ajayi, O.S., Fusuyi, A. S. (1995). The natural radioactivity of surface soil in Ijero-Ekiti. Nigeria. *Nig. J. of Phys.,* 7: 101-103.

Ajayi, O. S., Ajayi, I.R. (1999). Environmental gamma radiation levels of some areas of Ekiti and Ondo State, South Western Nigeria. *Nig. J. of Phys*., 11: 17-21.

Ajibade, A., Woakes, M. and Rahaman, M. (1987). Proterozoic crustal development in the Pan-African regime of Nigeria. *Geodynamics Series*. 17, 259-271.

Almeida, R. M. R., Lauria, D. C., Ferreira, A. C., Sracek, O. (2004). Groundwater radon, radium and uranium in Região dos Lagos, Rio de Janeiro State, Brazil. *Journal of Environmental Radioactivity*; 73 (3): 323–334.

Alnour, I., Wagiran, H., Ibrahim, N., Laili, Z., Omar, M., Hamzah, S. and Idi, B. Y. (2012). Natural radioactivity measurements in the granite rock of quarry sites, Johor, Malaysia. *Radiation Physics and Chemistry*. 81(12), 1842-1847.

Al-Sulaiti, H. (2011). *Determination of natural radioactivity levels in the State of Qatar using High Resolution Gamma-ray Spectroscopy*. Ph.D. Thesis. Universisty of Surrey. UK.

Anudu, G.K., Essien, B.I., Onuba, L.N., Ikpokonte, A.E. (2011). Lineament analysis and interpretation for assessment of groundwater potential of Wamba and adjoining areas, Nassarawa State, northcentral Nigeria. *Journal of applied technology in environmental sanitation,* 1, 185 – 198.

Auu, Gui Ah. (1983). PUSPATI TRIGA REACTOR FUEL WORTH MEASUREMENT. *Nuclear Science Journal*, 1, 9-12.

Bala, A.E. (2001). An evaluation of Landsat 5 Thematic Mapper data as a tool for groundwater investigation in Basement Complex rocks of Nigeria. *Unpublished PhD Thesis*, Ahmadu Bello University, Zaira, Nigeria.

Bala, A.E., Batalan, O., De Smedt, F. (2000).Using Landsat5 imagery in the assessment of groundwater resources in the crystalline rocks around Dutsin Ma, northwestern Nigeria. *Journal of Mining and Geology*, 36, 85 – 92.

Barongo, J. O., Palacky G. D. (1989). Investigation of electrical properties of weather layers in the Yale area, Western Kenya, using resistivity soundings. *Geophysics*,56, 133-138.

Black, R. R., Caby, R., Moussine-Pouchkine, A., Bayer, R., Bertrand, J.M., Boullier, A.M., Fabre, J., Lesquer, A. (1979). Evidence for Late Precambrian plate tectonics in West Africa. *Nature,* 278, 223 – 227.

Caby, R. (1989).Precambrian terrains of Benin, Nigeria and Northeast Brazil and the Late Proterozoic South Atlantic fit. *Geologic Society of American Special Paper*. 230, 145 – 158.

Cothern, R. C., P.A. Rebers , P. A. (1990) (Eds.) Radon, Radium and Uranium in drinking water, *Lewis Publishers*.

Council Directive 98/83/EY/, of 3 November. (1998), on the quality of water intended for human consumption, Official Journal of the European Communites, L 330, 05/12/1998 s. 0032-0054; 1996.

Crancon, P., van der Lee, J. (2003). Speciation and mobility of uranium (VI) in humic–containing soils. *Radiochimica Acta*; 91: 673–679.

Dada, S. S. (2008). Proterozoic evolution of the Nigeria – Boborema province. *Geol. Socei. Lond.Speci. Public.* 294, 121 – 136

De Beer, J. H., Blume J., (1985). Geophysical and hydrogeological investigation of the groundwater resources of western Hereroland, southwest African/Namibia. *Trans. Geol. Soc. S. Africa*,88, 483-493.

Deflorin, O., Surbeck, H. (2004). Natürliche Radionuklide in Grundwässern des Kantons Graubünden, In: Völkle H., Gobet M. Umweltradioaktivität und Strahlendosen in der Schweiz. Bern; *Bundesamt für Ge*sundheit.

Degueldre, C., Triay, I., Kim, J. I., Vilks, P., Laaksoharju, M., Miekeley, N. (2000). Groundwater colloid properties: a global approach. *Applied Geochemistry*,15, 1043–1051.

Delleur, J.W. (1999).The Handbook of Groundwater Engineering. *CRC Press*, New York.

Durrance, E. M. (1986). Radioactivity in Geology: Principles and Applications. New York, NY (USA). *John Wiley and Sons Inc*.

Edet, A. E., Okereke, C. S. (1997). Assessment of hydrogeological conditions in basement aquifers of the Precambrian Oban Massif, Southeastern Nigeria. *Journal of Applied Geophysics*, 36, 195-204.

Edet, A.E., Teme, C.S., Okereke, C.S., Esu, E.O. (1994). Lineament analysis for groundwater exploration in Precambrian Oban Massif and Obudu Plateau, S.E Nigeria. *Journal of Mining and Geology*,30, 87 – 95.

Eisenbud, M. and Gesell, T. (1997). Environmental Radioactivity from Natural, Industrial and Military Sources. *Acad. press, San Diego, CA,* 134-200.

Evan, R.D. (1969). Engineer's guide to elementary behaviour of radon daughters. *Health Phys*.,17, 229- 252.

Fernandez, F., Lozano, J. C., Comez, J.M.G. (1992) Natural Radionuclides in Ground Water in Western Spain. *Radiation Protection Dosimetry* ,45 (1–4): 227–229.

Fetter, C. W. (1994). *Applied Hydrogeology*, 3rd ed. Upper Saddle River, NJ: Prentice Hall, Inc

Figgins PE. (1961) Radiochemistry of Polonium. NAS-NS Publication 3037. Washington: U.S. Atomic Energy Commission.

Freeze, R.A. and Cherry, J.A. (1979). Groundwater. *Prentice Hall*, New Jersey, 604 pp

Galnett, R.H., Gardner, J.V. (1979). Use of radar for groundwater exploration in Nigeria. *West Africa.Proceedings of the 14th International Symposium on Remote Sensing of Environment, Ann Arbor, Michigan*.

Gans, I., Fusban, H.U., Wollenhaupt, H., Kiefer, J., Glöbel, B., Berlich, J., Porstendörfer, J. (1987). Radium 226 und Andere Natürliche Radionuklide im Trinkwasser und in Getränken in der Bundesrepublik Deutschland. WaBoLu-Hefte 4/87*, Institut für Wasser- Boden-und Lufthygiene des Bundesgesund-heitsamtes.*

Gbadebo, A.M. (2011). Natural redionuclides Distributions in granitic rocks and soils of abandoned quarry sites, Abeokuta, South western Nigeria. Asian Journal of Applied Sci.,4 : 176-185.

Godknows Igali. (2012). Nigeria Ranks 3rd in Poor Water Access, by WHO and UNICEF.11th Session of Development partners Coordinating Meeting, *Daily Triumph Newspaper*, May 10th .

Goki, N.G., Ugodulunwa, F.X.O., Ogunmola, J.K., Oha, I.A., Ogbole, J.O. (2010). Geological controls for groundwater distribution in the basement rocks of Kanke, central Nigeria from geophysical and remotely sensed data. *African Journal of Basic and Applied Sciences*,2, 104 – 110.

Greenberg, R. R., Bode, P. and De Nadai Fernades, E. A. (2011). Neutron activation analysis: A primary method of measurement. Spectrochimica Acta Part B: Atomic Spectroscopy. 66 (3), 193-241.

Grohmann, H.C., Riccomini, C., Machado-Alves, F. (2007). SRTM-based morphotectonic analysis of the Pocos de Caldas Alkaline massif, Southern Brazil. *Computers & Geosciences,* 33, 10 – 19.

Grzybowska, D., Wardaszko, T., Nidecka, J. (1983). Natural Radioactivity of Fresh Waters in Poland. Polskie *Archiwum Hydrobiologii*; 30 (4): 309–318.

Hamby, D.M., Tynybekov, A.K. (2002).Uranium, Thorium, and Potassium in soils along the shore of the lake Issyk-Kyol in the Kyrghyz Republic. *Environ. Monitor. Assess*., 73, 01-108.

Hostetler PB, Garrels RM. (1962).Transportation and Precipitation of Uranium and Vanadium at low temperatures with special reference to sandstone-type uranium deposits. *Economic Geology*, 57 (2): 137-167

Huikuri, P., Salonen, L., Raff, O. (1998). Removal of Natural Radionuclides from Drinking Water by Point of Entry Reverse Osmosis. *Desalination* ,119: 235-239.

Ibrahim, N.M., Abd El Ghani, A.H., Shawky, S.M., Ashraf, E.M., Faruk, M.A. (1993). Measurement of radioactivity level in soil in Nile Delta and Middle Egypt. *Health Phys*., 4,620-627.

IAEA, International Atomic Energy Agency. (1990). The Environmental Behaviour of Radium, Vienna: IAEA, *Technical Report Series* No. 310.

Internal Commission on Radiological Protection. (1993). Age-dependent Doses to Members of the Public from Intake of Radionuclides: Part 2 Ingestion Dose Coefficients, *Annals on the ICRP, ICRP publication 67, Oxford*: Pergamon Press.

Internal Commission on Radiological Protection. (1995).Age-dependent Doses to Members of the Public from Intake of Radionuclides: Part 3 Ingestion Dose Coefficients, *Annals on the ICRP, ICRP publication 69, Oxford:* Pergamon Press.

Internal Commission on Radiological Protection. (1991). Annual Limits on Intake of Radionuclides by Workers Based on the 1990 Recommendations. *Annals on the ICRP, ICRP publication*, 67, Oxford Press.

Internal Commission on Radiological Protection. (1990). Annual Limits on Intake of Radionuclides by Workers Based on the Recommendations, Annals on the ICRP, ICRP publication 67, *Oxford Press.*

International Atomic Energy Agency,IAEA. (1989). Construction and use of calibration Facilities for Radiometric Field Equipment. *Technical Reports Series no.309, IAEA,Vienna.*

Isam Salih, M. M., Pettersson, H. B. L., Lund, E. (2002). Uranium and thorium series radionuclides in Drinking water from drilled bedrock wells: Correlation to

Geology and Bedrock radioactivity and dose estimation. *Radiation Protection Dosimetry* 2002; 102 (3): 249–258.

Ivanovich, M., Harmon, R. S., (Eds.). (1982). Uranium series Disequilibrium. Application to Environmental Problems, *Clarendon Press, Oxford.*

Jang, J. H., Dempsey, B. A., and Burgos, W. D. (2006). Solubility of Schoepite: Comparison and selection of complexation and constants for U(VI). Water Res. 40, 2738-2740.

Jibiri, N. N., Mabawonku, A. O., Oridate, A. A., ujiagbedion. (1999). Natural radionuclides concentration level in soil and water around a cement factory at Eweoro, Ogun, Nigeria. Nig. J. of Phy. 11, 12-16.

Juntunen, R. (1991).Uranium and radon in wells drilled into bedrock in Southern Finland. Report of Investigation, Helsinki: *Geological Survey of Finland* (98).

Kafala, S. and MacMahon, T. (1993). Neutron activiation analysis without muclti element standards. Journal of radioanalytical and nuclear chemistry. 169 (1), 187-199.

Keller, G. V., Frischknecht, F. C. (1966). Pergamon Press, 1966 -Science - 519 pages

Knoll, G. F. (2000). *Radiation detection and measurements*. 3rd ed.. John Wiley & Sons, Inc. New York.

Kobal, I., Vaupotic, J., Mitic, D., Kristan, J., Ancik, M., Jerancic, S., Skofljanec, M. (1990). Natural radioactivity of fresh waters in Slovenia, Yugoslavia. *Environmental International*; 16 (2): 141–154. Koljonen T. (Ed.). (1992). The Geochemical Atlas of Finland, Part 2: Till. Espoo. *Geological Survey of Finland.*

Langmuir, D. (1978) .Uranium-solution equilibria at low temperatures with applications to sedimentary Ore deposits. *Geochimica Cosmochimica Acta* ,42 (6): 547-569.

Lee, S. K. (2007) *Natural background radiation in the Kinta District, Perak Malaysia.* Masters thesis, Universiti Teknologi Malaysia, Faculty of Science.

Lee, S.K., H. Wagiran, Ahmad T. R, Nursama H. A and A. K. Wood. (2009). Radiological Monitoring: Terrestrial Natural Radionuclides in Kinta District, Perak, Malaysia. *J. of Environ. Radioact*., 100, 368-374.

Lehtinen, M.,Nurmi,P., Ramo, T. (1998). Suomen Kalliopera 3000 Vuosimiljoonaa. Jyvaskyla:*Suomen Geologinen Seura*; (in Finnish).

Lieser, K. H., Ament, A., Hill, R., Singh, R. N., Stingl, U., Thybusch, B. (1990). Colloids in Groundwater and their Influence on Migration of Trace Elements and Radionuclides. *Radiochimica Ac*ta; 49 (2): 83–100.

Lohman, S.W. (1972). Groundwater Hydraulic. U.S Geological Survey professional paper, 708.

Lowder, V. M. (1990). Natural environmental radioactivity and radon gas. Proc. Of Int. Workshop on Radon Monitoring in radioprotection, environmental radioactivity and earth Sciences. *World Scientific Singapore*. P. 1-17. Malaysia. M.Sc thesis, Universiti Teknologi Malaysia.

Loxnachar, Thomas, E., Brown, Kirk ,W.,Cooper, Terence, H., Milford, Murray, H. (1999). Sustaining Our Soils and Society. American Geological Institute, Soil Science Society of America, USDA *Natural Resource Conservation Service publication.*

Lucas, H. F. (1985). ^{226}Ra and ^{228}Ra in water supplies: *Journal of the American Water Works Association,* v. 77. no. 9, p. 57–66.

Mäkeläinen, I., Salonen, L., Huikuri, P., Arvela, H. (2002). Dose received and cancer risk from natural radionuclides in drinking water in Finland. Proceedings of the 5th International Conference on High Levels of Natural Radiation and Radon Areas held in Munich, Germany on Sep 4-7, 2000. BfS Schriften. Strahlenhygine. High Levels of Natural Radiation and Radon Areas: *Radiation Dose and Health Effects*. Volume II: Poster Presentations. General Exposure Assessment; 24: 28-30.

Malczewski, D. ,Teper, L., and Dorda, J. (2004). Assessment of natural and anthropgenic radioactivity levels in rocks and soils in the environs of Świeradów Zdrój in Sudetes, Poland, by in situ gamma-ray spectrometry, *Journal ofEnvironmental Radioactivity* 73, 233–245.

Malczewski, D., Sitarek, A., Zaba, J. and Dorda, J. (2005) . Natural radioactivity of selected Crystalline rocks of Iera block, *Prze. Geol*. ,53 (3), 237-244.

Malczewski, D. and Żaba, J. (2007). ^{222}Rn and ^{220}Rn concentrations in soil gas of Karkonosze-Izera Block (Sudetes, Poland), Journal of Environmental Radioactivity 92, 144–164.

Maxwell, O., Wagiran, H., Ibrahim, N., Lee, S. K., Soheil, S. (2013a). Comparison of ^{238}U, ^{232}Th, and ^{40}K in different layers of subsurface structuresion Dei-Dei and Kubwa, Abuja, Northcentral Nigeria. *Radiation Physics and Chemistry*, 91, 70-80.

Maxwell, O., Wagiran, H., Ibrahim, N., Lee, S. K., Soheil, S. (2013b). Measurement of ^{238}U, ^{232}Th, and ^{40}K in boreholes at Gosa and Lugbe, Abuja, North Central Nigeria. *Radiation Protection Dosimetry* , pp 1-7.

Maxwell, O., Wagiran, H., Noorddin I., Oha I.A., Onwuka O. S., Soheil S. (2014). Integrated geoelectrical and structural studies for groundwater investigation in some parts of Abuja, Northcentral Nigeria. *Near Surface Geophysics*, 12, doi:10.3997/1873-0604.2014007.

Mbonu, P.D.C., Ebeniro, J. O.,Ofoegbu. C. O., Ekine, A.S. (1991). Geoelectrical Sounding for the determination of aquifer Characteristics in part of Umuahia area of Nigeria. *Geophysics*, 56, 284-291.

Mendoza, J.A and Dahlin T. (2008). Resistivity imaging in steep and weathered terrains. *Near Surface Geophysics* 6, 105–112.

Midtgård, A.K., Frengstad, B., Banks, D., Reidar Krog, J., Strand, T., Siewers, U., Lind, B. (1998) Drinking water from crystalline bedrock aquifers - not just H2O. *Mineralogical Society Bulletin*; December: 9–16.

National Academy of Science. (1995). Nitrate and Nitrite in Drinking Water. Washington, D.C.: *National Academy Press.*

National Research Council., (1999). Risk Assessment of Radon in Drinking Water. Washinton D.C.: *National Academy Press*.

Nikolakopoulos, K. G.; Kamaratakis, E. K; Chrysoulakis, N. (2006). " SRTM vs ASTER elevation product. Comparison for two regions in Crete, Greece". *International Journal of Remote Sensing* 27 (21).0143-1161.

Novotny. (2003). Water quality – diffuse pollution and wastewater management. 2nd edition, John Wiley and Sons, Inc., 43–50.

Nur. A., Ayuni, N. K. (2004). Hydrologeolectrical study in Jalingo Metropolis and environs of Taraba State, Northeastern Nigeria. *Global Journal of Geological Science* ,2, 101-109.

Obaje, N.G. (2009). Geology and mineral resources of Nigeria. *Lecture notes in earth sciences*, 120, pp 221.

Offodile, M. E. (1992). Groundwater study and development in Nigeria (1st Ed), ISBN, 978-30956-2-4, Pp. 306-308.

Okeyedi, A.S., Gbadedo, A.K., Arowolo, T.A., Mustapa, A.O., Tehokossa.,(2012). Measurement of Gamma-emitting Radionuclides in Rocks and Soil of Saunder Quarry Site, Abeokuta, Ogun State, Nigeria. Journal of Applied Sciences 12 (20) 2178 – 2181.

Oladapo, M. I., Akintorinwa, O.J. (2007). Hydrogeophysical study of Ogbesse, southwestern Nigeria. *Global Journal of Pure Sci*, 13, 55-61.

Olorunfemi, M. O., Okakune, E. T. (1992). Hydrogeological and Geological significance of Geoelectrical survey of Ile-Ife. *Nigeria Journal of Mining and Geology*,28, 221-222.

Olorunfemi, M. O., Fasuyi, S. A. (1993). Aquifer types and geoelectrical/hydrogeologic characteristics of the central basement terrain of Nigeria. *Journal of African Earth Sciences*, 16; 309-317.

Omeje M., H., Wagiran, N. Ibrahim, Oha I.A, Onwuka O.S., P.E Ugwuoke, Meludu, O. (2013). Geoelectrical investigation of aquifer problems in Gosa area of Abuja, Northcentral Nigeria. *International Journal of Physical Sciences, vol.* 8 (13), pp. 549-559.

Oyawoye, M. O. (1972). The basement complex of Nigeria. In T.F.J. Dessauvagie and A.J. Whiteman (eds). *African Geology, Ibadan*, 66 – 102.

Palacky, G.V. (1987). Resistivity characteristics of geologic target, in electromagnetic methods in applied geophysics, Vol. 1, Theory, 1351.

Peterson, R. E., Rockhold, M. L., Serne, R. J., Thorne, P. D. and Williams, M. D. (2008). Uranium contamination in the subsurface beneath the 300 Area, Hanford Site, Washington. Pacific Northwest National Laboratory (PNNL), Richland, WA (US).

Pfenning, G. , Klewe- Nebenius, H. , Seelmann-Eggebert, W.(1998). Chart of the Nuclides. *6th edition revised reprint.*

Plewa, M. and Plewa, S. (1992). Petrofizyka, Wydawnictwa Geologiczne, Warszawa, 248-271.

Powell, P., Bailey, R. J. , Jolly, P. K. (1987). Trace elements in British tap-water Supplies.

Przylibski, T. (2004) .Concentration of ^{226}Ra in rocks of the southern part of Lower Silesia (SW Poland), *Journal of Environmental Radioactivity* 75, 171–191

Swindon, WRc (Report PRD 706-M/1).

Pulawaski, B., Kurtn, K. (1977). Combined use of resistivity and seismic refraction methods in groundwater prospecting in crystalline areas. *Study project, Kenya, DANIDA* 5-33.

Rahaman, M.A. (1988). Recent advances in the study of the Basement Complex of Nigeria. Precambrian Geology of Nigeria. *Geol. Survey of Nigeria publication*, 11 – 43.

Reuter H.I, A. Nelson, Jarvis, A. (2007). An evolution of void filling interpolation methods For SRTM data. *International Journal of Geographic Information Science*, 21:9, 983–1008.

Reynolds J.M. (2011). An Introduction to Applied and Environmental Geophysics. *John Wiley & Sons Ltd*., England, vol. 2, 712 pp.

Saleh, M. A., Ramli, A. T., Alajerami, Y. and Aliyu, A. S. (2013). Assessment of natural radiation levels and associated dose rates from surface soils in pontian district, Johor, malaysia. J*ournal of Ovonic Research*. 9(1)

Salih, I., Bäckström, M., Karlsson, S., Lund, E., Pettersson, H.B.L. (2004) Impact of fluoride and other aquatic parameters on radon concentration in natural waters. *Applied Radiation and Isotopes* ,60 (1): 99–104.

Salonen, L. , Huikuri, P. (2000 & 2002). Elevated Level of Uranium Series Radionuclides in Private Water Supples in Finland, Proceedings of the 5th International Conference on High Levels of Natural Radiation and Radon Areas held in Munich, Germany on Sep. 4-7, BfS Schriften. Strahlenhygine. High levels of Natural Radiation and Radon Areas: *Radiation Dose and Health Effect*. Volume II: General Exposure Assessment; 24: 28-30.

Salolen L. (1994) . ^{238}U series radionuclides as a source of increased radioactivity in groundwater originating from Finnish bedrock. Future Groundwater Resources at Risk: *IAHS Pub*l. No. 222: 71-84.

Satpatty, B. N., Kanugo, B. N. (1976). Groundwater Exporation in Hard rock terrain, A case Study. *Geophysical prospecting*,24, 725-736.

Saumande, P., Reix, F., Beck, C . (1973)Etude de la radioactivté des eaux naturelles du Limousin: Le radium 226, l´uranium et le radon. *Bulletin De La Societe de Pharmacie de Strasbourg* , XVI (2): 141–152.

Shemang, E. N. (1993). Groundwater potentials of Kubami River Bassin, Zaria, Nigeria, from D.C Resistivity study. *Water Resources* 2, 36-41.

Silva, R., Nitsche, H. (1995). Actine Environmental Chemistry. *Radiochimica Acta*,70/71: 377-396.

Smith, B. M., Grune, W. N., Higgins, F.B. , Terril, J. G., Jr. (1961). Natural Radioactivity in Groundwater supplies in Maine and New Hampshire. *Journal of the American Water Works Association*; 53 (1), 75–88.

Smith, L. L. , Alvarado, J. S. , Markun, F. J. , Hoffmann, K. M. , Seely, D. C. , Shannon, R. T. (1997). An Evaluation of Radium-Specific, Solid-Phase Extraction Membranes. *Radioactivity & Radiochemistry*; 8 (1): 30–37.

SRTM. http://srtm.csi.cigar.org/ (Date of access 06/09/2010).

Stihi, C., Radulescu, C., Busuioc, G., I.V, Popescu, A, Gheboianu, Ene, A. (2011). Rom. Journ. Phys., 56, no.1–2, 257–264.

Suksi, J. (2001). Natural Uranium as a Tracer in Radionuclide Geosphere Transport Studies, Report Series in Radiochemistry 16/2001. Helsinki; *University of Helsink Department of Chemistry, Laboratory of Radiochemistry.*

Supian, B.S., Evans, C.J. (1992). Statistics and nuclear counting: theory, problems and solutions. Statistics and errors in measurements.Pp. 26-35.

Technical Procedure . (2003). NYE County Nuclear Waste Repository Project Office Field Collection, Logging, and Processing of Borehole Geologic Sample, pp 19.(TP 8.0,Rev. 15).

Thomas, R . (2004). Practical Guide to ICP-MS, MarcelDekker Inc.

Todd, K. D. (1980). Groundwater Hydrology, 2nd ed. New York: *John Wiley and Sons.*

Tsoulfanidis, N . (1995). Measurement and Detection of Radiation. *Taylor and Francis*.

Tarvainen, T. , Lahermo, P. , Hatakka, T. , Huikuri, P., Ilmasti, M., Juntunen, R., Karhu, J., Kortelainen, N., Nikkarinen, M., Vaisanen, U. (1999-2000).Chemical Composition of well water in Finland- Main results of the "One thousand wells" Project. *Geological Survey of Finland, Current Research ; Special Paper*, 31: 57-76.

Tzortzis, M., Tsertos, H. (2004). Determination of thorium, uranium and potassium Elemental concentrations in surface soils in Cyprus. *J. Environ. Radioact*. 77, 325-338.

Trimble, C.A. (1968). Absolute counting of alpha decay and the radioactivity in water from Hot spring National Park. *University of Arkansas*; Thesis.

Ulbak. K., Klinder, O. (1984). Radium and Radon in Danish Drinking Water. Radiation Protection Dosimetry; 7 (1–4): 87–89.

Ulrich, H. J., Degueldre, C. (1993). The sorption of 210Pb, 210Bi and 210Po on montmorillonite: a study with emphasis on reversibility aspects and on the effect of the radioactive decay of adsorbed nuclides. Radiochimica Acta, 62: 81–90.

United Nations Population Fund (UNFPA,(2013 &2014): http://nigeria.unfpa.org/abuja.html.

United Nations Scientific Committee on the Effects of Atomic Radiation., UNSCEAR. (1998). Sources, effects and risks of ionising radiations. New York.

United Nations Scientific Committee on the effects of Atomic Radiation, UNSCEAR. (2000). Sources, effect and risks of ionising radiation. *Report to the General Assembly with Scientific Annexes.* United Nations. New York.

United States Environmental Protection Agency. (2003). Current Drinking Water Standards, Ground water and drinking water protection agency, pp. 1–12.

U.S. Environmental Protection Agency (EPA) .(1999). Cancer risk coefficients for Environmental exposure to radionuclides. United State Environmental Protection Agency. Federal Guidance Report No -13(EPA. 402 R-99-001).

U.S. Environmental ProtectionAgency. (1993). Diffuse NORM Waste characterization and preliminary risk assessment, Washington, DC*: U.S. EPA*; RAE-9232/1-2, Draft Report.

Usikalu, M. A., Anoka, O. C. and Balogun, F. A. (2011). Radioactivity measurement s of the Jos Tin mine tailing in Northern Nigeria. Archives of Physics Research, 2 (2): 80-86.

U.S. Nuclear Regulatory Commission, NRC. (1988). Health risk of radon and other internally deposited alpha-emitters, Washington, DC. *Academia press; NRC. Report BEIR IV.*

U.S Soil Conservation Service. (1951). A report based on data gathered under cooporation agreement between the soil conservation service, the Idaho Agricultural experiment station. Gem country. *U.S Geological Survey.*

Vaaramaa, K., Lehto, J., Ervanne, H. (2003). Soluble and Particle-Bound ^{234,238}U, ^{226}Ra and ^{210}Po in ground waters. *Radiochimica Acta*; 91 (1): 21–27.

Valeriano, Márcio, M., Kuplich Tatiana, M., Storino Moisés , Amaral Benedito, D., Mendes, J. r., Jaime, N. L., Dayson, J. (2006).Modelling small watersheds in Brazilian Amazonia with Shuttle Radar Topographic Mission 90m data. *Comput. & Geosc.*32, 1169 – 1181.

Veeger, A. I., Ruderman, N. C. (1998) Hydrogeologic Controls on Radon-222 in a Buried Valley- Fractured Bedrock Aquifer System. *Ground Water*; 36 (4): 596–604.

Von Gunten, H.R., Benes, P. (1995). Speciation of Radionuclides in the Environment. Radiochimica Acta ; 69: 1–29.

Wright, R., Garbeil, H., Baloga, S., Mougin-Mark, P., (2006). An assessment of Shuttle Radar Topographic Mission digital elevation data for studies of volcano morphology. *Remote Sensing of Environment* 105, 41 – 53.

Williams, B. A., Brown, C. F., Um, W., Nimmons, M. J., Peterson, R. E., Bjornstad, B. N., Lanigan, D. C., Serne, R. J., Spane, F. A. and Rockhold, M. L. (2007). Limited field investigation report for uranium contamination in the 300 Area, 300-FF-5 operable unit, Hanford Site, Washington. Pacific Northwest National Laboratory (PNNL), Richland, WA (US).

World Health Organization (WHO). (2008). Meeting the MDG drinking water and sanitation target: the urban and rural challenge of the decade. WHO Library Cataloguing-in-Publication Data .

World Health Organization. (2004). 3rd Edition of Guidelines on Drinking Water Quality, *Geneva.*

WHO Lead. (1995). Environmental Health Criteria, *Geneva*, 165.

Xinwei, L., Xiaolon, Z. (2008). Natural radioactivity measurements in Rock samples of Chihua Mountain National Geological Park, China. *Radiat. Prot. Dosim.* 128, 77-82.

Ye-shin, K., Hoa-sung, P., Jin-yong, K., Sun-ku, P., Byong-wook, C., Ig-hwan, S., Dong Chun, S. (2004). Health risk assessment for uranium in Korean groundwater. *J. Environ. Radioactivity*, pp. 77-85.

Zelensky, A. V., Buzinny, M. G., Los, I. P. (1993). Measurement of ^{226}Ra, ^{222}Rn and Uranium in Ukrainian Groundwater using Ultra-low level liquid scintillation counting. In: Noakes JE, Schönhofer F, Polach HA. (Eds.) Advances in Liquid Scintillation Spectrometry 1992, RADIOCARBON; 405–411.

Zielinski, R. A., Asher-Bolinder, A., Meier, A. L. (1995). Uraniferous waters of the Arkansas River Valley, Colorado, U.S.A.: a function of geology and land use. *Applied Geochemistry*; 10: 133–144.

Zhuo, W., Iida, T., Yang, X. (2001).Occurrence of ^{222}Rn, ^{226}Ra, ^{228}Ra and U in groundwater in Fujian Province, China. *Journal of Environmental Radioactivity;* 53: 111–120.

Zohdy, A. A., Eaton, C.P., Mabey, D. R. (1974). Application of surface geophysics In groundwater investigation. Tech.Water resources investigation, Washington. *US. Geol. Survey.*

APPENDIX A:

Accessibility map of the study locations of Dei-Dei, Kubwa, Gosa and Lugbe showing positions of VES points for borehole locations in Abuja, North central Nigeria

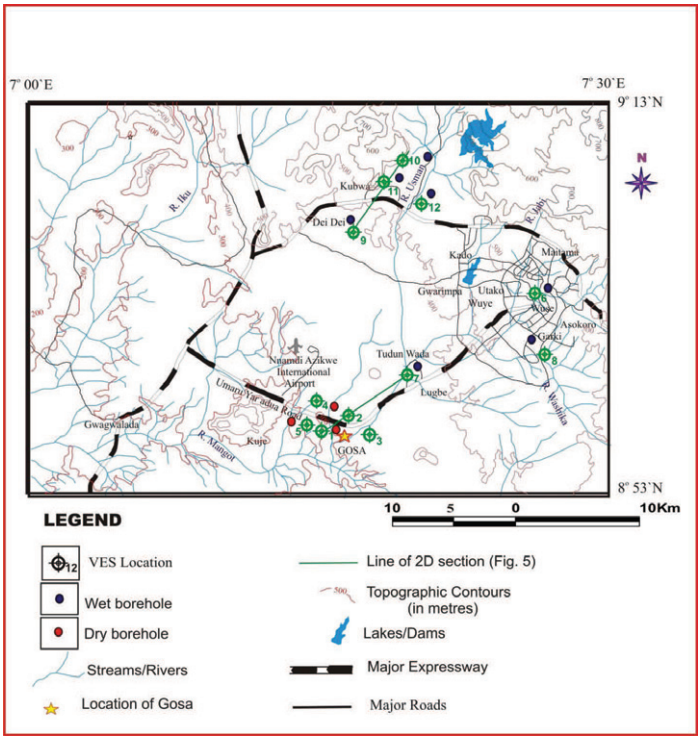

APPENDIX B:

Geological map of the study area (top) with schematic cross section (bottom) showing the rock types and the cross section of where the boreholes were drilled.

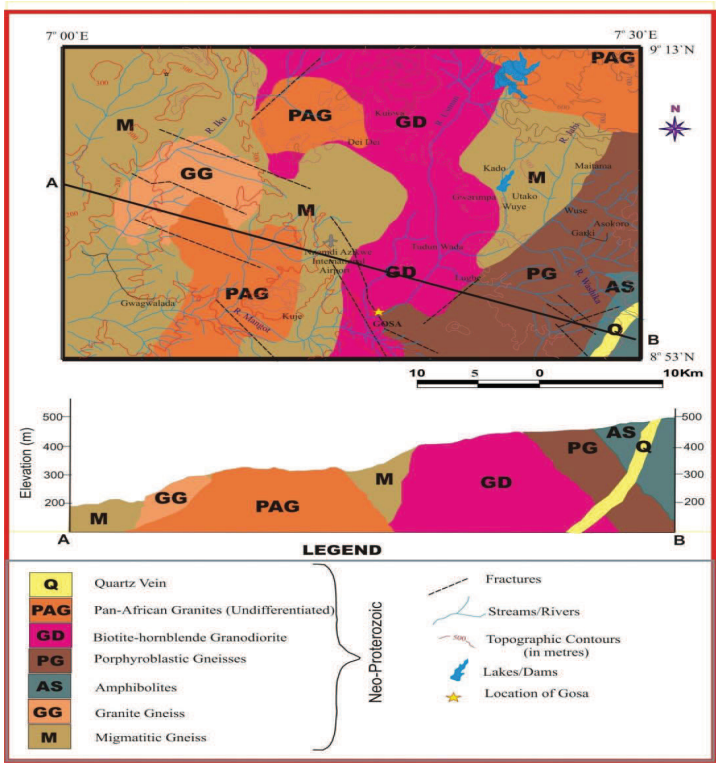

APPENDIX C:

88-LINEAMENT SRTM DATA EXTRACTED FOR THE STRUCTURAL MAP OF THE STUDY

Direction	Length (m)	Number Lines
0	4818	1
1	0	0
2	0	0
3	3245	1
4	0	0
5	8008	1
6	0	0
7	0	0
8	0	0
9	0	0
10	0	0
11	0	0
12	0	0
13	2915	1
14	0	0
15	10142	2
16	0	0
17	5049	1
18	14949	3
19	3179	1
20	6050	1
21	13189	2
22	7491	1
23	0	0
24	16775	3
25	5764	1
26	2365	1
27	3465	1
28	4312	1
29	17160	2
30	0	0
39	3366	1
40	9262	2
41	0	0
42	9405	1
43	1958	1
44	7942	2
45	0	0
46	8833	2
47	0	0
48	10637	2
49	0	0
50	7304	1
51	0	0
52	0	0
53	3047	1
54	4697	1
55	5115	1
56	0	0
57	0	0
58	2981	1
59	0	0
60	6237	1
61	9526	2
62	0	0
63	4807	1
64	13189	2
65	8382	2
66	0	0
67	0	0
68	0	0
69	8811	2
70	0	0

79	5632	1	119	0	0
80	0	0	120	0	0
81	4884	1	121	0	0
82	3586	1	122	0	0
83	0	0	123	0	0
84	5016	1	124	0	0
85	0	0	125	0	0
86	0	0	126	0	0
87	0	0	127	0	0
88	0	0	128	0	0
89	0	0	129	0	0
90	77	1	130	0	0
91	4268	1	131	0	0
92	0	0	132	0	0
93	0	0	133	0	0
94	0	0	134	0	0
95	0	0	135	0	0
96	0	0	136	0	0
97	0	0	137	0	0
98	0	0	138	0	0
99	0	0	139	0	0
100	0	0	140	0	0
101	0	0	141	0	0
102	0	0	142	0	0
103	0	0	143	396	1
104	0	0	144	0	0
105	0	0	145	0	0
106	0	0	146	0	0
107	0	0	147	0	0
108	5401	1	148	0	0
109	0	0	149	0	0
110	0	0	150	0	0
111	0	0	151	0	0
112	0	0	152	0	0
113	0	0	153	0	0
114	0	0	154	0	0
115	0	0	155	0	0
116	0	0	156	0	0
117	0	0	157	0	0
118	0	0	158	0	0

APPENDIX D

CALCULATION OF ^{238}U AND ^{232}TH IN THORIUM ORE (IAEA S-14) AND ^{40}K IN LAKE SEDIMENT (IAEA SL-2)

^{238}U:

Concentration of ^{238}U in Thorium ore (S-14) = 29 ppm

The weight of measured sample used from S-14 = 20.01 g

The concentration of ^{238}U in S-14 used = 29 x 20.01μg g^{-1} = 580.29 ppm

^{232}Th:

For ^{232}Th in Thorium ore (S-14) = 0.061 (wt. %) = $\frac{0.061 \times 100}{1000000} = 0.061 \times 10^{-4}$

= 610 ppm

The measure weight of S-14 used = 20.01 g

The concentration of ^{232}Th in S-14 used = 610 x 20.01 = 12206.1 ppm.

^{40}K:

Specific activity of ^{40}K = 240 Bq kg^{-1} (IAEA SL-2)

The weight of SL-2 used = 74.18 g

The activity of ^{40}K in SL-2 used = $\frac{240\ Bq}{1000\ g} \times 74.18\ g$ = 0.24 x 74.18 Bq

= 17.8 Bq

APPENDIX E

THE CONCENTRATION OF URANIUM AND THORIUM WAS CALCULATED USING THE FOLLOWING FORMULA

$$C_{samp} = \frac{W_{std} \times N_{samp}}{W_{samp} \times N_{std}} . C_{std} \qquad (3.19)$$

where

C_{samp}= concentration of sample collected (ppm)

C_{std}= concentration of the standard sample (ppm)

C_{std} = weight of the standard sample (g)

W_{samp} = weight of the sample collected (g)

N_{samp}= net counts of the photopeak area of the sample collected

N_{std} = net counts of the photopeak area of the standard sample.

The uncertainty of the sample concentration was calculated by using the accurate approach by Supian and Evans, 1992.

$$\Delta C_{samp}(ppm) = \left(\left(\frac{\Delta W_{std}}{W_{std}}\right)^2 + \left(\frac{\Delta W_{samp}}{W_{samp}}\right)^2 + \left(\frac{\Delta N_{samp}}{W_{samp}}\right)^2 \left(\frac{\Delta N_{std}}{N_{std}}\right)^2 \right)^{1/2} \text{X } C_{std} \qquad (3.20)$$

Conversion factors were used to convert ppm to Bq kg^{-1}. [^{238}U; 1ppm = 12.35 Bq kg^{-1}; ^{232}Th; 1ppm= 4.06 Bq kg^{-1}]. Whereas 1% of ^{40}K = 313 Bq kg^{-1} (IAEA, 1989).

The specific activity of potassium was calculated by using the formula:

$$A_{samp} = \frac{W_{std} \times N_{samp}}{W_{samp} \times N_{std}} . A_{std} \qquad (3.21)$$

where

A_{samp} = the specific activity of the sample collected (Bq Kg^{-1})

A_{std} = the specific activity of standard sample (Bq Kg^{-1})

W_{std} = the weight of the standard sample (Kg)

N_{samp} = the net counts of the photopeak area for the sample collected

W_{samp} = the weight of the sample collected (Kg)

N_{std} = the net counts of the photopeak area for the standard sample.

The uncertainty of the specific activity of potassium was calculated by using the following formula:

$$\Delta A_{samp}(ppm) = \left(\left(\frac{\Delta W_{std}}{W_{std}}\right)^2 + \left(\frac{\Delta W_{samp}}{W_{samp}}\right)^2 + \left(\frac{\Delta N_{samp}}{W_{samp}}\right)^2 \left(\frac{\Delta N_{std}}{N_{std}}\right)^2 \right)^{1/2} \text{X} \quad A_{std} \quad (3.22)$$

APPENDIX F:

Mathematical Model of Groundwater Flow in Homogeneous Isotropic Medium of Representative elementary volume (REV) of flow equation in porous media (modified after Delluleur, 1999)

MatLab software was used to determine the representative elementary volume of flow equation in porous media as shown in below. The result of the model of Equation (xiv) was discussed in Section 4.3.

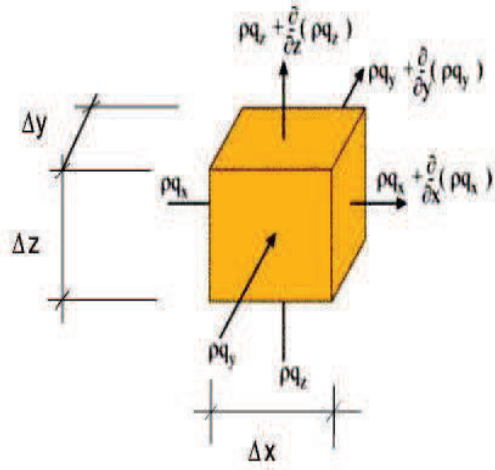

From Figure of REV , the relation of continuity equation that expresses the fundamental principle of mass conservation, stating that in a representative elementary volume (REV), the net result of inflow, I, minus outflow, O , is balanced by the change in mass storage, M in a given period of time:

$$I - O = \frac{\partial M}{\partial t} \quad \text{(i)}$$

I and O represent mass fluxes, expressed in mass per unit time (kg s^{-1}); they can be computed using Darcy's law, which is the constitutive law of the porous media. Equation (3.5) can also be written in the following form:

$$I - O = \delta \mathrm{M} \quad \text{(ii)}$$

where I and O now represent the mass inflow and the mass outflow, whose fundamental dimension is mass $[M]$.

Because Darcy's law is based on the difference of the hydraulic heads, in order to individualize the solution, the boundary conditions are needed. Finally, for transient simulations, the initial conditions meaning that the starting values for the state variables are necessary because the state variables are functions of location (spatial coordinates) and time. The continuity equation will lead to partial differential equations, for which analytical solutions exist only in a limited number of cases. Thus, numerical methods are largely employed to solve the usual practical problems of flow in porous media. The equation of continuity is obtained using the same principle for the unsaturated, respectively saturated media; there is only a small difference concerning the water content: for unsaturated media it is variable in time, while for saturated media it is a constant.

Continuity equation:

Consider a volume of soil (Figure 3.9), also called elementary control volume. The lengths of the three sides are $\Delta x, \Delta y$ and Δz ; the time step used for the discretization of the continuity equation is Δt. The water flux, q, flowing through the REV has the components q_x , q_y and q_z

Left side of the volume of the continuity equation:

The mass inflow I_x during the interval Δt through the left face of area $\Delta y\ \Delta z$ is:

$$I_x = \rho\, V_x = \rho q_x\, \Delta t\ \Delta y \Delta z \quad \text{(iii)}$$

where

V_x = volume of water through $\Delta y \Delta z$

q_x = specific discharge along x

Applying Taylor series expansion along x axis and keeping only the first two terms, the outflow O_x in the same interval Δt is

$$O_x = \rho V_{x+\Delta x} = \left[\rho q_x + \partial \frac{(\rho q_x)}{\partial x} \Delta x\right] \Delta t \Delta y \Delta z \qquad \text{(iv)}$$

The inflow minus outflow in the time interval Δt in the x direction is then:

$$I_x - \ O_x = -\frac{\partial(\rho q_x)}{\partial x} \Delta x \Delta y \Delta z \Delta t \qquad \text{(v)}$$

Thus, the same expressions can be obtained for the other two directions, so the balance of the total mass inflow and the total mass outflow is:

$$I_x - \ O_x = -\left[\frac{\partial(\rho q_x)}{\partial x} + \frac{\partial(\rho q_y)}{\partial y} + \frac{\partial(\rho q_z)}{\partial z}\right] \Delta x \Delta y \Delta z \Delta t \qquad \text{(vi)}$$

Taking into account the parenthesis represent a scalar called divergence:

$$div\ (\rho q) = \frac{\partial(\rho q_x)}{\partial x} + \frac{\partial(\rho q_y)}{\partial y} + \frac{\partial(\rho q_z)}{\partial z} \qquad \text{(vii)}$$

Equation (vii) can be written as:

$$I - O = -div\ (\rho q) \Delta x \Delta y \Delta z \Delta t \qquad \text{(viii)}$$

Right side of the continuity equation:

The mass M of water existing in a volume V_w can be expressed as:

$$M = \rho V_w \qquad \text{(ix)}$$

where ρ is the water density. At the same time, the volume of water V_w can be defined using the volumetric water content, θ as:

$$V_w = \theta V = \theta \Delta x \Delta y \Delta z \qquad \text{(x)}$$

Thus, the mass of groundwater $M(t)$ existing in REV at the moment t is:

$$M(t) = \rho\theta\Delta x\Delta y\Delta z \tag{xi}$$

At the moment $t + \Delta t$, the mass $M(t + \Delta t)$ can be approximated using the first two terms of the Taylor series expansion in the following form:

$$M(t + \Delta t) = M(t) + \frac{\partial M}{\partial t}\Delta t = M(t) + \frac{\partial(\rho\theta\Delta x\Delta y\Delta z)}{\partial t}\Delta t \tag{xii}$$

It follows that:

$$\delta\mathrm{M} = M(t + \Delta t) - M(t) = \frac{\partial(\rho\theta\Delta x\Delta y\Delta z)}{\partial t}\Delta t \tag{xiii}$$

The water density and the volumetric water content are functions of the spatial variables and of time: $\rho = \rho(x, y, z, t); \theta = \theta(x, y, z, t)$.

Density of water as well as the control volume varies in time due to the water pressure variation; still, the lateral deformations of the control volume are neglected, and only the vertical deformation is taken into account. As a result, the derivative in the relation (xiv) can be expressed as (Delleur, 1999):

$$\frac{\partial(\rho\theta\Delta x\Delta y\Delta z)}{\partial t} = \frac{\partial\rho}{\partial t}\,\theta\Delta x\Delta y\Delta z + \rho\frac{\partial\theta}{\partial t}\,\Delta x\Delta y\Delta z + \rho\,\theta\Delta x\Delta y\frac{\partial\Delta z}{\partial t} =$$

$$= \rho\left(\frac{\theta}{\rho}\frac{\partial\rho}{\partial t} + \frac{\partial\theta}{\partial t} + \frac{\partial\theta}{\Delta z}\frac{\partial\Delta z}{\partial t}\right)\Delta x\Delta y\Delta z \tag{xiv}$$

APPENDIX G:

Minimum Detectable Activity for Radioactivity Concentrations Using HPGe Spectrometry and NAA

Minimum detectable activity (MDA) measured using de-ionized double distilled water which detected the minimum activity using gamma ray counting with a certain degree of confidence (Knoll, 2000; Currie, 1968). The MDA was given by

$$MDA = \frac{L_d}{\varepsilon\, y\, T_b\, q} \quad (1)$$

where L_d is the detection limit

$$L_d = 2\, L_c = 2k\, \sigma_B \quad (2)$$

where σ_B is the uncertainty for counting of de-ionized water,

k = the probabilities for errors which is equal to 1.645 (Currie, 1968),

L_c = the critical level beyond which is the net signal cannot reliably be detected,

The value of minimum detectable activities (MDA) were 13 Bq kg^{-1} for ^{40}K, 1 Bq kg^{-1} for ^{238}U (^{226}Ra) and 2 Bq kg^{-1} for ^{232}Th for a counting time of 21600 s (IAEA, 1989; IAEA, 2003; Saleh et al 2013).

Detection Limit for Neutron Activation Analysis (NAA)

The limit of detection of a particular element refers to the lowest level to which an analytical signal can be distinguished at a specific confidence level from a background signal. The detection limit depends on the irradiation, the decay and the counting conditions (Currier, 1968, Greenberg et al., 2011; Kafala and MacMahon, 2007; Al-Sulaiti, 2011). The detection limit is often estimated by using Currie's formula (Currier, 1968).

The counting threshold of a particular element is defined for making decision if sample can be detected, namely, the critical level (L_c) according to Currie, L_c is defined as the level of the net signal above which the gross count can be considered to be statistically different from background signal. The critical level L_c is expressed as

$$L_c = K_\alpha \sigma_{net} = K\sqrt{2B} \quad (3)$$

where K_α is the coverage is factor being employed, and σ_{net} is the standard deviation of Gaussian distribution for the number of counts in the blank. σ_{net} which can be estimated from the following relation

$$\sigma_{net}{}^2 = \sigma_{S+B^2} + \sigma_{B^2} \quad (4)$$

where σ_{S+B^2} is the variance of the signal and σ_{B^2} is the variance of the blank. If σ_{net} is approximately independent of the signal level, then

$$\sigma_{net}{}^2 = \sigma_{S+B^2} + \sigma_{B^2} = 2\sigma_{B^2} \quad (5)$$

For a single count, $\sigma_B{}^2 = B$, and hence

$$\sigma_{net}{}^2 = 2B \quad (6)$$

Description level is subjected to two kinds of errors based on the net counts result of a particular element. If the net counts N_s is less than L_C, the element does not contain any count above this limit at 95 % confidence level. The probability of making an error in assuming a signal has been detected where no signal is actually presented; this type of error is called α. The net count, N_s, of element is given by

$$N_s = N_T - N_b \tag{7}$$

where N_b is the number of count recorded with a blank sample and N_T is the number of counts recorded with element of interest.

If the second type of error, β is implemented, then the possibility of not detecting the signal where one exists has to be taken into consideration. The detection limit L_d, can be described as the level of true net counts (signal). L_d can be written as

$$L_d = L_c + K_\beta \sigma_{net} = L_c + K_\beta \sqrt{2B} \tag{8}$$

where K_β is the coverage factor being employed in this case. If both types of errors are set to be equal then

$K_\alpha = K_\beta = K$

and thus

$$L_d = 2L_c = 2K\sigma_{net} = 2K\sqrt{2B} \tag{9}$$

In this case, the detection limit is simply twice the critical level.

$$L_d = K\sqrt{2B} = 1.645\sqrt{B} = 2.33\sqrt{B} \tag{10}$$

where, 1.645 is the value of μ to give a 95 % confidence level, B is the background area under the photopeak. The detection limit in unit of mass of an element is given by the following equation:

$$L_d = \frac{2.33\sqrt{B}}{T} \quad (11)$$

where T is called sensitivity of analysis, given as

$$T = \frac{CA}{m} = \left[\frac{N_a \theta P_\gamma \varepsilon}{w}\right] RSD \quad (12)$$

where w is the atomic weight; other parameters are R, the reaction rate per second, S, the saturation factor ($S = 1 - e^{-\lambda t_{ir}}$), D = $e^{-\lambda t_d}$; Decay factor, $C = (1 - e^{-\lambda t_m})/\lambda$; Counting factor, $R = \varphi_{th}\sigma_{eff}$ is the reaction rate, N_a is the Avogadro's number (mol^{-1}); θ is the isotopic abundance of target isotope N_o, m is the mass of the irradiated element (g), A is the net peak area, γ is the gamma ray abundance and ε is the peak efficiency of the detector.

The detection limit of elemental analysis investigated by neutron activation analysis for 228 and 278 energy (keV) for ^{238}U is 0.80 ppm. ^{232}Th with 312 energy (keV) has detection limit of 0.50 ppm.

APPENDIX H:

LIST OF PUBLICATIONS

Maxwell, O., Wagiran, H., Ibrahim, N., Lee, S. K., Soheil, S. (2013a). Comparison of ^{238}U, ^{232}Th, and ^{40}K in different layers of subsurface structuresion Dei-Dei and Kubwa, Abuja, Northcentral Nigeria. *Radiation Physics and Chemistry*, 91, 70-80.

Maxwell, O., Wagiran, H., Ibrahim, N., Lee, S. K., Soheil, S. (2013b). Measurement of ^{238}U, ^{232}Th, and ^{40}K in boreholes at Gosa and Lugbe, Abuja, North Central Nigeria. *Radiation Protection Dosimetry* , pp 1-7.

Maxwell, O., Wagiran, H., Noorddin I., Oha I.A., Onwuka O. S., Soheil S. (2014). Integrated Geoelectrical And Structural Studies For Groundwater Investigation In Some Parts Of Abuja, Northcentral Nigeria. *Near Surface Geophysics, 12,* Doi:10.3997/1873-0604.2014007.

OMEJE, M., H., Wagiran, N. Ibrahim, Oha I.A, Onwuka O.S., P.E Ugwuoke, Meludu, O. (2013). Geoelectrical investigation of aquifer problems in Gosa area of Abuja*, Northcentral Nigeria.* International Journal of Physical Sciences, vol. 8 (13), pp. 549-559.

Maxwell, O., Wagiran, H., Ibrahim, N., Lee, S. K., Soheil, S. (2014). Radiological monitoring of borehole at Dei-Dei in Abuja, Northcentral Nigeria. ICSED 2014: February 19-21, Singarpore (APCBEE Pocedia). *Singapore 2014 Published by Elsevier B.V. Selection and/or peer review under responsibility of Asia-Pacific Chemical, Biological & Environmental Engineering Society*.

Maxwell, O., Wagiran, H., Ibrahim, N., Lee, S. K., Soheil, S. (2014). Radiation Hazards on borehole drillers in Dei-Dei Abuja, North Central Nigeria. Proceeding of International Science Postgraduate Conference 2013

(ISPC2013) at Faculty of Science, Universiti Teknologi Malaysia.

O. Maxwell, H. Wagiran, S. Sabri, S. K. Lee and Z. Embong. (2014). Radioactivity Level and toxic elemental concentration in groundwater at Dei-Dei and Kubwa area of Abuja, Northcentral Nigeria. Submitted to *Journal of Radiation Physics and Chemistry.*

O. Maxwell, H. Wagiran, N. Ibrahim , S. Sabri and Z. Embong. (2014). Natural Radioactivity and Geological Influence on Subsurface Layers at Kubwa and Gosa Area of Abuja, Northcentral Nigeria. Submitted to *Journal of applied radiation and Isotopes.*

O. Maxwell, H. Wagiran, S. Sabri, S. K. Lee and Z. Embong. (2014). Health Risks Associated with Radionuclides of Subsurface Lithology on Borehole Drillers in Parts of Abuja, North Central Nigeria. Submitted to Journal of *Stochastic Environmental Research and Risk Assessment.*